SUPERSYMMETRIC YANG–MILLS THEORIES ON THE LATTICE

By

Anosh Joseph
B.Sc., Mahatma Gandhi University, 2001
M.Sc., Indian Institute of Technology–Madras, 2004

DISSERTATION

Submitted in partial fulfillment of the requirements for the
degree of Doctor of Philosophy in Physics
in the Graduate School of Syracuse University

August 2011

Advisor: Prof. Simon Catterall, Ph.D.

Abstract

This dissertation reviews the formulation of twisted supersymmetric Yang–Mills (SYM) theories in the continuum and also on the lattice. We focus on the maximally supersymmetric twisted SYM theories in four and two dimensions. The one-loop renormalization of the lattice four-dimensional SYM theory is investigated. We also study the thermal phase structure of the maximally supersymmetric SYM in two dimensions and possible black hole transitions in its dual gravitational theory, using numerical simulations of the lattice theory.

Contents

List of Tables

List of Figures

Preface

Implementation of supersymmetric Yang–Mills (SYM) theories on the lattice is an old problem in lattice field theory. It has resisted solution until recently, when new ideas drawn from topological field theories have been brought to bear on the question. The result has been the creation of a new class of lattice gauge theories, called "twisted SYM theories," in which the lattice action is invariant under one or more supersymmetries. The twisted SYM theories on the lattice are local, free of doublers, and also possess exact gauge-invariance. In principle, they form the basis for a truly non-perturbative definition of the continuum SYM theories. In this dissertation, we attempt to present a variety of lattice studies of sixteen supercharge SYM theories in four and two dimensions.

To make this dissertation as self contained as possible, we have included a set of introductory topics, such as constructing SYM theories in various dimensions, general properties of topological field theories, and their connections to SYM theories and lattice formulations, geometric structure of the resultant lattices, and simulation algorithms employed in the numerical studies to obtain some interesting results.

In Chapter 1, we introduce the four-dimensional $\mathcal{N} = 4$ SYM theory. We begin with various conditions that can be imposed on Dirac fermions in various dimensions to maintain the symmetry between the number of fermion and boson degrees of freedom in a given Yang-Mills theory coupled to spin-1/2 fermions. The conditions lead to Weyl, Majorana, and Weyl–Majorana fermions. The method of dimensional reduction is introduced next, and then this method is applied to the ten-dimensional $\mathcal{N} = 1$ SYM theory to obtain the $\mathcal{N} = 4$ SYM theory in four dimensions.

In Chapter 2, we introduce topological field theories, BRST invariance in gauge theories, and then focus on topological field theories of Witten type, which are the focus of our interest.

In Chapter 3, we show how to twist the supersymmetries of SYM theories with extended supersymmetries. The method of maximal twisting is discussed next, and then its relevance to the lattice constructions is explained. We give the twisted versions of the two-dimensional $\mathcal{N} = 2$ and four-dimensional $\mathcal{N} = 4$ SYM theories, exposing the nilpotent scalar supersymmetries appearing as a consequence of the twist. We also write down the action and scalar supersymmetries of these theories.

In Chapter 4, we introduce supersymmetric lattices, their geometric structure, ori-

entation of field operators, the lattice covariant derivatives, connection to Dirac-Kähler fermions, and discretized actions of the twisted SYM theories.

After these introductory Chapters, in Chapter 5, we present a part of the original work, where the $\mathcal{N} = 4$ SYM is studied at one-loop on a four-dimensional lattice. The lattice formulation under consideration retains one exact supersymmetry at non-zero lattice spacing. This feature, combined with gauge-invariance and the large point group symmetry of the lattice theory, can be used to show that that the only counterterms that appear at any order in perturbation theory correspond to renormalizations of existing terms in the bare lattice action. The analysis shows that no mass terms are generated at any finite order of perturbation theory. The one-loop renormalization coefficients are extracted by examining the fermion and auxiliary boson self-energies at one-loop. They all exhibit a common logarithmic divergence that can be absorbed by a single wavefunction renormalization. This finding implies that, at one-loop, only a fine tuning of the finite parts is required to regain full supersymmetry in the continuum limit.

In Chapter 6, we write down the algorithms to simulate the twisted SYM theories, as a prelude to the numerical study presented in the following Chapter. The Rational Hybrid Monte Carlo (RHMC) algorithm is presented, and the overall structure of the C++ code to simulate these theories is detailed.

In Chapter 7, we discuss the results of numerical simulations of (1+1)-dimensional sixteen supercharge $SU(N)$ Yang–Mills theory at finite temperature and compactified on a circle. For large N, this system is thought to provide a dual description of the decoupling limit of N coincident D1-branes on a circle. It has been proposed that, at large N, there is a phase transition at strong coupling related to the Gregory-Laflamme (GL) phase transition in the holographic gravity dual. In a high temperature limit, there was argued to be a deconfinement transition associated with the spatial Polyakov loop, and it has been proposed that this is the continuation of the strong coupling GL transition.

On the lattice, this theory is investigated for $SU(3)$ and $SU(4)$. The study of the time and space Polyakov loops in the lattice SYM theory show evidence supporting this transition. In particular, at strong coupling, the transition has the parametric dependence on coupling predicted by gravity. The GL phase transition temperature is estimated from the lattice data which, interestingly, is not yet known directly in the gravity dual.

We end with a set of conclusions and recommendations for the directions of future research.

Chapter 1

$\mathcal{N} = 4$ Super Yang–Mills Theory

Supersymmtric Yang–Mills (SYM) theories belong to an interesting class of quantum field theories. Among them, the four-dimensional SYM theory with sixteen supersymmetries is a very special quantum field theory in its own right. This theory exhibits many interesting properties. For zero theta angle, the four-dimensional SYM theory with a simple gauge group has just a single dimensionless coupling parameter, the gauge coupling parameter g. The classical version of this theory exhibits superconformal invariance, owing to the dimensionless nature of its coupling parameter. Its beta function vanishes identically to all orders in perturbation theory and the same is believed to be true at the nonperturbative level. This theory, therefore, is finite, with no renormalization at all. Its coupling parameter does not run, unlike most gauge theories, different values of g really give different theories, rather than being transmuted to a change of scale. Another interesting property exhibited by this theory is exact electric-magnetic duality that is, the invariance under the interchange of electric and magnetic quantum numbers, and also the replacement of g with $4\pi/g$. That is, the theory with a weak gauge coupling g is fully equivalent to the one with a strong gauge coupling $4\pi/g$.

In 1997, Maldacena proposed [1] a new duality relating Type II supergravity (a certain low energy limit of string theory) in $(d+1)$-dimensional anti-de Sitter (AdS) space and d-dimensional super conformal theories. This is known as the holographic principle. The $\mathcal{N} = 4$ SYM theory takes part in the most successful realization of holographic principle. This theory can be realized as the gauge theory living on a D3-brane of Type IIB superstring theory in $AdS_5 \times S^5$ space.

The action of $\mathcal{N} = 4$ SYM theory was given for the first time in 1977 in [2, 3] within the framework of string theory toroidal compactifications. This theory has the maximal amount of supersymmetry - sixteen real supercharges - for a four-dimensional field theory with global supersymmetry.

There exist different types of construction schemes for four-dimensional $\mathcal{N} = 4$ SYM theory. We follow the original work of Brink, Schwarz and Scherk [2], where it is constructed by dimensional reduction from ten dimensions.

1.1 Yang–Mills theory with fermions

We are interested in constructing a Yang–Mills theory coupled to spin-$\frac{1}{2}$ fermions in d spacetime dimensions with an additional symmetry: the number of bosonic and fermionic degrees of freedom are equal. We will call this symmetry supersymmetry.

A massless gauge potential in d dimensions has $d-2$ on-shell real degrees of freedom. A Dirac spinor in d dimensions has $2^{[d/2]}$ on-shell real degrees of freedom, where $[d/2]$ represents the integral part. These two numbers do not match in any dimension. In order to demand the additional symmetry, we will have to reduce the number of fermionic degrees of freedom by requiring the spinor to satisfy some supplementary conditions.

Let us consider a Yang–Mills theory coupled to massless spin-$\frac{1}{2}$ particles on a d-dimensional flat Minkowski space $\mathbb{R}^{1,(d-1)}$ with signature $g_{mn} = \text{diag}(-,+,+,\cdots,+)$, where $m, n = 0, 1, 2, \cdots, (d-1)$. The metric is

$$ds^2 = \sum_{m,n} g_{mn} dx^m dx^n = -(dx^0)^2 + (dx^1)^2 + \cdots + (dx^{(d-1)})^2 \ . \tag{1.1}$$

The theory has a gauge field A_m taking values in the real Lie algebra of a compact gauge group G. The gauge field takes values in anti-hermitian matrices, in the adjoint representation of G. The covariant derivative D_m is

$$D_m = \partial_m + A_m \ , \tag{1.2}$$

The corresponding curvature F_{mn} is

$$F_{mn} = [D_m, D_n] = \partial_m A_n - \partial_n A_m + [A_m, A_n] \ . \tag{1.3}$$

We add a fermionic term to the d-dimensional Yang–Mills action. The fermions are contained in a Dirac spinor λ taking values in the Lie algebra of G.

The action is

$$S = \text{Tr} \int d^d x \Big(-\frac{1}{4} F_{mn} F^{mn} + i\overline{\lambda} \Gamma^m D_m \lambda \Big) \ , \tag{1.4}$$

where Γ^m are the d-dimensional gamma matrices. Since anti-hermitian matrices generate the Lie algebra in our case, the trace Tr is negative definite.

We examine the dimensions in which the action (1.4) permits the extra symmetry - supersymmetry - between the gauge bosons and the fermions without the addition of other fields. The requirement of same number of bosonic and fermionic degrees of freedom is essential for field theories that transform as linear representations of supersymmetry. Since the spinor degrees of freedom grow faster than that of gauge bosons, we will reduce the number of spinor degrees of freedom by imposing some additional conditions on the fermions. Before we choose those conditions, a familiarization with spinor representations in arbitrary dimensions would be useful.

1.2 Spinors in higher dimensions

The Lorentz group, the symmetry group of Minkowski space, admits finite-dimensional representations. Spinors appear as fields that transform under finite-dimensional representations of the Lorentz group.

We use the language of Clifford algebras to discuss the spinor representations in d dimensions. A Clifford algebra is a set of matrices (we call them gamma matrices) satisfying the anticommutation relations:

$$\{\Gamma_m, \Gamma_n\} = 2g_{mn} \ , \tag{1.5}$$

where $m, n = 0, 1, \cdots (d-1)$.

Given such a set of matrices, we see that the following antisymmetric matrices,

$$\Sigma^{mn} = -\frac{i}{4}[\Gamma^m, \Gamma^n] = -\Sigma^{nm} \ , \tag{1.6}$$

satisfy the commutation relations of the Lorentz group generators:

$$i[\Sigma^{mn}, \Sigma^{sr}] = \eta^{ns}\Sigma^{mr} + \eta^{mr}\Sigma^{ns} - \eta^{nr}\Sigma^{ms} - \eta^{ms}\Sigma^{nr} \ . \tag{1.7}$$

The matrices Σ^{mn} give a d-dimensional representation of the Lorentz algebra. They are a set of antisymmetric tensors transforming according to the d-dimensional Lorentz vector representation of $SO(1, d-1)$. They act on the space of fields called Dirac spinors. The algebra generated by Σ^{mn} yield the spinor representation of $SO(1, d-1)$.

The d-dimensional representation of the Lorentz algebra generated by Σ^{mn} is not always an irreducible representation. To see if a given representation is reducible or not, we need to consider separately the case where d is an odd or even dimension.

We begin with the construction of gamma matrices in even dimensions, $d = 2k + 2$, where $k = 1, 2, \cdots$. We group the gamma matrices into a set of raising and lowering operators [4, 5]

$$u_0^{\pm} = \frac{1}{2}(\pm\Gamma_0 + \Gamma_1) \ , \tag{1.8}$$

$$u_a^{\pm} = \frac{1}{2}(\Gamma_{2a} \pm i\Gamma_{2a+1}) \ , \tag{1.9}$$

where $a = 1, \cdots, k$. These operators satisfy the following anticommutation relations:

$$\{u_i^+, u_j^-\} = \delta_{ij} \ , i, j = 0, 1, \cdots, k \tag{1.10}$$

$$\{u_i^+, u_j^+\} = \{u_i^-, u_j^-\} = 0 \ , \tag{1.11}$$

along with the conditions:

$$(u_i^+)^2 = (u_i^-)^2 = 0 \ . \tag{1.12}$$

We can let u_i^- operators act repeatedly on any spinor state to reach a spinor $|\xi\rangle$ annihilated by all u_i^-'s

$$u_i^-|\xi\rangle = 0, \quad \text{for all } i \ . \tag{1.13}$$

Now we can let the creation operator u_i^+ act on $|\xi\rangle$, at most once each, in all possible ways to obtain a spinor representation. The spinor states obtained in that way are given in table 1.1.

states	$\|\xi\rangle$	$u_i^+\|\xi\rangle$	$u_i^+u_j^+\|\xi\rangle$	$\cdots$	$(u_k^+u_{(k-1)}^+\cdots u_0^+)\|\xi\rangle$
number	1	$k+1$	${}_{k+1}C_2$	$\cdots$	1

Table 1.1: Spinor states and their corresponding numbers.

The total number of states is

$$1+(k+1)+\ {}_{k+1}C_2+\cdots+1=\sum_{n=0}^{k+1}\ {}_{k+1}C_n=2^{k+1}=2^{d/2}\ . \tag{1.14}$$

This representation has dimension 2^{k+1}. The spinor representation is given by

$$|s_0s_1\cdots s_k\rangle=(u_k^+)^{s_k+\frac{1}{2}}\cdots(u_0^+)^{s_0+\frac{1}{2}}|\xi\rangle\ , \tag{1.15}$$

where each of s_i is $\pm\frac{1}{2}$. The $|\xi\rangle$ we started with contains all $s_i=-\frac{1}{2}$.

The matrix elements of Γ^m can be derived from the definitions and the anticommutation relations by taking the $|s_0s_1\cdots s_k\rangle$ as a basis.

The generators $\Sigma_{2i,2i-1}$ form a commuting set. We consider the operator

$$S_i\equiv\Sigma_{2i,2i-1}=u_i^+u_i^--\frac{1}{2}\ . \tag{1.16}$$

The basis vectors $|s_0s_1\cdots s_k\rangle$ defined above form simultaneous eigenstates of all the S_i's with eigenvalues s_i,

$$S_i|s_0s_1\cdots s_k\rangle=s_i|s_0s_1\cdots s_k\rangle\ . \tag{1.17}$$

The half-integer eigenvalues show that this is a spinor representation. The spinors form the 2^{k+1}-dimensional Dirac representation of the Lorentz algebra $SO(1,2k+1)$. For example, in $d=4$, the states $|\pm\frac{1}{2},\pm\frac{1}{2}\rangle$ form a four component Dirac spinor.

Noting that increasing d by two doubles the size of Dirac matrices, we can give an iterative expression for gamma matrices in even dimensions starting in $d=2$.

The gamma matrices in $d=2$ are:

$$\Gamma^0=\begin{pmatrix}0&1\\-1&0\end{pmatrix},\quad \Gamma^1=\begin{pmatrix}0&1\\1&0\end{pmatrix}\ . \tag{1.18}$$

Then in $d=2k+2$ with $k=1,2,\cdots$ we have,

$$\Gamma^m=\gamma^m\otimes\begin{pmatrix}-1&0\\0&1\end{pmatrix},\quad m=0,\cdots,d-3\ , \tag{1.19}$$

$$\Gamma^{(d-2)}=\mathbb{I}\otimes\begin{pmatrix}0&1\\1&0\end{pmatrix}, \tag{1.20}$$

$$\Gamma^{(d-1)}=\mathbb{I}\otimes\begin{pmatrix}0&-i\\i&0\end{pmatrix}\ , \tag{1.21}$$

with γ^m the $2^k\times2^k$ Dirac matrices in $d-2$ dimensions and $\mathbb{I}$ the $2^k\times2^k$ identity. The 2×2 matrices act on the index s_k, which is added in going from $2k$ to $2k+2$ dimensions.

For representations in odd dimensions, we need to add a new gamma matrix Γ_{d+1} to the Γ_m matrices. Let us define Γ_{d+1} in the following section.

1.2.1 Weyl spinors

Since the generators Σ^{mn} are quadratic in the gamma matrices, the spinor states $|s_0 s_1 \cdots s_k\rangle$ with even and odd numbers of $+\frac{1}{2}$s do not mix. This indicates that the Dirac representations in even dimensions are reducible representations of the Lorentz algebra.

We define a new gamma matrix:

$$\Gamma_{d+1} = i^{-k}\Gamma_0\Gamma_1\cdots\Gamma_{d-1} \ , \tag{1.22}$$

which has the properties:

$$(\Gamma_{d+1})^2 = 1, \quad \{\Gamma_{d+1}, \Gamma^m\} = 0, \quad [\Gamma_{d+1}, \Sigma^{mn}] = 0 \ . \tag{1.23}$$

All the Dirac spinor states are eigenstates to Γ_{d+1}

$$\Gamma_{d+1}|s_0 s_1 \cdots s_k\rangle = \pm|s_0 s_1 \cdots s_k\rangle \ , \tag{1.24}$$

with eigenvalue $+1$ for even numbers of $s_i = +\frac{1}{2}$ and -1 for odd ones.

Since Γ_{d+1} commutes with the generators of the Lorentz algebra Σ^{mn} cannot furnish an irreducible representation of $SO(1, d-1)$. The Dirac representation, let us denote it by $\mathbb{S}$, breaks down into two 2^k dimensional irreducible representations $\mathbb{S}^+$ and $\mathbb{S}^-$. These representations are called Weyl (or chiral) representations, and they can be obtained by projecting out the two subspaces using Γ_{d+1}. We define a projection operator:

$$\mathbb{P}^\pm = \frac{1}{2}(\mathbb{I} \pm \Gamma_{d+1}) \ . \tag{1.25}$$

The Lorentz generators and representation now split into two parts:

$$\Sigma^\pm_{mn} = \mathbb{P}^\pm\Sigma_{mn}, \quad \mathbb{S}^\pm = \mathbb{P}^\pm\mathbb{S} \ . \tag{1.26}$$

The spinors obtained in this way are called Weyl spinors.

In $d = 4$, the Dirac representation is the familiar four-dimensional one, which separates into two two-dimensional Weyl representations distinguished by their eigenvalue under the chirality operator Γ_5.

$$\mathbf{4}_{\text{Dirac}} = \mathbf{2} + \mathbf{2'} \ . \tag{1.27}$$

Here we have labeled a representation $\mathbb{S}$ by its dimension (in boldface). In $d = 10$, the representations are:

$$\mathbf{32}_{\text{Dirac}} = \mathbf{16} + \mathbf{16'} \ . \tag{1.28}$$

To get representations in odd dimensions, $d = 2k + 3$, we simply add Γ_{d+1} to the gamma matrices for $d = 2k + 2$. The set of creation and annihilation operators is the same as that of $d = 2k+2$. This is now an irreducible representation of the Lorentz algebra because Σ^{md} anticommutes with Γ_{d+1}. Thus, there is a single spinor representation of $SO(1, 2k + 2)$, which has dimension 2^{k+1}. There is no chirality in odd dimensions.

For k even, the Weyl irreducible representations are equivalent to complex conjugates of each other. While for k odd each Weyl representation is equivalent to its own complex conjugate. The Weyl representations can only be real for $k = 1$ (mod) 4 and must be pseudo-real for $k = 3$ (mod) 4.

The Lorentz generators Σ_{mn} in odd dimensional case furnish an irreducible representation of the Lorentz group by themselves. In each odd dimension, the fundamental spinor representation is either real or pseudo-real.

1.2.2 Majorana spinors

The above construction of the irreducible representations of gamma matrices shows that, in even dimensions, $d = 2k+2$, the irreducible representations are unique up to a change of basis. That is, for any set of gamma matrices $\{\Gamma^m\}$ and $\{\Gamma^{m'}\}$ both satisfying the Clifford algebra, there exists a nonsingular matrix M, such that

$$\Gamma_m = M\Gamma'_m M^{-1}, \quad \text{for all } m = 0, 1, \cdots d-1 \ . \tag{1.29}$$

Thus, the matrices $(\Gamma^m)^*$ and $-(\Gamma^m)^*$ satisfy the same Clifford algebra as Γ^m. This implies that the Dirac representation is its own conjugate in even dimensions.

We can impose a condition that relates the spinor state $|\xi\rangle^*$ to $|\xi\rangle$. This condition must be consistent with Lorentz transformations and so must have the form:

$$|\xi\rangle^* = B|\xi\rangle \ , \tag{1.30}$$

with B, a nonsigular matrix satisfying

$$B\Sigma^{mn}B^{-1} = -(\Sigma^{mn})^* \ . \tag{1.31}$$

Such a condition, called the Majorana (or reality) condition, is consistent only if $BB^* = 1$.

Using the reality and anticommutation properties of the gamma matrices, one finds

$$B^*B = (-1)^{k(k+1)/2} \ \text{ or } \ (-1)^{k(k-1)/2} \ . \tag{1.32}$$

Thus, a Majorana condition is possible only if $k = 0$ or 3 (mod) 4 for the first case, and for $k = 0$ or 1 (mod) 4 for the second case. If $k = 0$, both conditions are possible, but they are physically equivalent, being related by a similarity transformation.

The Majorana condition on a Dirac spinor λ is:

$$\lambda = C\overline{\lambda}^T \ , \tag{1.33}$$

where C is the charge conjugation matrix. It transforms the Lorentz representation matrices in the following way:

$$C\Sigma^{mn}C^{-1} = -\Sigma^{mnT} \ . \tag{1.34}$$

1.2.3 Weyl–Majorana spinors

Imposing a Majorana condition on a Weyl spinor requires the Weyl spinor representation to be conjugate to itself. For k odd, which is $d = 0$ or 4 (mod) 8, it is therefore not possible to impose both the Majorana and Weyl conditions on a spinor: one can impose one or the other. Precisely for $k = 0$ (mod) 4, which is $d = 2$ (mod) 8, a spinor can simultaneously satisfy the Majorana and Weyl conditions.

We can have Majorana spinors in $d = 2, 3, 4, 8, 9, 10$, and Weyl spinors in $d = 2, 4, 6, 8, 10$. For the cases $d = 4, 8$, while one can, in principle, impose a Majorana condition, this condition is incompatible with the Weyl condition and, thus, there are no

d	Majorana	Weyl	Weyl–Majorana	min. rep.
2	yes	self	yes	1
3	yes	-	-	2
4	yes	complex	-	4
5	-	-	-	8
6	-	self	-	8
7	-	-	-	16
8	yes	complex	-	16
9	yes	-	-	16
10	yes	self	yes	16

Table 1.2: We can impose various conditions on $SO(1, d-1)$ Dirac spinors in various dimensions. A dash indicates that the condition cannot be imposed. For the Weyl representation, it is indicated whether these are conjugate to themselves (self) or to each other (complex). The smallest representation in each dimension, counting the number of real components, is given in the final column.

d	A_m	λ_D	λ_M	λ_W	λ_{MW}
3	**1**	2	**1**	-	-
4	**2**	4	**2**	**2**	-
6	**4**	8	-	**4**	-
10	**8**	32	16	16	**8**

Table 1.3: Conditions on spinor degrees of freedom in various dimensions.

Weyl–Majorana spinors for $d = 4, 8$. For $d = 2, 10$, we can impose both Majorana and Weyl conditions, that is, we have Weyl–Majorana spinors. The Weyl–Majorana spinors in $d = 2$ and $d = 10$ have particular importance because of their relevance to string theory.

Imposing a Majorana or Weyl condition on the spinor, though, reduces its degrees of freedom, each by a factor of one half. Starting with $d = 3$, the various possibilities for matching the degrees of freedom of a gauge field A_m to those of Dirac λ_D, Majorana λ_M, Weyl λ_W and Weyl–Majorana λ_{MW} spinors are shown in table 1.3.

Note that in $d > 10$ there are no solutions to our matching problem on fermion-gauge boson degrees of freedom. That is, $d = 10$ is the highest dimension in which we can have a SYM action (on a flat spacetime without adding extra fields).

1.3 Super Yang–Mills theory in ten dimensions

The SYM action in ten dimensions has the form

$$S = \mathrm{Tr} \int d^{10}x \Big(-\frac{1}{4} F_{mn} F^{mn} + i\overline{\lambda}\Gamma^m D_m \lambda \Big) \,, \tag{1.35}$$

where F_{mn} is the ten-dimensional curvature, $m,n = 0,1,\cdots,9$; λ is a Weyl–Majorana spinor (it is known as a gaugino) with its 8 degrees of freedom matching with those of the ten-dimensional gauge field A_m. The Dirac spinor in ten dimensions has 32 degrees of freedom. This can be reduced to 16 by imposing the Weyl condition (decomposing λ in to chiral and antichiral parts $\lambda_\pm$ by applying the projection operator $\mathbb{P}_\pm$). Imposing the Majorana condition $\lambda = C\overline{\lambda}^T$ on this Weyl spinor further reduces the number of degrees of freedom down to 8. Thus we obtain a Weyl–Majorana spinor with 8 degrees of freedom matching with those of the gauge field.

The action (1.35) is invariant under a set of transformations of the fields, called the supersymmetry transformations

$$\delta_S A_m = i\overline{\alpha}\Gamma_m\lambda \ , \tag{1.36}$$

$$\delta_S \lambda = \Sigma_{mn}F^{mn}\alpha \ , \tag{1.37}$$

where the constant spinor field parameter α is a single Weyl–Majorana spinor parameterizing the supersymmetry transformations. This is referred to as $\mathcal{N}=1$ supersymmetry. In $d=10$, there are 16 real supercharges corresponding to these transformations.

The symbol δ_S stands for the *supersymmetric variation*. For a generic field Φ, it means:

$$\delta_S\Phi = \sum_{a=1}^{16}[\epsilon^a Q_a, \Phi\} \ , \tag{1.38}$$

where Q_a are the sixteen supersymmetries. The symbol $[A,B\}$ denotes the graded commutator $AB - (-1)^{|A||B|}BA$. For a field X, we have $|X| = 1$ when it is fermionic and $|X| = 0$ when it is bosonic.

1.4 Dimensional reduction to four dimensions

We are interested in constructing $\mathcal{N}=4$ SYM theory in four dimensions. To obtain this theory, we dimensionally reduce the ten-dimensional $\mathcal{N}=1$ SYM theory down to four dimensions.

1.4.1 The method of dimensional reduction

Let us consider compactifying one spatial dimension of $\mathbb{R}^{1,(d-1)}$ on a circle of radius R, that is,

$$\mathbb{R}^{1,(d-1)} \longrightarrow \mathbb{R}^{1,(d-2)} \times S^1. \tag{1.39}$$

The coordinates x^m, $m = 0,1,\cdots,(d-1)$ of $\mathbb{R}^{1,(d-1)}$ decompose into x^μ of $\mathbb{R}^{1,(d-2)}$ and the compactified spatial dimension y of S^1. The limit $R \to 0$, in which the compactified dimension shrinks to zero size, is called 'dimensional reduction'. To understand what happens to spacetime fields under this action, we begin with the simplest case of a complex scalar field φ with periodic boundary conditions on S^1. This field has the Fourier expansion:

$$\varphi(x^\mu, y) = \sum_{n\in\mathbb{Z}} \varphi_n(x^\mu)\frac{e^{iny/R}}{\sqrt{2\pi R}} \ . \tag{1.40}$$

The kinetic part of the action for this field becomes:

$$\begin{aligned} S_{KE}^{(d)} &= \int d^d x^m \varphi^\dagger \Big(\Box_{(d)} - m^2 \Big) \varphi \\ &= \int d^{(d-1)} x^\mu \int dy \varphi^\dagger \Big(\Box_{(d-1)} + \frac{\partial^2}{\partial y^2} - m^2 \Big) \varphi \\ &= \int d^{(d-1)} x^\mu \sum_{n \in \mathbb{Z}} \varphi_n^\dagger(x^\mu) \Big(\Box_{(d-1)} - m^2 - \frac{n^2}{R^2} \Big) \varphi_n(x^\mu) \ . \end{aligned} \tag{1.41}$$

The Fourier modes $\varphi_n(x^\mu)$ acquire curvature dependent masses $m^2 + n^2/R^2$. In the limit $R \to 0$, the modes φ_n for $n \neq 0$ become infinitely massive. It would cost an infinite amount of energy to excite such modes, and they therefore decouple from the theory. The only mode that survives in this limit is the zero mode φ_0, with the kinetic action:

$$S_{KE}^{(d-1)} = \int d^{(d-1)} x^\mu \varphi_0^\dagger \Big(\Box_{(d-1)} - m^2 \Big) \varphi_0 \ . \tag{1.42}$$

We can extend the method of dimensional reduction to more than one space dimensions. Consider compactification on a torus $\mathbb{T}^k = S^1 \times S^1 \cdots S^1$, k times, with each circle of radius R. The spacetime becomes:

$$\mathbb{R}^{1,(d-1)} \longrightarrow \mathbb{R}^{1,d-1-k} \times \mathbb{T}^k \ . \tag{1.43}$$

The Lorentz group splits in the following way:

$$SO(1, d-1) \to SO(1, d-1-k) \times \text{isometries on } \mathbb{T}^k \ . \tag{1.44}$$

The representations of the fields also take new forms. The covariant derivative, $D_m = \partial_m + A_m$, acting on the zero mode of a field simply reduces to D_μ for $m = \mu$. The components of the covariant derivative in the reduced directions, D_i for $i = 1, \cdots, k$, acting on a zero mode is just A_i on the mode. The gauge field components in the reduced dimensions, A_i $i = 1, \cdots k$, become a collection of scalar fields.

In the limit $R \to 0$, the isometries on $\mathbb{T}^k$ become the rotations on $\mathbb{R}^k$, and we have the splitting:

$$SO(1, d-1) \to SO(1, d-1-k) \times SO(k) \ . \tag{1.45}$$

A spinor field decomposes into direct sums of representations of $SO(1, d-1-k)$ because of the tensor product structure of the Clifford algebra. The Lorentz group splitting is the same as in (1.45).

1.4.2 From $\mathcal{N} = 1$, $d = 10$ SYM to $\mathcal{N} = 4$, $d = 4$ SYM

Dimensional reduction of ten-dimensional $\mathcal{N} = 1$ SYM theory down to four dimensions leads to an $\mathcal{N} = 4$ SYM with the same number of supersymmetries.

The Lorentz group $SO(1, 9)$ splits according to

$$SO(1, 9) \to SO(1, 3) \times SO(6) \ . \tag{1.46}$$

We will also be using the notation of *Spin* group, the double cover of the Lorentz group, in the later sections. The double cover splits according to

$$Spin(1,9) \to Spin(1,3) \times Spin(6) \approx Spin(1,3) \times SU(4) \ . \tag{1.47}$$

Dimensional reduction of the theory on a six dimensional torus $\mathbb{T}^6$ gives rise to a multiplet of four-dimensional fields possessing an additional $SO(6) \sim SU(4)$ global symmetry. This internal rotational symmetry is known as the R-symmetry, $SO_R(6)$, of the dimensionally reduced theory.

After dimensional reduction, the ten-dimensional gauge field reduces to a four dimensional real vector A_μ, $\mu = 0, 1, 2, 3$, transforming under the $SO(1,3)$ symmetry. The reduced components of the gauge field A_i, $i = 1, 2, \cdots, 6$ become six real scalars. The $SO_R(6)$ becomes an internal symmetry mixing between these scalars. They transform as the second rank complex self-dual **6** of $SU(4)$.

The Clifford algebra splits up as follows:

$$\Gamma_\mu = \gamma_\mu \otimes \mathbb{I}_8, \quad \Gamma_i \approx \gamma_{pq} = \gamma_5 \otimes \begin{pmatrix} 0 & \rho_{pq} \\ \rho^{pq} & 0 \end{pmatrix} \ , \tag{1.48}$$

where γ_μ, $\mu = 0, 1, 2, 3$, are the ordinary 4×4 gamma matrices, and the 4×4 ρ matrices, with $p, q = 1, 2, 3, 4$, are given by

$$(\rho_{pq})_{rs} = \epsilon_{pqrs}, \quad (\rho^{pq})_{rs} = \frac{1}{2}\epsilon^{pqkl}\epsilon_{klrs} \ , \tag{1.49}$$

and the chirality matrix Γ_{11}, in terms of our usual γ_5 is:

$$\Gamma_{11} = \Gamma_0 \cdots \Gamma_9 = \gamma_5 \otimes \mathbb{I}_8 \ . \tag{1.50}$$

Finally, the ten-dimensional charge conjugation matrix is related to the four dimensional matrix C by

$$C_{10} = C \otimes \begin{pmatrix} 0 & \mathbb{I}_4 \\ \mathbb{I}_4 & 0 \end{pmatrix} \ . \tag{1.51}$$

Imposing both Majorana and Weyl conditions on the Dirac spinor results in the structure

$$\lambda = \begin{pmatrix} L\chi^s \\ \\ R\widetilde{\chi}_s \end{pmatrix} \ , \tag{1.52}$$

where $L = \frac{1}{2}(\mathbb{I} + \gamma_5)$ and $R = \frac{1}{2}(\mathbb{I} - \gamma_5)$; $s = 1, 2, 3, 4$; and $\widetilde{\chi}_s = C\overline{\chi}^{sT}$. We have four left-handed and four right-handed (Weyl) spinors.

The spinor index **16** separates into $(\mathbf{2}, \mathbf{4}) + (\overline{\mathbf{2}}, \overline{\mathbf{4}})$ under $SO(1,3) \times SO(6)$. The ten-dimensional spinor becomes four Weyl spinors.

Thus the dimensionally reduced action is

$$\begin{aligned} S \ = \ & \int d^4x \mathrm{Tr} \Big(-\frac{1}{4}F_{\mu\nu}F^{\mu\nu} - \frac{1}{2}D_\mu A_i D^\mu A_i + \frac{1}{4}[A_i, A_j]^2 \Big) \\ & -\frac{i}{2}\mathrm{Tr}\ (\overline{\lambda}\Gamma^\mu D_\mu \lambda + i\overline{\lambda}\Gamma_i[A_i, \lambda]) \ . \end{aligned} \tag{1.53}$$

The supersymmetry transformation laws take the following form after dimensional reduction

$$\delta A_\mu = -i\overline{\alpha}\Gamma_\mu\lambda \ , \tag{1.54}$$

$$\delta A_i = -i\overline{\alpha}\Gamma_i\lambda \ , \tag{1.55}$$

$$\delta\lambda = \Big(\frac{1}{2}F_{\mu\nu}\Gamma^{\mu\nu} + D_\mu A_j\Gamma^{\mu j} + \frac{i}{2}[A_i, A_j]\Gamma^{ij}\Big)\alpha \ . \tag{1.56}$$

Chapter 2

Topological Field Theory

Supersymmetric fields theories naively break supersymmetry when they are discretized on a lattice. Topological field theories provide a crucial insight into establishing the compatibility between SYM theories and lattice discretization. Certain supersymmetric field theories with extended supersymmetries can be discretized on a lattice while preserving at least one supersymmetry. The continuum limit of these discretized theories turn out to have a structure similar to that of topological field theories. In this Chapter we briefly introduce a class of topological field theories and show how their structure is compatible with discretization on the lattice.

As the name suggests, topological field theories are characterized by observables (correlations functions) which depend only on the topology (global features) of the space on which these theories are constructed. The non-dependence on local features implies that the observables of topological field theories are independent of the metric of the space on which they are defined.

The origin of topological field theories goes back to the work of Schwarz and Witten. In 1978, Schwarz showed [6] that Ray-Singer torsion[1] could be represented as the partition function of a certain quantum field theory. In 1982, the work of Witten [7] provided a framework for understanding Morse theory[2] in terms of supersymmetric quantum mechanics. These two field theory constructions represent the prototype of all known topological field theories.

There are two general classes of topological field theories: they are known as Witten and Schwarz type. In Witten type topological field theories, the classical action is trivial (zero or a topological invariant). In Schwarz type theories, classical actions are non-trivial. The prototype example of a Witten type theory is the Donaldson theory[3]; the best known example of Schwarz type theory is the Chern-Simons theory.

[1] Ray-Singer torsion is a particular topological invariant of Riemannian manifolds.

[2] Morse theory is a method to determine the topology of a manifold from the critical points of only one suitable function on the manifold.

[3] Donaldson theory is the study of smooth 4-manifolds using gauge theory techniques.

2.1 Yang–Mills theory and BRST invariance

Let us begin our brief description of topological field theory focusing only on Witten type theory, as only this type eventually leads to a discretization on the lattice.

We look at a conventional nonabelian field theory with gauge symmetry. The best example is Yang–Mills theory in four dimensions. The classical action is a combination of gauge field Lagrangian and Dirac Lagrangian. It is:

$$S_c = \int d^4x \mathrm{Tr} \left(-\frac{1}{4} F_{\mu\nu} F^{\mu\nu} + \overline{\psi}(\Gamma^\mu D_\mu - m)\psi \right) , \tag{2.1}$$

where the trace is over the generators of the gauge group G and the fermion multiplet ψ belongs to an irreducible representation of G. The field strength is:

$$F^A_{\mu\nu} = \partial_\mu A^A_\nu - \partial_\mu A^A_\nu + f^{ABC} A^B_\mu A^C_\nu , \tag{2.2}$$

where f^{ABC} are the structure constants of G. The covariant derivative is defined in terms of the representation matrices T^A by

$$D_\mu = \partial_\mu + A^A_\mu T^A \tag{2.3}$$

The gauge-fixed (quantum) action after Faddeev-Popov gauge-fixing is:

$$S_q = S_c + \int d^4x \mathrm{Tr} \left(\frac{1}{2\xi} (\partial^\mu A^A_\mu)^2 + \overline{c}^A (-\partial^\mu D^{AC}_\mu) c^C \right) , \tag{2.4}$$

where ξ is a gauge parameter, and c and $\overline{c}$ are the Faddeev-Popov ghost and anti-ghost fields.

The Faddeev-Popov ghost fields serve as negative degrees of freedom to cancel the effects of unphysical time-like and longitudinal polarization states of gauge bosons A_μ, and thus make the gauge theory a complete interacting theory.

There is a beautiful formal tool to implement this cancellation, known as the BRST formulation [8, 9].

Let us rewrite the gauge-fixed action by introducing a new commuting scalar field B^A to expose the the symmetry associated with the BRST technique:

$$S_q = S_c + \int d^4x \mathrm{Tr} \left(-\frac{\xi}{2} (B^A)^2 + B^A \partial^\mu A^A_\mu + \overline{c}^A (-\partial^\mu D^{AC}_\mu) c^C \right) . \tag{2.5}$$

The new field B^A is not a normal propagating field, as it has a quadratic term without derivatives. These type of fields, which appear in the functional integral part but have no independent dynamics, are called auxiliary fields. We can eliminate them by using the equations of motion. We could also get rid of the dependence on B by integrating it in a functional integral with a standard Euclidean measure $[dB]$. This would bring us back to (2.4), the Faddeev-Popov gauge-fixed action.

The BRST symmetry has a continuous parameter that is an anticommuting number. Let us denote it by ϵ (we call this the BRST parameter), and consider the following

infinitesimal transformation of the fields in the action:

$$\begin{aligned}
\delta A_\mu^A &= \epsilon D_\mu^{AC} c^C && (2.6)\\
\delta\psi &= i\epsilon c^A T^A \psi && (2.7)\\
\delta c^A &= -\frac{1}{2}\epsilon f^{ABC} c^B c^C && (2.8)\\
\delta\overline{c}^A &= \epsilon B^A && (2.9)\\
\delta B^A &= 0 && (2.10)
\end{aligned}$$

The BRST transformation above is a global symmetry of the gauge-fixed action for any value of the gauge parameter ξ.

The BRST transformation has one more remarkable feature, which is a natural consequence of its anticommuting nature. Let $Q\Phi$ be the BRST transformation of the generic field Φ of the theory:

$$\delta\Phi = \epsilon Q\Phi \ . \tag{2.11}$$

Then the BRST variation of $Q\Phi$ vanishes:

$$Q^2\Phi = 0 \ . \tag{2.12}$$

That is, the BRST operator Q is nilpotent.

The BRST operator gives a precise relation between the unphysical gauge boson polarization states and anti-ghosts as positive and negative degrees of freedom. We can use the principle of BRST symmetry to remove the unphysical gauge boson polarizations in nonabelian gauge theories. The complete quantum action, S_q, which comprises the classical action S_c together with the necessary gauge-fixing and ghost terms, is, by construction, Q-invariant.

The change in gauge field A_μ^A involves the ghost field c^A. In the infinitesimal gauge symmetry (Yang–Mills symmetry), transformation for A_μ^A given by $A_\mu^A \to A_\mu^A - (D_\mu\theta)^A$ we can replace the gauge parameter $-\theta^A$ by the ghost field c^A. That is, gauge-invariant quantities are also BRST-invariant. We also see that all observables are given by BRST-invariant expressions, since all observables in a gauge theory must be gauge-invariant.

With the BRST transformations, we can write:

$$S_q = S_c + \mathcal{Q}\int d^4x \Big[\overline{c}^A\Big(\partial^\mu A_\mu^A - \frac{\xi}{2}B^A\Big)\Big] \ . \tag{2.13}$$

We can show that the vacuum expectation value of $\mathcal{Q}\mathcal{O}$ for any (not necessarily $\mathcal{Q}$ invariant) functional $\mathcal{O}$ is zero. We write:

$$\langle\mathcal{O}\rangle = \int [dA][dc][d\overline{c}]\ \mathcal{O}(A,c,\overline{c})e^{-S_q(A,c,\overline{c})} \ . \tag{2.14}$$

Let us rename the variables of integration in the following way:

$$\begin{aligned}
A_\mu^{A'} &= A_\mu^A + \delta A_\mu^A \ , && (2.15)\\
c^{A'} &= c^A + \delta c^A \ , && (2.16)\\
\overline{c}^{A'} &= \overline{c}^A + \delta\overline{c}^A \ . && (2.17)
\end{aligned}$$

where $\delta = \epsilon\mathcal{Q}$ is the BRST variation with ϵ an arbitrary Grassmann number. The vacuum expectation value of $\mathcal{O}$ becomes:

$$\langle\mathcal{O}\rangle = \int [dA'][dc'][d\overline{c}']\ \mathcal{O}(A', c', \overline{c}')e^{-S_q(A',c',\overline{c}')} \ . \tag{2.18}$$

Assuming that the measure of integration is invariant, which it should be for consistency of the theory, we get the vacuum expectation value of $\mathcal{O}$:

$$\begin{aligned}\langle\mathcal{O}\rangle &= \int [dA][dc][d\overline{c}]\ (\mathcal{O} + \delta\mathcal{O})e^{-S_q - \delta S_q} \ , \\ &= \langle\mathcal{O}\rangle + \langle\delta\mathcal{O}\rangle \ ,\end{aligned} \tag{2.19}$$

since $\delta S_q = 0$. The change $\delta\mathcal{O}$ is the BRST variation of the operator $\mathcal{O}$. We can thus write the above equation as

$$\langle\mathcal{Q}\mathcal{O}\rangle = 0 \ . \tag{2.20}$$

2.2 Introducing topological field theory

Now that we are familiar with the basics of BRST quantization of gauge theories, we can move on to introducing topological field theories. We define a topological field theory as follows [10]:

A topological field theory consists of:

(a.) A collection of fields Φ (which are Grassmann graded) defined on a Riemannian manifold (M, g),

(b.) A nilpotent operator Q, which is odd with respect to the Grassmann grading,

(c.) Physical states defined to be Q-cohomology classes,

(d.) An energy-momentum tensor which is Q-exact, i.e.,

$$T_{\alpha\beta} = QV_{\alpha\beta}(\Phi, g) \ , \tag{2.21}$$

for some functional $V_{\alpha\beta}$ of the fields and the metric.

The collective field content of the theory Φ includes the gauge field, ghosts, and multipliers. The theory has local gauge symmetry, and, as we briefly discussed before in the case of Yang–Mills, we can construct a BRST type operator Q that is nilpotent. We denote the variation of any functional $\mathcal{O}(\Phi)$ as:

$$\delta\mathcal{O} = Q\mathcal{O} \ . \tag{2.22}$$

The physical Hilbert space is defined by the condition:

$$Q\ |\text{phys}\rangle = 0 \ . \tag{2.23}$$

Furthermore, a physical state of the form:

$$|\text{phys}\rangle = |\text{phys}\rangle + Q|\chi\rangle \tag{2.24}$$

is equivalent to $|\text{phys}\rangle$, for any state $|\chi\rangle$. A state is called Q-closed if it is annihilated by Q, while a state is called Q-exact if it is of form $Q|\chi\rangle$. Thus the physical Hilbert space splits into different equivalence classes called *Q-cohomology classes*.

We take Q to be metric independent, which is the simplest situation to deal with, also the best choice of connecting SYM theories with global supersymmetries. For a theory defined on some manifold M, with a metric $g_{\alpha\beta}$, the energy-momentum tensor $T_{\alpha\beta}$ is defined by the change in the action under an infinitesimal deformation of the metric:

$$\delta_g S_q = \frac{1}{2}\int_M d^n x\sqrt{g}\delta g^{\alpha\beta}T_{\alpha\beta} \ . \tag{2.25}$$

We assume that the functional measure in the path integral is both Q-invariant and metric independent.

We now consider the change in the partition function:

$$Z = \int [d\Phi] e^{-S_q} \ , \tag{2.26}$$

under the infinitesimal change in the metric:

$$\begin{aligned}
\delta_g Z &= \int [d\Phi] e^{-S_q}(\delta_g S_q) \ , \\
&= \int [d\Phi] e^{-S_q}\Big(-\frac{1}{2}\int_M d^n x\sqrt{g}\delta g^{\alpha\beta}T_{\alpha\beta}\Big) \ , \\
&= \int [d\Phi] e^{-S_q}\Big(-\frac{1}{2}\int_M d^n x\sqrt{g}\delta g^{\alpha\beta}QV_{\alpha\beta}\Big) \ .
\end{aligned}$$

Let us denote:

$$\chi = -\frac{1}{2}\int_M d^n x\sqrt{g}\delta g^{\alpha\beta}V_{\alpha\beta} \ . \tag{2.27}$$

Thus, we have

$$\delta_g Z = \int [d\Phi] e^{-S_q} Q\chi = \langle Q\chi\rangle = 0 \ . \tag{2.28}$$

Thus, the partition function Z is independent of metric deformations. It depends not on the local structure of the manifold, but only on global properties. That is, Z is a topological invariant.

We can now move on to finding other metric independent correlation functions in the theory. Let us consider the vacuum expectation value of an observable $\mathcal{O}(\Phi)$:

$$\langle\mathcal{O}\rangle = \int [d\Phi] e^{-S_q}\mathcal{O} \ , \tag{2.29}$$

and look for the conditions that are sufficient for this expectation value to be a topological invariant, that is, for $\delta_g\langle\mathcal{O}\rangle$ to be zero.

Proceeding as before, we find:

$$\delta_g\langle\mathcal{O}\rangle = \int [d\Phi] e^{-S_q}(\delta_g\mathcal{O} - \delta_g S_q\cdot\mathcal{O}) \ . \tag{2.30}$$

Assuming that $\mathcal{O}$ enjoys the properties:

$$\delta_g \mathcal{O} = QR \text{ and } Q\mathcal{O} = 0 \ , \tag{2.31}$$

for some R, we have that

$$\delta_g \langle \mathcal{O} \rangle = \langle QR \rangle + \langle \mathcal{Q}(\chi \mathcal{O}) \rangle = 0 \ . \tag{2.32}$$

Now, it is clear that if $\mathcal{O} = Q\mathcal{O}'$, for some $\mathcal{O}'$, we automatically have $\langle \mathcal{O} \rangle = 0$. Thus BRST invariant operators that are not Q-exact are topological invariants if they satisfy the condition $\delta_g \mathcal{O} = QR$.

In the case of Witten type theories, the complete quantum action S_q, which comprises the classical action plus all the necessary gauge-fixing and ghost terms, can be written as a BRST commutator, i.e.,

$$S_q = QV \ , \tag{2.33}$$

for some functional $V(\Phi, g)$ of the fields, and Q is the nilpotent BRST charge.

By using the Q-exact nature of the action, we can prove that the partition function Z and the above class of topological invariant correlators are also exact at the semi-classical level. Let us introduce a dimensionless parameter β to rescale the action $S_q \to \beta S_q$ and then consider the variation of the partition function under a change in β:

$$\begin{aligned} \delta_\beta Z &= -\int [d\Phi] e^{-\beta S_q} S_q \delta\beta \\ &= -\int [d\Phi] e^{-\beta S_q} (QV) \ \delta\beta = 0 \ . \end{aligned} \tag{2.34}$$

This shows that Z is independent of β, as long as β is non-zero[4]. We can evaluate the partition function in the large-β limit. Such a limit corresponds to the semi-classical approximation, in which the path integral is dominated by fluctuations around the classical minima. In Witten type theories, such an approximation is exact. We can also establish the semi-classical exactness of the topologically invariant correlation functions in a similar way.

It should be noted that topological field theories do not admit dynamical excitations. That is, these theories have no propagating degrees of freedom. In Witten type theories, the BRST operator Q plays the role of a supersymmetry charge as well. The classical action for Witten type theories is:

$$S_c = 0 \ , \tag{2.35}$$

or a topological invariant. This action admits a large amount of topological shift symmetry:

$$A_\mu^{A'} = A_\mu^A + \epsilon_\mu^A \ . \tag{2.36}$$

From the structure of the topological shift symmetry, we can see that each bosonic field has a Q-superpartner. We have defined our theory by the requirement that physical states are annihilated by Q. Hence, the superpartners are interpreted as ghosts, leading

[4]Setting β to zero is not allowed, as the path integral requires a damping factor.

to a total of zero degrees of freedom. The energy of any physical state in these theories is zero, and, hence, there are no physical excitations.

Thus, the number of degrees of freedom in a Witten type topological field theory and a conventional supersymmetric field theory are quite different. There are no physical degrees of freedom at all in Witten type theories. This may seem a little strange since from what we have described above topological field theories are also supersymmetric theories in their own right with supersymmetry charge $\mathcal{Q}$. If we think of them as topological field theories, they have to satisfy the requirement that they have no degrees of freedom, while, on the other hand, if we think of them as supersymmetric field theories, we require them to have both bosonic and fermionic states. These two requirements do not contradict with each other if we look at these theories from the point of view of the so-called *twisting* of the supersymmetry. (We will describe the details of twisting in Chapter 3.) In the context of the lattice supersymmetry constructions, we are strongly dependent on this view point.

We can construct topological field theories from SYM theories through the twisting process. The zero degrees of freedom restriction would then be equivalent to a projection to the vacuum states of the supersymmetric gauge theory. Once $\mathcal{Q}$ is chosen, we can change the physical interpretation of the supersymmetric gauge theory in the following way to make it a topological field theory: We restrict our interest to $\mathcal{Q}$-invariant path integrals, observables, and states, and we consider anything of the form $\mathcal{Q}\mathcal{O}$, for any operator $\mathcal{O}$, to be trivial. Thus, the interesting observables or states lie in the cohomology groups of $\mathcal{Q}$. Theories obtained after these restrictions are topological field theories.

Since we will be interested in dynamical excitations of the (twisted) supersymmetric gauge theories, we will not impose these restrictions on path integrals, observables, and states, but treat the theory as merely a twisted version of the original supersymmetric theory that exposes a nilpotent supersymmetry explicitly.

2.3 Constructing a topological field theory

The original construction of topological quantum field theory by Witten [11] showed that Donaldson theory can be realized as a four-dimensional "twisted" $\mathcal{N} = 2$ SYM theory. There are different approaches to deriving the action of Witten's theory and a topological field theory in general. We briefly describe them below. We will be interested in the third method, the method of twisting.

2.3.1 Gauge-fixing topological shift symmetry

Beaulieu and Singer [12], and Brooks, Montano and Sonnenschein [13] noted that Witten's theory can be derived by gauge-fixing the local transformation

$$\delta A_\mu^A = \theta_\mu^A \ , \tag{2.37}$$

where A_μ^A is a gauge field in the adjoint representation. The gauge-fixing has two steps: BRST gauge-fixing to expose fermionic symmetries and Yang–Mills gauge-fixing of the

gauge field. They started with a classical action that is BRST and Yang–Mills gauge-invariant. The set of classical actions that satisfy these conditions are the trivial classical action $S_c = 0$ and actions that are topological invariants (such as the theta term).

The gauge-fixing condition that leads to Witten's theory corresponds to gauge field configurations with vanishing instanton curvature,

$$F^+_{\mu\nu} = F_{\mu\nu} + \widetilde{F}_{\mu\nu} = 0 \ . \tag{2.38}$$

A series of topological gauge-fixing steps generate a set of ghosts and ghost for ghost fields, leading to Witten's $\mathcal{N} = 2$ SYM action in four dimensions [11].

2.3.2 Quantization through Batalin-Vilkovisky procedure

The basic idea here [14] is to regard the instanton equation $F^+_{\mu\nu} = 0$ as arising from a suitable classical action involving a linear combination of the $F^+_{\mu\nu}$ and an auxiliary self-dual field $G_{\mu\nu}$. The equation of motion for $G_{\mu\nu}$ becomes the Langevin equation for the system. This theory has an on-shell reducibility. Quantizing the theory with this on-shell reducibility requires us to make use of the Batalin-Vilkovisky quantization procedure [15]. The result is the quantum action of $\mathcal{N} = 2$, $d = 4$ SYM theory given by Witten [11].

2.3.3 Twisting the supercharges of Yang–Mills theory

There is yet another way to understand the origin of the action given in [11]. This is the most useful way for us in the context of lattice supersymmetry. The motivation here is to obtain the (scalar) BRST supercharge by "twisting" a set of conventional (spinorial) supercharges. After twisting, we obtain an action that bears a formal similarity to that of Witten's four-dimensional $\mathcal{N} = 2$ SYM theory. The twisting procedure can obviously be applied to various classes of SYM theories with extended supersymmetries.

It should be noted that, it is most natural to use Euclidean signature in constructing topological quantum field theories. Twisting of the supersymmetries does not work well in Lorentz signature in any event.

Chapter 3

Twisted Super Yang–Mills Theories

In Chapter 2 we briefly mentioned that we can twist the supersymmetries of SYM theories to derive topological field theories. Since topological field theories are most naturally related to Euclidean signature, we will be focusing on SYM theories on Euclidean spacetime. Our interest in constructing SYM theories on the lattice also require these theories to have a flat Euclidean signature. Although twisting does not work well in Lorentz signature, we can usually return to Lorentz signature, if the theory is constructed on a manifold of type $M = \mathbb{R} \times W$, by simply taking Lorentz signature on $\mathbb{R}$.

We are specifically interested in the method of twisting, as it provides a way of studying a class of SYM theories on a flat Euclidean spacetime lattice. All SYM theories do not admit twisting; only SYM theories with extended supersymmetries ($\mathcal{N} > 1$) undergo twisting. Among the set of extended SYM theories, we focus on a special class of SYM theories that can be *maximally twisted*.

In Chapter 1, we showed that SYM theories can be constructed only in certain spacetime dimensions. The theories we construct in that way are $\mathcal{N} = 1$ SYM theories. We can construct SYM theories with extended supersymmetries through the method of dimensional reduction. In table 3.1, we show how a set of SYM theories with extended supersymmetries can be obtained through the dimensional reduction of a set of $\mathcal{N} = 1$ theories in higher dimensions. Here (a, a) represents left and right-handed supersymmetries.

Theories with extended supersymmetries in d dimensions contain a (Euclidean) spacetime rotation group $SO(d)$ and an R-symmetry group, which we denote by G_R. Supersymmetric theories typically have global chiral symmetries that do not commute with the supercharges. They are called "R-symmetries." These symmetries turn out to play a crucial role in twisting. We are interested in the full twist of the Lorentz group - called *maximal twisting*. Construction of a manifestly supersymmetric d-dimensional Yang–Mills theory through twisting requires the R-symmetry group to contain $SO(d)$ as a subgroup. That is, there should exist a nontrivial homomorphism from the Euclidean Lorentz group $SO(d)_E$ to the R-symmetry group G_R. In table 3.2 we list a set of Eu-

$\mathcal{N}=1,\ d=10$	$\mathcal{N}=1,\ d=6$	$\mathcal{N}=1,\ d=4$
$\downarrow$	$\downarrow$	$\downarrow$
$\mathcal{N}=2,\ d=6$	$\mathcal{N}=2,\ d=4$	$\mathcal{N}=2,\ d=3$
$\downarrow$	$\downarrow$	$\downarrow$
$\mathcal{N}=4,\ d=4$	$\mathcal{N}=4,\ d=3$	$\mathcal{N}=(2,2),\ d=2$
$\downarrow$	$\downarrow$	
$\mathcal{N}=8,\ d=3$	$\mathcal{N}=(4,4),\ d=2$	
$\downarrow$		
$\mathcal{N}=(8,8),\ d=2$		

Table 3.1: Dimensional reduction of a set of $\mathcal{N}=1$ SYM theories and their daughter theories in lower dimensions. Here (a,a) represents left- and right-handed supersymmetries.

Theory	Lorentz symmetry	R-symmetry	Maximal twist
$d=2,\mathcal{N}=2$	$SO(2)$	$SO(2)\times U(1)$	Yes
$d=2,\mathcal{N}=4$	$SO(2)$	$SO(4)\times SU(2)$	Yes
$d=2,\mathcal{N}=8$	$SO(2)$	$SO(8)$	Yes
$d=3,\mathcal{N}=1$	$SO(3)$	$U(1)$	No
$d=3,\mathcal{N}=2$	$SO(3)$	$SO(3)\times SU(2)$	Yes
$d=3,\mathcal{N}=4$	$SO(3)$	$SO(7)$	Yes
$d=4,\mathcal{N}=1$	$SO(4)$	$U(1)$	No
$d=4,\mathcal{N}=2$	$SO(4)$	$SO(2)\times SU(2)$	No
$d=4,\mathcal{N}=4$	$SO(4)$	$SO(6)$	Yes

Table 3.2: Euclidean SYM theories with symmetry groups and possibilities of maximal twist.

clidean SYM theories with their Lorentz and R-symmetries, and the existence of maximal twist in each case.

The constraint on the size of R-symmetry group excludes the (twisted) lattice formulation of some interesting class of theories, such as $\mathcal{N}=2$ SYM (the Seiberg-Witten theory) in four dimensions or generic $\mathcal{N}=1$ supersymmetric QCD theories.

The well known $\mathcal{N}=4$ SYM in four dimensions can be twisted in three different ways [16, 17, 18] but only one of them, introduced by Marcus [18], undergo maximal twisting and, thus, leads to a lattice construction of this theory. The other two twists cannot be implemented on a lattice in a gauge covariant way.

The twists of three-dimensional $\mathcal{N}=4$ and $\mathcal{N}=8$ and two-dimensional $\mathcal{N}=(8,8)$, $\mathcal{N}=(4,4)$ theories are presented by Blau and Thompson [19].

3.1 Twisting in d dimensions

In this section, we briefly review the maximal twists of extended SYM theories in the continuum formulation on $\mathbb{R}^d$. From the list we created above we see that the R-symmetry group possess an $SO(d)_R$ subgroup for six of the theories. The theories that allow maximal twisting have the property:

$$SO(d)_E \times SO(d)_R \subset SO(d)_E \times G_R \ . \tag{3.1}$$

To construct the twisted theory, we embed a new rotation group $SO(d)'$ into the diagonal sum of $SO(d)_E \times SO(d)_R$, and declare this $SO(d)'$ as the new Lorentz symmetry of the theory. This is called the *twisted rotation group*.

The details of twist construction are slightly different in each case. We focus on the general idea of twisting first and then go on to the special cases of interest in later sections. Let us assume that a fermionic field, which is a spacetime spinor, is in the spinor representation of the R-symmetry group $SO(d)_R$ as well[1]. After twisting, the fermions become integer spin representations of the twisted rotation group $SO(d)'$, since the product of two half-integer spins is always an integer spin. The fermions still preserve their Grassmann odd nature, but they are now irreducible antisymmetric tensor fields of the twisted rotation group. They can be expressed as a direct sum of scalars, vectors, anti-symmetric tensors, and other higher p-forms.

The bosons of the theory, Grassmann even fields, transform as vectors $\mathbf{d}$ under the $SO(d)'$ - the gauge bosons V_μ transform as $(\mathbf{d}, \mathbf{1})$, and the scalars B_μ transform as $(\mathbf{1}, \mathbf{d})$ under the $SO(d)_E \times SO(d)_R$. If there are more than d scalars in the untwisted theory (for example, $\mathcal{N} = 4$, $d = 4$ theory has six scalars), they become either 0-forms or d-forms under $SO(d)'$.

It is clear now why we have used the the name maximal twist for this type of twisting. The twisting procedure involves the twisting of the full Lorentz symmetry group instead of twisting a subgroup of it. The four dimensional $\mathcal{N} = 2$ theory can only admit a *half twisting* as its R-symmetry group is not as large as the Lorentz rotation group $SO(4)_E$. The other two theories, $\mathcal{N} = 1$ in $d = 4$ and $\mathcal{N} = 1$ in $d = 3$ do not admit a nontrivial twisting as there is no nontrivial homomorphism from their Euclidean rotation group to their R-symmetry group.

The supersymmetries also take new forms under the twisted rotation group. They also transform like twisted fermions, in integer spin representations of the twisted rotation group. The scalar component $\mathcal{Q}$ of the twisted supersymmetries is nilpotent

$$\mathcal{Q}^2 = 0 \ . \tag{3.2}$$

The twisted superalgebra implies that the momentum P_a is now the Q-variation of something. That is, it is Q-exact. This fact renders it plausible that the entire energy momentum tensor may be Q-exact in twisted theories. This, in turn, implies that the entire action of the theory could be written in a Q-exact form $S = Q\Lambda$. (In some cases, for example, $\mathcal{N} = 4$ in $d = 4$ case, the twisted action is a sum of Q-exact and Q-closed

[1]It is the spin group $Spin(d)$ to be more precise, but using $SO(d)$ will also lead to same results.

terms.) The subalgebra $Q^2 = 0$ of the twisted supersymmetry algebra does not produce any spacetime translations. We can use this fact to carry the twisted theory easily onto the lattice.

On a flat Euclidean spacetime, the twisted theory is merely a rewriting of the physical theory, and, indeed, possesses all supersymmetries of the physical theory. The twisted SYM theory can be made topological by interpreting the scalar supercharge $\mathcal{Q}$ as a BRST operator. Then the observables of the physical theory are restricted only to a set of topological observables, appropriately defined correlators of the twisted operators.

Although the twisted formulation of supersymmetry goes back to Witten [11] in the topological field theory construction of four-dimensional $\mathcal{N} = 2$ SYM theory in the context of Donaldson invariants, this formulation had been anticipated in earlier lattice work using Dirac-Kähler fields [20, 21, 22, 23, 24]. The precise connection between Dirac-Kähler fermions and topological twisting was found by Kawamoto and collaborators [25, 26, 27]. They observed that the 0-form supercharge that arises after twisting is a scalar that squares to zero and constitutes a closed subalgebra of the full twisted superalgebra. It is this scalar supersymmetry that can be made manifest in the lattice action, even at finite lattice spacing [28, 29, 30, 31, 32, 33, 34, 35].

3.2 Twisted $\mathcal{N} = 2$, $d = 2$ SYM theory

We begin with a simple example of the twist construction: the two-dimensional $\mathcal{N} = 2$ SYM theory. This theory can be obtained by the dimensional reduction of four-dimensional $\mathcal{N} = 1$ SYM theory. The global symmetry of the four-dimensional theory:

$$SO(4)_E \times U(1) \ , \tag{3.3}$$

where $SO(4)_E$ is the Euclidean Lorentz symmetry and $U(1)$ is the chiral symmetry, splits in the following way, after dimensional reduction, to become the global symmetry of the two-dimensional theory

$$G = SO(2)_E \times SO(2)_{R_1} \times U(1)_{R_2} \ . \tag{3.4}$$

Here, $SO(2)_E$ is the Euclidean Lorentz symmetry; $SO(2)_{R_1}$ is rotational symmetry along reduced dimensions and $U(1)_{R_2}$ is the chiral $U(1)$ symmetry of the theory. We rewrite the symmetry group of the theory as:

$$SO(2)_E \times SO(2)_{R_1} \times U(1)_{R_2} \sim SO(2)_E \times SO(2)_{R_1} \times SO(2)_{R_2} \ . \tag{3.5}$$

Since the internal symmetry group contains two $SO(2)$'s, we can maximally twist this theory in two ways. They are called the A-model and the B-model twist [36]. In the A-model twist, the twisted rotation is defined as the diagonal $SO(2)$ subgroup of the product of the Lorentz rotation $SO(2)_E$ and the (chiral) $SO(2)_{R_2}$ symmetry. In the B-model twist, the twisted rotation group is the diagonal $SO(2)$ subgroup of the product of the Lorentz rotation $SO(2)_E$ and the (internal) $SO(2)_{R_1}$ symmetry.

We will be focusing on the B-model twist picture (it is also known as *self-dual twist*), since the form of the twisted action resembles that of the orbifold constructions [37, 38, 39, 40], a complementary and equivalent approach to lattice supersymmetry.

The fermions and supersymmetries are now decomposed into integer spin representations of the twisted rotation group - there is a 0-form η, a 1-form ψ_a and a 2-form χ_{ab}:

supercharges:	$\mathcal{Q}$	$\mathcal{Q}_a$	$\mathcal{Q}_{ab}$
fermions:	η	ψ_a	χ_{ab}
number of fields:	1	2	1

Under the twisted symmetry $SO(2)' \times U(1)_{R_2}$, the fermions transform as

$$\eta \oplus \psi_a \oplus \chi_{ab} \longrightarrow \mathbf{1}_{\frac{1}{2}} \oplus \mathbf{2}_{-\frac{1}{2}} \oplus \mathbf{1}_{\frac{1}{2}} \tag{3.6}$$

The gauge field A_a transform as $(\mathbf{2},\mathbf{1})_0$, and the scalars B_a transform as $(\mathbf{1},\mathbf{2})_0$ under the rotation group $SO(2)_E \times SO(2)_{R_1} \times U(1)_{R_2}$. In the new rotation group $SO(2)' \times U(1)_{R_2}$, they transform as $(\mathbf{2})_0$. Naturally we can combine the gauge field and scalars to obtain a complexified gauge field in this type of twist, that is,

$$\mathcal{A}_a = A_a + iB_a \text{ and } \overline{\mathcal{A}}_a = A_a - iB_a. \tag{3.7}$$

Thus, the complexified gauge bosons transform as

$$\mathcal{A}_a \oplus \overline{\mathcal{A}}_a \longrightarrow \mathbf{2}_0 \oplus \mathbf{2}_0 \ . \tag{3.8}$$

3.2.1 Supersymmetry transformations and twisted action

The twisting process produces a nilpotent supercharge $\mathcal{Q}$; it acts on the twisted fields in the following way:

$$\mathcal{Q}\mathcal{A}_a = \psi_a \tag{3.9}$$
$$\mathcal{Q}\psi_a = 0 \tag{3.10}$$
$$\mathcal{Q}\overline{\mathcal{A}}_a = 0 \tag{3.11}$$
$$\mathcal{Q}\chi_{ab} = -\overline{\mathcal{F}}_{ab} \tag{3.12}$$
$$\mathcal{Q}\eta = d \tag{3.13}$$
$$\mathcal{Q}d = 0 \tag{3.14}$$

where d is an auxiliary field introduced for the off-shell completion of the supersymmetry algebra. It has equations of motion:

$$d = [\overline{\mathcal{D}}_a, \mathcal{D}_a] \ . \tag{3.15}$$

The twisted theory has complexified covariant derivatives and field strengths. For a generic field Φ, we have:

$$\mathcal{D}_a\Phi \equiv \partial_a\Phi + [\mathcal{A}_a, \Phi], \quad \overline{\mathcal{D}}_a\Phi \equiv \partial_a\Phi + [\overline{\mathcal{A}}_a, \Phi] \ . \tag{3.16}$$

The field strength takes the form:

$$\mathcal{F}_{ab} = [\mathcal{D}_a, \mathcal{D}_b], \quad \overline{\mathcal{F}}_{ab} = [\overline{\mathcal{D}}_a, \overline{\mathcal{D}}_b] \ . \tag{3.17}$$

The action of the twisted theory can be expressed in a $\mathcal{Q}$-exact form:

$$S = \mathcal{Q}\int d^2x \mathrm{Tr}\ \Lambda \tag{3.18}$$

$$= \mathcal{Q}\int d^2x \mathrm{Tr}\left(\chi_{ab}\mathcal{F}_{ab} + \eta[\overline{\mathcal{D}}_a, \mathcal{D}_a] - \frac{1}{2}\eta d\right) . \tag{3.19}$$

After $\mathcal{Q}$-variation and integrating out the field d yields

$$S = \int d^2x \mathrm{Tr}\left(- \overline{\mathcal{F}}_{ab}\mathcal{F}_{ab} + \frac{1}{2}[\overline{\mathcal{D}}_a, \mathcal{D}_a]^2 - \chi_{ab}\mathcal{D}_{[a}\psi_{b]} - \eta\overline{\mathcal{D}}_a\psi_a\right) . \tag{3.20}$$

The action is $\mathcal{Q}$-invariant by construction

$$\mathcal{Q}S = \mathcal{Q}^2\Lambda = 0 . \tag{3.21}$$

This theory can be made topological by regarding $\mathcal{Q}$ as a BRST charge.

3.2.2 The twisted supersymmetry algebra

The two-dimensional supersymmetry algebra of the untwisted $\mathcal{N}=2$ theory has the form

$$\{Q_{\alpha i}, Q_{\beta j}\} = 2\delta_{ij}\gamma^a_{\alpha\beta}P_a , \tag{3.22}$$

where $Q_{\alpha i}$ is supercharge, the left-indices $\alpha(=1,2)$ and the right-indices $i(=1,2)$ are Lorentz spinor and internal spinor suffixes labeling two different $\mathcal{N}=2$ supercharges, respectively. We can take these operators to be Majorana in two dimensions. P_a is the generator of translation.

The process of twisting leads to the decomposition of the above supercharges with double spinor indices into scalar, vector and pseudo-scalar components:

$$Q_{\alpha i} = (\mathbb{I}\mathcal{Q} + \gamma^a\mathcal{Q}_a + \gamma^5\widetilde{\mathcal{Q}})_{\alpha i}, \quad \widetilde{\mathcal{Q}} = \epsilon_{ab}\mathcal{Q}_{ab} . \tag{3.23}$$

These are the twisted supercharges of the two-dimensional $\mathcal{N}=2$ SYM theory. The supersymmetry relations can be rewritten by the twisted generators in the following form:

$$\{\mathcal{Q}, \mathcal{Q}_a\} = P_a, \quad \{\widetilde{\mathcal{Q}}, \mathcal{Q}_a\} = -\epsilon_{ab}P^b , \tag{3.24}$$

$$\mathcal{Q}^2 = \widetilde{\mathcal{Q}}^2 = \{\mathcal{Q}, \widetilde{\mathcal{Q}}\} = \{\mathcal{Q}_a, \mathcal{Q}_b\} = 0 . \tag{3.25}$$

This is the twisted $\mathcal{N}=d=2$ supersymmetry algebra.

3.2.3 Connection with Dirac-Kähler fermions

The supercharges and fermions become tensorial in their representations as a result of twisting. The twisted fermions appearing in the matrix form (3.23) can be considered as components of a geometrical object called a Dirac-Kähler field [27]

$$\Psi = (\eta, \psi_a, \chi_{ab}) . \tag{3.26}$$

If we take a standard free fermion action for a theory with two degenerate Majorana species and replace the fermions by matrices, we find that the action can be easily written as [27]

$$S_F = \mathrm{Tr}\ \Psi^\dagger \gamma_a \partial_a \Psi \ . \tag{3.27}$$

Expanding the matrices into (real) components $(\eta, \psi_a, \chi_{ab})$ and doing the trace yields

$$S_F = \frac{1}{2}\eta \partial_a \psi_a + \chi_{ab} \partial_{[a} \psi_{b]} \ . \tag{3.28}$$

This geometrical rewriting of the fermionic action yields the so-called Dirac-Kähler action, which is most naturally rewritten using the language of differential forms as [41]

$$S_F = \langle \Psi \cdot (d - d^\dagger)\Psi \rangle \ . \tag{3.29}$$

Here d and $d^\dagger$ are the usual exterior derivative and its adjoint. Their action of d on general rank p-antisymmetric tensors (forms) $\omega_{[\mu_1 \cdots \mu_p]}$ yields a rank $p+1$ tensor with components $\omega_{[\mu_1 \cdots \mu_p \mu_{p+1}]}$ and the square bracket notation indicates complete antisymmetrization between all indices. The dot notation just indicates that corresponding tensor components are multiplied and integrated over space. The operator $d^\dagger$ maps rank p tensors to rank $p-1$. This recasting of the action in geometrical terms not only yields a nilpotent supersymmetry but allows us to discretize the action without inducing fermion doubles [42].

The choice of maximal twisting gives rise to twisted fermions that are just sufficient to saturate a single Dirac-Kähler field [43] and, thus, leads to a lattice construction that does not suffer from the fermion doubling problem.

3.3 Twisted $\mathcal{N} = 4$, $d = 4$ SYM theory

We begin with looking at the symmetries of the ten-dimensional $\mathcal{N} = 1$ SYM theory as the theory we are interested in is obtained by the dimensional reduction of it down to four dimensions. Taking spinors into consideration, the rotational symmetry group of the ten-dimensional theory is $Spin(10)$. The ten-dimensional Dirac spinors are in the spin representations $\mathbb{S}^+$ and $\mathbb{S}^-$ of rank 16. These representations are complex conjugates of each other in Euclidean spacetime. We can define a Euclidean chirality operator Γ^E_{11} in ten dimensions. It acts on the spin representations by a multiplication by $\mp i$. (In (1.24), the chirality operator acts on Lorentz representations of Dirac spinor.), that is,

$$\Gamma^E_{11} \mathbb{S}^\pm = \mp i \ \mathbb{S}^\pm \ . \tag{3.30}$$

If ϵ is the infinitesimal Grassmann valued parameter generating supersymmetry transformations then

$$\Gamma^E_{11} \epsilon = -i\epsilon \ . \tag{3.31}$$

After dimensional reduction, the ten-dimensional Euclidean rotation symmetry group reduces to

$$Spin(10)_E \to Spin(4)_E \times Spin(6)_R \ ,$$

where $Spin(4)_E \sim SU(2) \times SU(2)$ is the four-dimensional rotational symmetry group on $\mathbb{R}^4$ and $Spin(6)_R \sim SU(4)_R$ is the global R-symmetry group of the dimensionally reduced theory.

The ten-dimensional chirality operator also splits into two $\Gamma_{11}^E \to \widehat{\Gamma}^E \widetilde{\Gamma}^E$, where $\widehat{\Gamma}^E$ measures the $Spin(4)$ chirality and $\widetilde{\Gamma}^E$ measures the $Spin(6)$ chirality. Thus, in four dimensions, the chirality condition becomes

$$\Gamma_{11}^E \epsilon = \widehat{\Gamma}^E \widetilde{\Gamma}^E \epsilon \ . \tag{3.32}$$

The complexification of $Spin(4)$ is $SL(2,\mathbb{C}) \times SL(2,\mathbb{C})$ and the two spin representations corresponding to the two eigenvalues of $\widehat{\Gamma}^E$ are $(\mathbf{2},\mathbf{1})$ and $(\mathbf{1},\mathbf{2})$ of $SL(2,\mathbb{C}) \times SL(2,\mathbb{C})$[2]. They are pseudo-real in Euclidean dimensions. The spin representations of $Spin(6)$ are the defining four-dimensional representation $\mathbf{4}$ of $SU(4)_R$ and its dual $\overline{\mathbf{4}}$. Thus, the four-dimensional fermion fields transform under

$$Spin(4) \times Spin(6) \sim SL(2,\mathbb{C}) \times SL(2,\mathbb{C}) \times Spin(6) \tag{3.33}$$

as

$$(\mathbf{2},\mathbf{1},\overline{\mathbf{4}}) \oplus (\mathbf{2},\mathbf{1},\mathbf{4}) \ . \tag{3.34}$$

The supersymmetries also transform the same way under $Spin(4) \times Spin(6)$.

Now we introduce the maximal twisting of this theory. This twist was originally introduced by Marcus [18]. This twist plays a crucial role in the Geometric Langlands program [44] as well.

There is a nontrivial homomorphism from the four-dimensional rotation group $Spin(4)$ to the R-symmetry group $Spin(6)$ of the theory. That means there exists maximal twisting of the theory. We replace the $Spin(4)$ rotation group with a different subgroup $Spin'(4)$ of $Spin(4) \times Spin(6)$. Though the new $Spin'(4)$ group is isomorphic to the original rotational symmetry $Spin(4)$, and acts on $\mathbb{R}^4$ the same way that $Spin(4)$ does, it acts differently on the $\mathcal{N}=4$ gauge theory.

We choose the homomorphism from $Spin(4)$ to $Spin(6)$, such that the action of $Spin'(4)$ on $\mathbb{S}^+$ has a non-zero invariant vector. Since the supersymmetry generator ϵ takes values in $\mathbb{S}^+$ (See (3.30) and (3.31) above), a choice of an invariant vector in $\mathbb{S}^+$ will give us a $Spin'(4)$-invariant supersymmetry. We will call it $\mathcal{Q}$. This is a scalar symmetry under the $Spin'(4)$ group, and it will automatically obey $\mathcal{Q}^2 = 0$.

We describe below how the fields transform under the twisted rotation group. From the twist construction, we want the $\mathbf{4}$ of $Spin(6)$ $(= SU(4)_R)$ to transform as $(\mathbf{2},\mathbf{1}) \oplus (\mathbf{1},\mathbf{2})$ of $Spin(4) (= SU(2) \times SU(2))$. The $\overline{\mathbf{4}}$ of $Spin(6)$, which is the complex conjugate of the $\mathbf{4}$, transforms the same way under $Spin(4)$, since the $(\mathbf{2},\mathbf{1})$ and $(\mathbf{1},\mathbf{2})$ of $Spin(4)$ are pseudo-real.

We can embed the $Spin(4) (= SU(2) \times SU(2))$ in $Spin(6)$ $(= SU(4)_R)$. This embedding commutes with the additional $U(1)$ group. So our embedding is such that the $\mathbf{4}$ of $Spin(6)$ transforms under $SU(2) \times SU(2) \times U(1)$ as $(\mathbf{2},\mathbf{1})^1 \oplus (\mathbf{1},\mathbf{2})^{-1}$. The $\overline{\mathbf{4}}$ transforms as the complex conjugate of this, or $(\mathbf{2},\mathbf{1})^{-1} \oplus (\mathbf{1},\mathbf{2})^1$.

[2]The two-dimensional representation of the first $SL(2,\mathbb{C})$ tensored with the trivial one-dimensional representation of the second $SL(2,\mathbb{C})$ gives $(\mathbf{2},\mathbf{1})$, and vice versa gives $(\mathbf{2},\mathbf{1})$.

We could also use the language of SO groups to describe the twist instead of $Spin$ groups. To do so, we use the fact that the fundamental six-dimensional vector representation $\mathbf{6}$ of $SO(6)$ is, in terms of $Spin(6) = SU(4)_R$, the same as antisymmetric part of $\mathbf{4}\otimes\mathbf{4}$. So $\mathbf{6}$ is the antisymmetric part of $(\mathbf{2},\mathbf{1})^1 \oplus (\mathbf{1},\mathbf{2})^{-1}$, which is $(\mathbf{2},\mathbf{2})^0 \oplus (\mathbf{1},\mathbf{1})^2 \oplus (\mathbf{1},\mathbf{1})^{-2}$. Here $(\mathbf{2},\mathbf{2})$ is the same as the vector representation $\mathbf{4}$ of $SO(4)$. So the $\mathbf{6}$ of $SO(6)$ decomposes into the sum of a vector $\mathbf{4}$ and two scalars of $SO(4)$.

We can likewise analyze how the supersymmetries transform under $Spin'(4)$. The $\overline{\mathbf{4}}$ of $Spin(6)$ transforms as $(\mathbf{2},\mathbf{1})^{-1} \oplus (\mathbf{1},\mathbf{2})^1$ of $Spin'(4)\times U(1)$, and the $\mathbf{4}$ as $(\mathbf{2},\mathbf{1})^1 \oplus (\mathbf{1},\mathbf{2})^{-1}$. So using (3.34)

$$(\mathbf{2},\mathbf{1},\overline{\mathbf{4}}) \oplus (\mathbf{2},\mathbf{1},\mathbf{4}) \ ,$$

the supersymmetries that transform as $(\mathbf{2},\mathbf{1})$ of $Spin(4)$ transform under $Spin'(4)\times U(1)$ as

$$(\mathbf{2},\mathbf{1})^0 \otimes ((\mathbf{2},\mathbf{1})^{-1} \oplus (\mathbf{1},\mathbf{2})^1) = (\mathbf{1},\mathbf{1})^{-1} \oplus (\mathbf{3},\mathbf{1})^{-1} \oplus (\mathbf{2},\mathbf{2})^1 \ , \tag{3.35}$$

and the supersymmetries that transform as $(\mathbf{1},\mathbf{2})$ of $Spin(4)$ transform under $Spin'(4)\times U(1)$ as

$$(\mathbf{1},\mathbf{2})^0 \otimes ((\mathbf{2},\mathbf{1})^{-1} \oplus (\mathbf{1},\mathbf{2})^1) = (\mathbf{1},\mathbf{1})^{-1} \oplus (\mathbf{1},\mathbf{3})^{-1} \oplus (\mathbf{2},\mathbf{2})^1 \ . \tag{3.36}$$

Thus, the supercharges and fermions transform under the new rotation group

$$SU(2)' \times SU(2)' \times U(1)$$

as

$$(\mathbf{1},\mathbf{1})^{-1} \oplus (\mathbf{2},\mathbf{2})^1 \oplus [(\mathbf{3},\mathbf{1}) \oplus (\mathbf{1},\mathbf{3})]^{-1} \oplus (\mathbf{2},\mathbf{2})^1 \oplus (\mathbf{1},\mathbf{1})^{-1} \ , \tag{3.37}$$

or equivalently under the rotation group

$$SO(4)' \times U(1)$$

as

$$\mathbf{1}^{-1} \oplus \mathbf{4}^1 \oplus \mathbf{6}^{-1} \oplus \mathbf{4}^1 \oplus \mathbf{1}^{-1} \ . \tag{3.38}$$

As a result of this choice of embedding, the twisted theory contains supersymmetries and fermions in integer spin representations. They transform as scalars, vectors and higher rank p-form tensors:

supercharges:	$\mathcal{Q}$	$\mathcal{Q}_\mu$	$\mathcal{Q}_{\mu\nu}$	$\bar{\mathcal{Q}}_\mu$	$\bar{\mathcal{Q}}$
fermions:	η	ψ_μ	$\chi_{\mu\nu}$	$\bar{\psi}_\mu$	$\bar{\eta}$
number of fields:	1	4	6	4	1

The four gauge bosons transform as $(\mathbf{2},\mathbf{2})^0$ under the twisted rotation group. We label them as a vector field A_μ. Similarly, four of the six scalars of the theory are now elevated to the same footing as the gauge bosons; they also transform as $(\mathbf{2},\mathbf{2})^0$ under the twisted rotation group. We label them as a vector field B_μ. The two other scalars remain as singlets under the twisted rotation group. We label them by ϕ and $\bar{\phi}$. Thus the bosons of the twisted theory transform as:

$$SU(2)' \times SU(2)' \times U(1) \to (\mathbf{1},\mathbf{1})^1 \oplus (\mathbf{2},\mathbf{2})^0 \oplus (\mathbf{2},\mathbf{2})^0 \oplus (\mathbf{1},\mathbf{1})^{-1} \ , \tag{3.39}$$

or equivalently

$$SO(4)' \times U(1) \to \mathbf{1}^1 \oplus \mathbf{4}^0 \oplus \mathbf{4}^0 \oplus \mathbf{1}^{-1} \ . \tag{3.40}$$

We parametrize the bosonic field content of the theory by

bosons:	ϕ	A_μ	B_μ	$\bar{\phi}$
number of fields:	1	4	4	1

3.3.1 Supersymmetry transformations and twisted action

The two vector fields A_μ and B_μ of the twisted $\mathcal{N}=4$, $d=4$ theory transform the same way under the twisted rotation group. We can describe the twisted theory in a compact way if we combine the vector fields into a complex vector field $\mathcal{A}_\mu$ [18]:

$$\mathcal{A}_\mu \equiv A_\mu + iB_\mu \ , \tag{3.41}$$
$$\overline{\mathcal{A}}_\mu \equiv A_\mu - iB_\mu \ . \tag{3.42}$$

We can now define three covariant derivatives and field strengths[3] using these connections:

$$D_\mu \cdot \equiv \partial_\mu + [A_\mu, \ \cdot \ ], \quad F_{\mu\nu} \equiv [D_\mu, D_\nu] \ , \tag{3.43}$$
$$\mathcal{D}_\mu \cdot \equiv \partial_\mu + [\mathcal{A}_\mu, \ \cdot \ ], \quad \mathcal{F}_{\mu\nu} \equiv [\mathcal{D}_\mu, \mathcal{D}_\nu] \ , \tag{3.44}$$
$$\overline{\mathcal{D}}_\mu \cdot \equiv \partial_\mu + [\overline{\mathcal{A}}_\mu, \ \cdot \ ], \quad \overline{\mathcal{F}}_{\mu\nu} \equiv [\overline{\mathcal{D}}_\mu, \overline{\mathcal{D}}_\nu] \ . \tag{3.45}$$

We will go one more step further to make contact with the lattice construction. We assemble the complexified gauge fields and the two scalar fields into a single five-component complexified connection:

$$\mathcal{A}_a = \Big(\mathcal{A}_\mu \equiv A_\mu + iB_\mu, \ \ \mathcal{A}_5 \equiv A_5 + iB_5\Big) \ , \quad a = 1, \cdots, 5 \ ; \mu = 1, \cdots, 4 \tag{3.46}$$

where the fifth component $\mathcal{A}_5 = \phi$ and $\overline{\mathcal{A}}_5 = \overline{\phi}$. Correspondingly, we package the fermions in the $SU(5)\times U(1)$ representation (which is a subgroup of $SO(10)$, the Lorentz symmetry group of the ten-dimensional theory) - they become five-dimensional scalar, vector and antisymmetric tensors $(\eta, \psi_a, \chi_{ab})$. The original twisted theory will then be obtained by simple dimensional reduction of a theory in five dimensions. A similar language arises in the orbifold construction of this theory [40] where the fermions and bosons transform in the representations of $SU(5) \times U(1)$:

bosons:	$\mathbf{10}$	$\rightarrow$	$\mathbf{5} \oplus \overline{\mathbf{5}}$
fermions:	$\mathbf{16}$	$\rightarrow$	$\mathbf{1} \oplus \mathbf{5} \oplus \overline{\mathbf{10}}$

In addition to these fields, we introduce one auxiliary bosonic scalar field d for off-shell completion of the scalar supersymmetry.

The nilpotent scalar supersymmetry $\mathcal{Q}$ now acts on these fields in a simple manner

$$\mathcal{Q}\mathcal{A}_a = \psi_a \tag{3.47}$$
$$\mathcal{Q}\psi_a = 0 \tag{3.48}$$
$$\mathcal{Q}\overline{\mathcal{A}}_a = 0 \tag{3.49}$$
$$\mathcal{Q}\chi_{ab} = -\overline{\mathcal{F}}_{ab} \tag{3.50}$$
$$\mathcal{Q}\eta = d \tag{3.51}$$
$$\mathcal{Q}d = 0 \tag{3.52}$$

[3] We employ an anti-hermitian basis for the generators $U(N)$.

The action of the twisted theory can now be expressed in a compact five-dimensional form, as a linear combination of $\mathcal{Q}$-exact and $\mathcal{Q}$-closed terms:

$$S = \mathcal{Q}\Lambda + S_{\mathcal{Q}-\text{closed}} \ , \tag{3.53}$$

where

$$\Lambda = \int \text{Tr} \left(\chi_{ab}\mathcal{F}_{ab} + \eta[\overline{\mathcal{D}}_a, \mathcal{D}_a] - \frac{1}{2}\eta d \right) , \tag{3.54}$$

and

$$S_{\mathcal{Q}-\text{closed}} = -\frac{1}{2}\int \ \text{Tr}\ \epsilon_{abcde}\chi_{de}\overline{\mathcal{D}}_c\chi_{ab} \ . \tag{3.55}$$

The invariance of the $\mathcal{Q}$-closed term is a result of the Bianchi identity (or Jacobi identity for covariant derivatives)

$$\epsilon_{abcde}\overline{\mathcal{D}}_c\overline{\mathcal{F}}_{de} = \epsilon_{abcde}[\overline{\mathcal{D}}_c, [\overline{\mathcal{D}}_d, \overline{\mathcal{D}}_e]] = 0 \ . \tag{3.56}$$

Carrying out the $\mathcal{Q}$-variation and subsequently eliminating the auxiliary field d using the equation of motion, we can write down the action in terms of the propagating fields:

$$\begin{aligned} S \ = \ \int \text{Tr} \Big(& - \overline{\mathcal{F}}_{ab}\mathcal{F}_{ab} + \frac{1}{2}[\overline{\mathcal{D}}_a, \mathcal{D}_a]^2 - \chi_{ab}\mathcal{D}_{[a}\psi_{b]} - \eta\overline{\mathcal{D}}_a\psi_a \\ & - \frac{1}{2}\epsilon_{abcde}\chi_{de}\overline{\mathcal{D}}_c\chi_{ab}\Big). \end{aligned} \tag{3.57}$$

We can obtain the twisted theory in four dimensions by dimensional reduction of this theory along the 5th direction. We write down the decomposition of five-dimensional fields into four-dimensional fields as follows

$$\mathcal{A}_a \ \rightarrow \ \mathcal{A}_\mu \oplus \phi \tag{3.58}$$

$$\mathcal{F}_{ab} \ \rightarrow \ \mathcal{F}_{\mu\nu} \oplus \mathcal{D}_\mu\phi \tag{3.59}$$

$$[\overline{\mathcal{D}}_a, \mathcal{D}_a] \ \rightarrow \ [\overline{\mathcal{D}}_\mu, \mathcal{D}_\mu] \oplus [\overline{\phi}, \phi] \tag{3.60}$$

$$\psi_a \ \rightarrow \ \psi_\mu \oplus \overline{\eta} \tag{3.61}$$

$$\chi_{ab} \ \rightarrow \ \chi_{\mu\nu} \oplus \overline{\psi}_\mu \tag{3.62}$$

The action (5.6), after dimensional reduction, yields:

$$\begin{aligned} S \ = \ \int \text{Tr} \Big(& - \mathcal{F}_{\mu\nu}\mathcal{F}_{\mu\nu} + \frac{1}{2}[\overline{\mathcal{D}}_\mu, \mathcal{D}_\mu]^2 + \frac{1}{2}[\overline{\phi}, \phi]^2 + (\overline{\mathcal{D}}_\mu\overline{\phi})(\mathcal{D}_\mu\phi) - \chi_{\mu\nu}\mathcal{D}_{[\mu}\psi_{\nu]} \\ & - \overline{\psi}_\mu\mathcal{D}_\mu\overline{\eta} - \overline{\psi}[\phi, \psi_\mu] - \eta\overline{\mathcal{D}}_\mu\psi_\mu - \eta[\overline{\phi}, \overline{\eta}] - \chi^*_{\mu\nu}\overline{\mathcal{D}}_\mu\overline{\psi}_\nu - \frac{1}{2}\chi^*_{\mu\nu}[\overline{\phi}, \chi_{\mu\nu}]\Big), \end{aligned} \tag{3.63}$$

where the last two terms arise from the dimensional reduction of the $\mathcal{Q}$-closed term with χ^*, the Hodge dual of χ, defined as $\chi^*_{\mu\nu} = \frac{1}{2}\epsilon_{\mu\nu\rho\lambda}\chi_{\rho\lambda}$ and $\overline{\psi}_\mu = \frac{1}{2}\chi_{5\mu}$.

The twisted supersymmetry transformations take the following form after dimensional reduction to four dimensions:

$$\begin{aligned} & \mathcal{Q}\mathcal{A}_\mu = \psi_\mu, \quad \mathcal{Q}\psi_\mu = 0 \\ & \mathcal{Q}\overline{\mathcal{A}}_\mu = 0, \quad \mathcal{Q}\chi_{\mu\nu} = -\overline{\mathcal{F}}_{\mu\nu} \\ & \mathcal{Q}\eta = d, \quad \mathcal{Q}d = 0, \quad \mathcal{Q}\phi = \overline{\eta} \\ & \mathcal{Q}\overline{\eta} = 0, \quad \mathcal{Q}\overline{\psi}_\mu = \overline{\mathcal{D}}_\mu\phi \\ & \mathcal{Q}\overline{\phi} = 0 \end{aligned} \tag{3.64}$$

Chapter 4

Supersymmetric Lattices

Supersymmetric field theories resisted discretization on the lattice for a long time since they were discovered. The central part of the difficulty is that naive discretizations of continuum supersymmetric field theories break supersymmetry completely, and radiative effects lead to a profusion of relevant supersymmetry breaking counterterms in the renormalized lattice action. In order to arrive at a supersymmetric theory in the continuum limit, the coefficients to these counterterms must be carefully fine tuned as the lattice spacing is sent to zero. This fine tuning process turned out to be both unnatural and practically impossible in most of the cases. We can easily identify the problem with discretization just by looking at the supersymmetry algebra. It naively breaks on the lattice. There are no infinitesimal translation generators on a discrete spacetime so that the algebra $\{Q, \overline{Q}\} = \gamma_a P_a$ is already broken at the classical level. An equivalent way to realize this difficulty is looking at the supersymmetry variation on the lattice. A naive supersymmetry variation of a naively discretized supersymmetric theory fails to yield zero as a consequence of the failure of the Leibniz rule when applied to lattice difference operators.

At present we have a new set of theoretical tools and ideas to construct a family of lattice models that retain exactly some of the continuum supersymmetry at non-zero lattice spacing. The basic idea is to maintain a particular subalgebra of the full supersymmetry algebra in the lattice theory. The hope is that this exact symmetry will constrain the effective lattice action and protect the theory from dangerous supersymmetry violating counterterms. The resultant supersymmetric lattice theories are local and free of doublers, and, in the case of Yang-Mills theories, also possess exact gauge-invariance. In principle, they form the basis for a truly non-perturbative definition of the continuum supersymmetric field theory.

Having a lattice formulation of supersymmetric gauge theories is very advantageous, as it opens up a large arena of theoretical and numerical investigations. For example, the availability of a supersymmetric lattice construction for the four dimensional $\mathcal{N} = 4$ SYM theory is clearly very exciting from the point of view of exploring the connection

between gauge theories and string/gravitational theories. The lattice formulation of this theory is important in its own right, even without the connection to string theory – it provides a non-perturbative formulation of a supersymmetric theory.

The geometric structure of twisted SYM theories allows them to be easily transported onto the lattice. The fermions manifest themselves in integer spin representations of the twisted rotation group. They carry the structure of anti-symmetric tensor fields. They also fill out the right number of ingredients to build a single Dirac-Kähler field. Such a construction suitably evades the fermion doubling problem on the lattice. The nilpotent supercharge exposed by the process of twisting does not generate translations. This property makes the twisted theory to be discretized keeping the nilpotent scalar supersymmetry unbroken. All these unique features make the twisted continuum theory well qualified to undergo discretization. We follow a geometric discretization scheme to construct lattice versions of the twisted SYM theories [45, 46, 42, 47, 29, 48] and it is detailed below.

4.1 Geometric structure of continuum and lattice action

We begin the description of the lattice formulation by looking at the general structure of the continuum gauge theory. The bosonic and fermionic fields are in integer spin representations of the twisted rotation group. The fermions are p-forms, that is, they are tensor fields in general. We take the gauge group to be $U(N)$ and represent all the fields in the adjoint representation of this gauge group. The continuum action, defined on a d-dimensional flat Euclidean spacetime has the following properties.

The action is Lorentz invariant, and it consists of complex covariant derivatives $\mathcal{D}_a$ and $\overline{\mathcal{D}}_a$ associated with a complex (not hermitian) connection $\mathcal{A}_a$ and its complex conjugate $\overline{\mathcal{A}}_a$, respectively, and a set of (bosonic and/or fermionic) tensor fields, $\{f^{(\pm)}_{a_1\cdots a_p}\}$, that is,

$$S_{\rm cont} = S_{\rm cont}\Big(\mathcal{D}_a, \overline{\mathcal{D}}_a, \{f^{(\pm)}_{a_1\cdots a_p}\}\Big) \ . \tag{4.1}$$

The covariant derivatives can act on the tensor fields in a curl-like or a divergence-like operation. The curl-like operation gives

$$\begin{aligned} \mathcal{D}_a\{f^{(\pm)}_{a_1\cdots a_p}(x)\} &= \partial_a\{f^{(\pm)}_{a_1\cdots a_p}(x)\} + [\mathcal{A}_a(x), \{f^{(\pm)}_{a_1\cdots a_p}(x)\}] \ , & (4.2)\\ \overline{\mathcal{D}}_a\{f^{(\pm)}_{a_1\cdots a_p}(x)\} &= \partial_a\{f^{(\pm)}_{a_1\cdots a_p}(x)\} + [\overline{\mathcal{A}}_a(x), \{f^{(\pm)}_{a_1\cdots a_p}(x)\}] \ , & (4.3)\end{aligned}$$

while the divergence-like operation gives

$$\begin{aligned} \mathcal{D}_{a_i}\{f^{(-)}_{a_1\cdots a_p}(x)\} &= \partial_{a_i}\{f^{(-)}_{a_1\cdots a_p}(x)\} + [\mathcal{A}_{a_i}(x), \{f^{(-)}_{a_1\cdots a_p}(x)\}] \ , & (4.4)\\ \overline{\mathcal{D}}_{a_i}\{f^{(+)}_{a_1\cdots a_p}(x)\} &= \partial_{a_i}\{f^{(+)}_{a_1\cdots a_p}(x)\} + [\overline{\mathcal{A}}_{a_i}(x), \{f^{(+)}_{a_1\cdots a_p}(x)\}] \ , & (4.5)\end{aligned}$$

where $(1 \le i \le p)$.

We choose a hypercubic abstract lattice to write down the lattice versions of the SYM theories[1]. The p-form fields are mapped to lattice fields living on p-cells of the lattice. The p-cell lattice field can have two possible orientations. This orientation is physical and determines how the lattice fields are gauge rotated on the lattice. So we need to choose an orientation that respects gauge symmetry on the lattice. We choose the fields to be positively oriented, that is, the orientation of the field corresponds to the one in which the link vector has positive components with respect to the coordinate basis.

We replace the complexified connections $\mathcal{A}_a$ and $\overline{\mathcal{A}}_a$ with the following link fields on the lattice:

$$\mathcal{A}_a(x) \;\to\; e^{\mathcal{A}_a(\boldsymbol{n})} \equiv \mathcal{U}_a(\boldsymbol{n}) \;, \tag{4.6}$$

$$\overline{\mathcal{A}}_a(x) \;\to\; e^{\overline{\mathcal{A}}_a(\boldsymbol{n})} \equiv \overline{\mathcal{U}}_a(\boldsymbol{n}) \;, \tag{4.7}$$

where $\boldsymbol{n}$ denotes the integer valued lattice site.

The lattice action contains a set of site, link and p-form fields:

$$S_{\text{latt}} = S_{\text{latt}}\Big(\mathcal{U}_a(\boldsymbol{n}), \overline{\mathcal{U}}_a(\boldsymbol{n}), \{f^{(\pm)}_{a_1\cdots a_p}(\boldsymbol{n})\}\Big) \;. \tag{4.8}$$

The fields on the lattice can be regarded as variables living on orientable links. As a result of this prescription the lattice variables $\mathcal{U}_a(\boldsymbol{n})$, $\overline{\mathcal{U}}_a(\boldsymbol{n})$, $\{f^{(+)}_{a_1\cdots a_p}(\boldsymbol{n})\}$, $\{f^{(-)}_{a_1\cdots a_p}(\boldsymbol{n})\}$ live on links $(\boldsymbol{n}, \boldsymbol{n}+\widehat{\boldsymbol{\mu}}_a)$, $(\boldsymbol{n}+\widehat{\boldsymbol{\mu}}_a, \boldsymbol{n})$, $(\boldsymbol{n}, \boldsymbol{n}+\widehat{\boldsymbol{\mu}}_{a_1}+\cdots+\widehat{\boldsymbol{\mu}}_{a_p})$ and $(\boldsymbol{n}+\widehat{\boldsymbol{\mu}}_{a_1}+\cdots+\widehat{\boldsymbol{\mu}}_{a_p}, \boldsymbol{n})$ respectively. A site variable $\eta(\boldsymbol{n})$ lives on a link $(\boldsymbol{n}, \boldsymbol{n})$.

For $G(\boldsymbol{n}) \in U(N)$, the lattice variables translate under the gauge transformations in the following way:

$$\mathcal{U}_a(\boldsymbol{n}) \;\to\; G(\boldsymbol{n})\mathcal{U}_a(\boldsymbol{n})G^\dagger(\boldsymbol{n}+\widehat{\boldsymbol{\mu}}_a) \tag{4.9}$$

$$\overline{\mathcal{U}}_a(\boldsymbol{n}) \;\to\; G(\boldsymbol{n}+\widehat{\boldsymbol{\mu}}_a)\overline{\mathcal{U}}_a(\boldsymbol{n})G^\dagger(\boldsymbol{n}) \tag{4.10}$$

$$\{f^{(+)}_{a_1\cdots a_p}(\boldsymbol{n})\} \;\to\; G(\boldsymbol{n})\{f^{(+)}_{a_1\cdots a_p}(\boldsymbol{n})\}G^\dagger(\boldsymbol{n}+\widehat{\boldsymbol{\mu}}_{a_1}+\cdots+\widehat{\boldsymbol{\mu}}_{a_p}) \tag{4.11}$$

$$\{f^{(-)}_{a_1\cdots a_p}(\boldsymbol{n})\} \;\to\; G(\boldsymbol{n}+\widehat{\boldsymbol{\mu}}_{a_1}+\cdots+\widehat{\boldsymbol{\mu}}_{a_p})\{f^{(-)}_{a_1\cdots a_p}(\boldsymbol{n})\}G^\dagger(\boldsymbol{n}) \tag{4.12}$$

Notice that these transformations respect the p-cell and orientation assignments of lattice fields.

The covariant derivatives $\mathcal{D}_a$ ($\overline{\mathcal{D}}_a$) in the continuum become forward and backward covariant differences $\mathcal{D}^{(+)}_a$ ($\overline{\mathcal{D}}^{(+)}_a$) and $\mathcal{D}^{(-)}_a$ ($\overline{\mathcal{D}}^{(-)}_a$), respectively. They act on the lattice fields $f^{(\pm)}_{a_1\cdots a_p}(\boldsymbol{n})$ in the following way:

$$\mathcal{D}^{(+)}_b f^{(+)}_{a_1\cdots a_p}(\boldsymbol{n}) \equiv \mathcal{U}_b(\boldsymbol{n})f^{(+)}_{a_1\cdots a_p}(\boldsymbol{n}+\widehat{\boldsymbol{\mu}}_b) - f^{(+)}_{a_1\cdots a_p}(\boldsymbol{n})\mathcal{U}_b(\boldsymbol{n}+\widehat{\boldsymbol{\mu}}) \tag{4.13}$$

$$\mathcal{D}^{(+)}_b f^{(-)}_{a_1\cdots a_p}(\boldsymbol{n}) \equiv \mathcal{U}_b(\boldsymbol{n}+\widehat{\boldsymbol{\mu}})f^{(-)}_{a_1\cdots a_p}(\boldsymbol{n}+\widehat{\boldsymbol{\mu}}_b) - f^{(-)}_{a_1\cdots a_p}(\boldsymbol{n})\mathcal{U}_b(\boldsymbol{n}) \tag{4.14}$$

$$\overline{\mathcal{D}}^{(+)}_b f^{(+)}_{a_1\cdots a_p}(\boldsymbol{n}) \equiv f^{(+)}_{a_1\cdots a_p}(\boldsymbol{n}+\widehat{\boldsymbol{\mu}}_b)\overline{\mathcal{U}}_b(\boldsymbol{n}+\widehat{\boldsymbol{\mu}}) - \overline{\mathcal{U}}_b(\boldsymbol{n})f^{(+)}_{a_1\cdots a_p}(\boldsymbol{n}) \tag{4.15}$$

$$\overline{\mathcal{D}}^{(+)}_b f^{(-)}_{a_1\cdots a_p}(\boldsymbol{n}) \equiv f^{(-)}_{a_1\cdots a_p}(\boldsymbol{n}+\widehat{\boldsymbol{\mu}}_b)\overline{\mathcal{U}}_b(\boldsymbol{n}) - \overline{\mathcal{U}}_b(\boldsymbol{n}+\widehat{\boldsymbol{\mu}})f^{(-)}_{a_1\cdots a_p}(\boldsymbol{n}) \tag{4.16}$$

where we have defined $\widehat{\boldsymbol{\mu}} = \sum_{i=1}^{p} \widehat{\boldsymbol{\mu}}_{a_i}$.

[1]Later we will see that there are more exotic lattice choices that expose the maximum amount of symmetry and thus impose stronger constraints on the counterterms on the lattice. We can write down a set of transformation rules that connects the basis vectors of such lattices with those of the hypercubic lattice.

4.1.1 Prescription for discretization

Thus, from a given continuum twisted action in d dimensions, we can construct the lattice action using the following prescription for discretization.

(i.) For complexified gauge bosons in the continuum $\mathcal{A}_a(x)$ and $\overline{\mathcal{A}}_a(x)$, we introduce lattice link fields $\mathcal{U}_a(\boldsymbol{n}) = e^{\mathcal{A}_a(\boldsymbol{n})}$ and $\overline{\mathcal{U}}_a(\boldsymbol{n}) = e^{\overline{\mathcal{A}}_a(\boldsymbol{n})}$.

(ii.) A continuum p-form field will be mapped to a corresponding lattice p-form field associated with a p-dimensional hypercubic lattice. The lattice site $(\boldsymbol{n})$ is spanned by the (positively oriented) unit vectors $\{\widehat{\boldsymbol{\mu}}_{a_1} \cdots \widehat{\boldsymbol{\mu}}_{a_p}\}$. The continuum fields become link variables and live on oriented links. The continuum complex covariant derivatives $\mathcal{D}_a$ and $\overline{\mathcal{D}}_a$ become link variables $\mathcal{U}_a(\boldsymbol{n})$ and $\overline{\mathcal{U}}_a(\boldsymbol{n})$, and they live on the links $(\boldsymbol{n}, \boldsymbol{n}+\widehat{\boldsymbol{\mu}}_a)$ and $(\boldsymbol{n}+\widehat{\boldsymbol{\mu}}_a, \boldsymbol{n})$, respectively. The tensor fields $f^{(+)}_{a_1\cdots a_p}(x)$ and $f^{(-)}_{a_1\cdots a_p}(x)$ become lattice variables $f^{(\pm)}_{a_1\cdots a_p}(\boldsymbol{n})$ living on links $(\boldsymbol{n}, \boldsymbol{n}+\widehat{\boldsymbol{\mu}}_{a_1}+\cdots+\widehat{\boldsymbol{\mu}}_{a_p})$ and $(\boldsymbol{n}+\widehat{\boldsymbol{\mu}}_{a_1}+\cdots+\widehat{\boldsymbol{\mu}}_{a_p}, \boldsymbol{n})$, respectively.

(iii.) The gauge transformations of lattice variables are given in (4.9)-(4.12).

(iv.) The curl-like complex covariant derivatives become forward covariant differences given in (4.2)-(4.3).

(v.) The divergence-like complex covariant derivatives become backward covariant differences given in (4.4)-(4.5).

4.2 Two-dimensional lattice $\mathcal{N} = 2$ SYM theory

As a result of the geometrical discretization prescription the two-dimensional $\mathcal{N} = 2$ lattice SYM theory lives on a two-dimensional square lattice spanned by two orthogonal basis vectors. The fermionic and bosonic fields live on sites, links and body diagonal of the lattice unit cell.

The lattice covariant forward difference operator $\mathcal{D}^{(+)}_a$ acts on the lattice scalar and vector fields in the following way:

$$\mathcal{D}^{(+)}_a f(\boldsymbol{n}) = \mathcal{U}_a(\boldsymbol{n}) f(\boldsymbol{n}+\widehat{\boldsymbol{\mu}}_a) - f(\boldsymbol{n})\mathcal{U}_a(\boldsymbol{n}) \ , \tag{4.17}$$

$$\mathcal{D}^{(+)}_a f_b(\boldsymbol{n}) = \mathcal{U}_a(\boldsymbol{n}) f_b(\boldsymbol{n}+\widehat{\boldsymbol{\mu}}_a) - f_b(\boldsymbol{n})\mathcal{U}_a(\boldsymbol{n}+\widehat{\boldsymbol{\mu}}_b) \ , \tag{4.18}$$

where $\widehat{\boldsymbol{\mu}}_a$ is the unit vector along the $\boldsymbol{a}$ direction; there are two unit vectors: $(\widehat{\boldsymbol{\mu}}_1, \widehat{\boldsymbol{\mu}}_2)$. We have replaced the continuum complex gauge fields $\mathcal{A}_a$ by non-unitary link fields $\mathcal{U}_a = e^{\mathcal{A}_a}$.

The lattice covariant backward difference operator $\overline{\mathcal{D}}^{(-)}_a$ replaces the continuum covariant derivative in divergence-like operations and its action on (positively oriented) lattice vector fields can be obtained by requiring that it to be the adjoint to $\mathcal{D}^{(+)}_a$. Thus, its action on lattice vectors is

$$\overline{\mathcal{D}}^{(-)}_a f_a(\boldsymbol{n}) = f_a(\boldsymbol{n})\overline{\mathcal{U}}_a(\boldsymbol{n}) - \overline{\mathcal{U}}_a(\boldsymbol{n}-\widehat{\boldsymbol{\mu}}_a) f_a(\boldsymbol{n}-\widehat{\boldsymbol{\mu}}_a) \ . \tag{4.19}$$

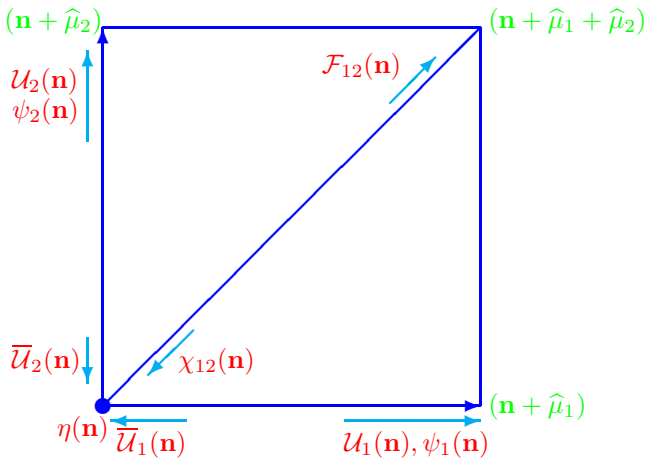

Figure 4.1: Orientations of twisted fields on a two-dimensional lattice.

The nilpotent scalar supersymmetry acts on the lattice fields in the following way:

$$\begin{aligned}
\mathcal{Q}\mathcal{U}_a(\boldsymbol{n}) &= \psi_a(\boldsymbol{n}) && (4.20)\\
\mathcal{Q}\psi_a(\boldsymbol{n}) &= 0 && (4.21)\\
\mathcal{Q}\overline{\mathcal{U}}_a(\boldsymbol{n}) &= 0 && (4.22)\\
\mathcal{Q}\chi_{ab}(\boldsymbol{n}) &= \mathcal{F}^{\dagger}_{ab}(\boldsymbol{n}) && (4.23)\\
\mathcal{Q}\eta(\boldsymbol{n}) &= d(\boldsymbol{n}) && (4.24)\\
\mathcal{Q}d(\boldsymbol{n}) &= 0 && (4.25)
\end{aligned}$$

The lattice field strength can be written as:

$$\mathcal{F}_{ab}(\boldsymbol{n}) = \mathcal{D}^{(+)}_a\mathcal{U}_b(\boldsymbol{n}) = \mathcal{U}_a(\boldsymbol{n})\mathcal{U}_b(\boldsymbol{n}+\widehat{\boldsymbol{\mu}}_a) - \mathcal{U}_b(\boldsymbol{n})\mathcal{U}_a(\boldsymbol{n}+\widehat{\boldsymbol{\mu}}_b)\ . \tag{4.26}$$

It reduces to the continuum (complex) field strength in the naive continuum limit and is automatically antisymmetric in the indices.

The supersymmetry transformations on the lattice, associated with the nilpotent supersymmetry, imply that the fermion fields $\psi_a(\boldsymbol{n})$ have the same orientation as their superpartners, the gauge links $\mathcal{U}_a(\boldsymbol{n})$, and run from $\boldsymbol{n}$ to $(\boldsymbol{n}+\widehat{\boldsymbol{\mu}}_a)$. However, the field $\chi_{ab}(\boldsymbol{n})$ must have the same orientation as $\mathcal{F}^{\dagger}_{ab}(\boldsymbol{n})$ and hence is to be assigned to the negatively oriented link running from $(\boldsymbol{n}+\widehat{\boldsymbol{\mu}}_a+\widehat{\boldsymbol{\mu}}_b)$ to $\boldsymbol{n}$. The negative orientation is crucial for allowing us to write down gauge-invariant expressions for the fermion kinetic term. The scalar fields $\eta(\boldsymbol{n})$ and $d(\boldsymbol{n})$ can be taken to transform simply as site fields.

4.2.1 Gauge transformations on the lattice

The gauge transformation properties of the lattice fields conveniently summarize these link mappings and orientations:

$$\begin{aligned}
\eta(\boldsymbol{n}) &\rightarrow G(\boldsymbol{n})\eta(\boldsymbol{n})G^\dagger(\boldsymbol{n}) && (4.27)\\
\psi_a(\boldsymbol{n}) &\rightarrow G(\boldsymbol{n})\psi_a(\boldsymbol{n})G^\dagger(\boldsymbol{n}+\widehat{\boldsymbol{\mu}}_a) && (4.28)\\
\chi_{ab}(\boldsymbol{n}) &\rightarrow G(\boldsymbol{n}+\widehat{\boldsymbol{\mu}}_a+\widehat{\boldsymbol{\mu}}_b)\chi_{ab}(\boldsymbol{n})G^\dagger(\boldsymbol{n}) && (4.29)\\
\mathcal{U}_a(\boldsymbol{n}) &\rightarrow G(\boldsymbol{n})\mathcal{U}_a(\boldsymbol{n})G^\dagger(\boldsymbol{n}+\widehat{\boldsymbol{\mu}}_a) && (4.30)\\
\overline{\mathcal{U}}_a(\boldsymbol{n}) &\rightarrow G(\boldsymbol{n}+\widehat{\boldsymbol{\mu}}_a)\overline{\mathcal{U}}_a(\boldsymbol{n})G^\dagger(\boldsymbol{n}) && (4.31)
\end{aligned}$$

The action is again $\mathcal{Q}$-exact on the lattice: $S=\mathcal{Q}\Lambda$, where

$$\Lambda=\sum_{\boldsymbol{n}}\mathrm{Tr}\,\Big(\chi_{ab}(\boldsymbol{n})\mathcal{D}_a^{(+)}\mathcal{U}_b(\boldsymbol{n})+\eta(\boldsymbol{n})\overline{\mathcal{D}}_a^{(-)}\mathcal{U}_a(\boldsymbol{n})-\frac{1}{2}\eta(\boldsymbol{n})d(\boldsymbol{n})\Big)\,. \tag{4.32}$$

Acting with the $\mathcal{Q}$ transformation shown above and again integrating out the auxiliary field d, we derive the gauge and $\mathcal{Q}$-invariant lattice action:

$$\begin{aligned}
S \;=\; &\sum_{\boldsymbol{n}}\mathrm{Tr}\,\Big(\mathcal{F}_{ab}^\dagger(\boldsymbol{n})\mathcal{F}_{ab}(\boldsymbol{n})+\frac{1}{2}\Big(\overline{\mathcal{D}}_a^{(-)}\mathcal{U}_a(\boldsymbol{n})\Big)^2\\
&-\chi_{ab}(\boldsymbol{n})\mathcal{D}_{[a}^{(+)}\psi_{b]}(\boldsymbol{n})-\eta(\boldsymbol{n})\overline{\mathcal{D}}_a^{(-)}\psi_a(\boldsymbol{n})\Big)\,. \qquad (4.33)
\end{aligned}$$

It is interesting to see that each term in the action forms a closed loop on the two-dimensional lattice. This is a requirement for preserving the gauge symmetry on the lattice.

4.3 Four-dimensional lattice $\mathcal{N}=4$ SYM theory

The way we discretized the two-dimensional $\mathcal{N}=2$ theory on a two-dimensional square lattice immediately motivates us to choose the discretization of the four-dimensional $\mathcal{N}=4$ theory on a four-dimensional hypercubic lattice. The fermions of the four-dimensional theory live on p-cells of the hypercubic lattice unit cell, associating themselves with the p-form representation of the continuum $SO(4)$ symmetry. The fermionic content of the hypercubic lattice construction manifest themselves as an explicit realization of Dirac-Kähler fermions. The bosons are also distributed on this lattice in orientations consistent with those of the fermions. The symmetry of the hypercubic lattice action is S_4, much smaller than the symmetry of the hypercube itself, due to the orientation assignment of the fields.

The gauge link fields $\mathcal{U}_a(\boldsymbol{n})$, $a=1,2,3,4$, live on elementary coordinate directions in the unit cell of the hypercube pointing in the direction $(\boldsymbol{n},\boldsymbol{n}+\widehat{\boldsymbol{\mu}}_a)$. The superpartners of the gauge link fields, $\psi_a(\boldsymbol{n})$, also live on the same links and oriented identically. The field $\overline{\mathcal{U}}_a(\boldsymbol{n})$ is oriented in the opposite direction $(\boldsymbol{n}+\widehat{\boldsymbol{\mu}}_a,\boldsymbol{n})$. The complexified field strength $\mathcal{F}_{ab}(\boldsymbol{n})$ runs along the direction $(\boldsymbol{n},\boldsymbol{n}+\widehat{\boldsymbol{\mu}}_a+\widehat{\boldsymbol{\mu}}_b)$. By exact supersymmetry, this implies that the field $\chi_{ab}(\boldsymbol{n})$ (and thus $\overline{\mathcal{F}}_{ab}(\boldsymbol{n})$) runs in the opposite direction.

The assignment of $\mathcal{U}_5(\boldsymbol{n})$ (and, thus, that of $\psi_5(\boldsymbol{n})$) is not immediately obvious. The Dirac-Kähler decomposition demands a 4-form. This motivates assigning the lattice field to the body diagonal of the unit hypercube, which is a 4-cell. It is oriented along the vector $\widehat{\boldsymbol{\mu}}_5 = (-1,-1,-1,-1)$. We see that this assignment ensures that $\widehat{\boldsymbol{\mu}}_1 + \widehat{\boldsymbol{\mu}}_2 + \cdots + \widehat{\boldsymbol{\mu}}_5 = 0$, and it is crucial for constructing gauge-invariant quantities on the lattice.

The basis vectors $\widehat{\boldsymbol{\mu}}_a$ of the hypercubic lattice are thus defined as[2]

$$\begin{aligned}
\widehat{\boldsymbol{\mu}}_1 &= (1,0,0,0) \\
\widehat{\boldsymbol{\mu}}_2 &= (0,1,0,0) \\
\widehat{\boldsymbol{\mu}}_3 &= (0,0,1,0) \\
\widehat{\boldsymbol{\mu}}_4 &= (0,0,0,1) \\
\widehat{\boldsymbol{\mu}}_5 &= (-1,-1,-1,-1)
\end{aligned} \tag{4.34}$$

Though the four-dimensional fields come with five indices they are all taken care of with suitable orientation assignments consistent with the lattice gauge symmetry.

On the hypercubic lattice the action of the four-dimensional theory takes the following form

$$\begin{aligned}
S &= \sum_{\boldsymbol{n},a,b,c,d,e} \Big\{ \mathcal{Q}\ \mathrm{Tr}\left[\chi_{ab}\mathcal{D}_a^{(+)}\mathcal{U}_b(\boldsymbol{n}) - \eta(\boldsymbol{n})\Big(\overline{\mathcal{D}}_a^{(-)}\mathcal{U}_a(\boldsymbol{n}) - \frac{1}{2}d(\boldsymbol{n})\Big)\right] \\
&\quad -\frac{1}{2}\mathrm{Tr}\ \epsilon_{abcde}\chi_{de}(\boldsymbol{n}+\widehat{\boldsymbol{\mu}}_a+\widehat{\boldsymbol{\mu}}_b+\widehat{\boldsymbol{\mu}}_c)\mathcal{D}_c^{\dagger(-)}\chi_{ab}(\boldsymbol{n}+\widehat{\boldsymbol{\mu}}_c)\Big\}\ .
\end{aligned} \tag{4.35}$$

where the lattice field strength is given by

$$\mathcal{F}_{ab}(\boldsymbol{n}) \equiv \mathcal{D}_a^{(+)}\mathcal{U}_b(\boldsymbol{n}) = \Big(\mathcal{U}_a(\boldsymbol{n})\mathcal{U}_b(\boldsymbol{n}+\widehat{\boldsymbol{\mu}}_a) - \mathcal{U}_b(\boldsymbol{n})\mathcal{U}_a(\boldsymbol{n}+\widehat{\boldsymbol{\mu}}_b)\Big)\ . \tag{4.36}$$

and the covariant difference operators appearing in this expression are given by

$$\mathcal{D}_c^{(+)}f(\boldsymbol{n}) = \mathcal{U}_c(\boldsymbol{n})f(\boldsymbol{n}+\widehat{\boldsymbol{\mu}}_c) - f(\boldsymbol{n})\mathcal{U}_c(\boldsymbol{n}) \tag{4.37}$$

$$\mathcal{D}_c^{(+)}f_d(\boldsymbol{n}) = \mathcal{U}_c(\boldsymbol{n})f_d(\boldsymbol{n}+\widehat{\boldsymbol{\mu}}_c) - f_d(\boldsymbol{n})\mathcal{U}_c(\boldsymbol{n}+\widehat{\boldsymbol{\mu}}_d) \tag{4.38}$$

$$\overline{\mathcal{D}}_c^{(-)}f_c(\boldsymbol{n}) = f_c(\boldsymbol{n})\overline{\mathcal{U}}_c(\boldsymbol{n}) - \overline{\mathcal{U}}_c(\boldsymbol{n}-\widehat{\boldsymbol{\mu}}_c)f_c(\boldsymbol{n}-\widehat{\boldsymbol{\mu}}_c) \tag{4.39}$$

$$\overline{\mathcal{D}}_c^{(-)}f_{ab}(\boldsymbol{n}) = f_{ab}(\boldsymbol{n})\overline{\mathcal{U}}_c(\boldsymbol{n}-\widehat{\boldsymbol{\mu}}_c) - \overline{\mathcal{U}}(\boldsymbol{n}+\widehat{\boldsymbol{\mu}}_a+\widehat{\boldsymbol{\mu}}_b-\widehat{\boldsymbol{\mu}}_c)f_{ab}(\boldsymbol{n}-\widehat{\boldsymbol{\mu}}_c) \tag{4.40}$$

The supersymmetry transformations on the lattice fields are almost identical to their continuum counterparts:

$$\mathcal{Q}\mathcal{U}_a(\boldsymbol{n}) = \psi_a(\boldsymbol{n}) \tag{4.41}$$

$$\mathcal{Q}\psi_a(\boldsymbol{n}) = 0 \tag{4.42}$$

$$\mathcal{Q}\overline{\mathcal{U}}_a(\boldsymbol{n}) = 0 \tag{4.43}$$

$$\mathcal{Q}\chi_{ab}(\boldsymbol{n}) = -\overline{\mathcal{F}}^L_{ab}(\boldsymbol{n}) \tag{4.44}$$

$$\mathcal{Q}\eta(\boldsymbol{n}) = d \tag{4.45}$$

$$\mathcal{Q}d(\boldsymbol{n}) = 0 \tag{4.46}$$

[2]These vectors are related to the $\boldsymbol{r}$-charges defined in the orbifold formulation of the four-dimensional $\mathcal{N}=4$ lattice SYM theory [40].

After the $\mathcal{Q}$-variation, as performed in the continuum, and integrating out the auxiliary field d, the final lattice action is:

$$\begin{aligned} S &= \sum_{\boldsymbol{n}} \mathrm{Tr}\,\Big[\mathcal{F}^{L\dagger}_{ab}\mathcal{F}^{L}_{ab} + \frac{1}{2}\Big(\overline{\mathcal{D}}^{(-)}_{a}\mathcal{U}_a(\boldsymbol{n})\Big)^2 - \chi_{ab}(\boldsymbol{n})\mathcal{D}^{(+)}_{[a}\psi_{b]}(\boldsymbol{n}) - \eta(\boldsymbol{n})\mathcal{D}^{\dagger(-)}_{a}\psi_a(\boldsymbol{n}) \\ &\quad -\frac{1}{2}\epsilon_{abcde}\chi_{de}(\boldsymbol{n}+\widehat{\boldsymbol{\mu}}_a+\widehat{\boldsymbol{\mu}}_b+\widehat{\boldsymbol{\mu}}_c)\overline{\mathcal{D}}^{(-)}_{c}\chi_{ab}(\boldsymbol{n}+\widehat{\boldsymbol{\mu}}_c)\Big]\ . \end{aligned} \tag{4.47}$$

To see that this action targets the continuum twisted theory one needs to expand $\mathcal{U}_a$ about the unit matrix [40][3]

$$\mathcal{U}_a(\boldsymbol{n}) = \mathbb{I}_N + \mathcal{A}_a(\boldsymbol{n})\ , \tag{4.48}$$

$$\overline{\mathcal{U}}_a(\boldsymbol{n}) = \mathbb{I}_N - \overline{\mathcal{A}}_a(\boldsymbol{n})\ . \tag{4.49}$$

While the supersymmetric invariance of the $\mathcal{Q}$-exact term is manifest in the lattice theory it is not immediately clear that the $\mathcal{Q}$-closed term remains supersymmetric after discretization. Interestingly, this can be shown using a remarkable property of the discrete field strength, which can be shown to satisfy an exact Bianchi identity just as for the continuum [47].

$$\epsilon_{abcde}\overline{\mathcal{D}}^{(-)}_{c}\overline{\mathcal{F}}_{ab}(\boldsymbol{n}+\widehat{\boldsymbol{\mu}}_c) = 0\ . \tag{4.50}$$

4.3.1 The A_4^* lattice construction

There exists a more symmetric lattice than the hypercubic lattice for the four-dimensional $\mathcal{N}=4$ theory. This lattice is called the A_4^* lattice. On this lattice, we treat all five basis vectors equally and they are oriented in such a way that the basis vectors connect the center of a 4-simplex to its corners. Having a most symmetric lattice is advantageous because the greater the symmetry is, the fewer relevant or marginal operators will exist on the lattice.

The lattice possesses an S^5 point group symmetry, which is the Weyl group of $SU(5)$. We briefly described the $SU(5)\times U(1)$ decomposition of the fields of the four-dimensional $\mathcal{N}=4$ SYM theory in Sec. 3.3.1. The discretization prescription for such a decomposition of the fields would be the A_4^* lattice. A specific basis for the A_4^* lattice is given in the form of five lattice vectors:

$$\widehat{\boldsymbol{e}}_1 = \Big(\frac{1}{\sqrt{2}},\frac{1}{\sqrt{6}},\frac{1}{\sqrt{12}},\frac{1}{\sqrt{20}}\Big) \tag{4.51}$$

$$\widehat{\boldsymbol{e}}_2 = \Big(-\frac{1}{\sqrt{2}},\frac{1}{\sqrt{6}},\frac{1}{\sqrt{12}},\frac{1}{\sqrt{20}}\Big) \tag{4.52}$$

$$\widehat{\boldsymbol{e}}_3 = \Big(0,-\frac{2}{\sqrt{6}},\frac{1}{\sqrt{12}},\frac{1}{\sqrt{20}}\Big) \tag{4.53}$$

$$\widehat{\boldsymbol{e}}_4 = \Big(0,0,-\frac{3}{\sqrt{12}},\frac{1}{\sqrt{20}}\Big) \tag{4.54}$$

$$\widehat{\boldsymbol{e}}_5 = \Big(0,0,0,-\frac{4}{\sqrt{20}}\Big) \tag{4.55}$$

[3]To leading order this is equivalent to the more conventional expression $\mathcal{U}_a(\boldsymbol{n}) = e^{\mathcal{A}_a(\boldsymbol{n})}$. We will see that the linear representation offers important advantages over the exponential in our later calculations.

These lattice vectors connect the center of a 4-simplex to its five corners. They are related to the $SU(5)$ weights of the 5 representation. The unit cell of the A_4^* lattice is a compound of two 4-simplices corresponding to the 5 (formed by the basis vectors $\widehat{\boldsymbol{e}}_m$) and $\overline{5}$ (formed by the basis vectors $-\widehat{\boldsymbol{e}}_m$) representations of $SU(5)$. The basis vectors satisfy the relations

$$\sum_{m=1}^{5}\widehat{\boldsymbol{e}}_m=0;\quad \widehat{\boldsymbol{e}}_m\cdot\widehat{\boldsymbol{e}}_n=\left(\delta_{mn}-\frac{1}{5}\right)$$
$$\sum_{m=1}^{5}(\widehat{\boldsymbol{e}}_m)_\mu(\widehat{\boldsymbol{e}}_m)_\nu=\delta_{\mu\nu};\quad \mu,\nu=1,\cdots,4.$$

Notice also that S^5 is a subgroup of the twisted rotation symmetry group $SO(4)'$ and that the lattice fields transform in reducible representations of this discrete group - for example, the vector $\mathcal{A}_a$ decomposes into a four component vector $\mathcal{A}_\mu$ and a scalar field ϕ under $SO(4)'$. Invariance of the lattice theory with respect to these discrete rotations then guarantees that the theory will inherit full invariance under twisted rotations in the continuum limit.

Proceeding in this manner, it is possible to assign all the remaining fields to links on the A_4^* lattice. Since $\psi_a(\boldsymbol{n})$ is a superpartner of $\mathcal{U}_a(\boldsymbol{n})$ it must also reside on the link connecting $\boldsymbol{n}\to\boldsymbol{n}+\widehat{\boldsymbol{e}}_a$. Conversely the field $\mathcal{U}_a^\dagger(\boldsymbol{n})$ resides on the oppositely oriented link from $\boldsymbol{n}\to\boldsymbol{n}-\widehat{\boldsymbol{e}}_a$. The ten fermions $\chi_{ab}(\boldsymbol{n})$ are then chosen to reside on new fermionic links $\boldsymbol{n}+\widehat{\boldsymbol{e}}_m+\widehat{\boldsymbol{e}}_n\to\boldsymbol{n}$, while the singlet fermionic field $\eta(\boldsymbol{n})$ is assigned to the degenerate link consisting of a single site $\boldsymbol{n}$.

The integer-valued lattice site $\boldsymbol{n}$ can be related to the physical location in spacetime using the A_4^* basis vectors $\widehat{\boldsymbol{e}}_a$.

$$\boldsymbol{R}=a\sum_{\nu=1}^{4}(\mu_\nu\cdot\boldsymbol{n})\widehat{\boldsymbol{e}}_\nu=a\sum_{\nu=1}^{4}n_\nu\widehat{\boldsymbol{e}}_\nu\ , \tag{4.56}$$

where a is the lattice spacing. On using the fact that $\sum_m\widehat{\boldsymbol{e}}_m=0$, we can show that a small lattice displacement of the form $d\boldsymbol{n}=\widehat{\boldsymbol{\mu}}_m$ corresponds to a spacetime translation by $(a\widehat{\boldsymbol{e}}_m)$:

$$d\boldsymbol{R}=a\sum_{\nu=1}^{4}(\mu_\nu\cdot d\boldsymbol{n})\widehat{\boldsymbol{e}}_\nu=a\sum_{\nu=1}^{4}(\widehat{\boldsymbol{\mu}}_\nu\cdot\widehat{\boldsymbol{\mu}}_m)\widehat{\boldsymbol{e}}_\nu=a\widehat{\boldsymbol{e}}_m\ . \tag{4.57}$$

In the next Chapter, we will use the A_4^* lattice construction to study the one-loop renormalization of the $\mathcal{N}=4$, $d=4$ SYM theory.

Chapter 5

Lattice $\mathcal{N} = 4$ SYM Theory at One-loop

In Chapter 1, we briefly discussed how special the four-dimensional $\mathcal{N} = 4$ SYM theory is and also mentioned that it plays a crucial role in the holographic principle. The dual of $\mathcal{N} = 4$ SYM theory is a string theory in $AdS_5 \times S^5$ space. We can study the dynamics of the gauge theory in various limits of its coupling parameter. We could also learn a lot about the dual string theory by studying the gauge theory. The lattice formulation of four-dimensional $\mathcal{N} = 4$ SYM theory would be very advantageous as it would give a non-perturbative definition of the gauge theory and open up a new window to explore its strong coupling dynamics. Indeed, such a lattice construction would allow for a systematic study of its dual string theory. In Chapter 4, we have written down the lattice version of this theory. We wrote down the the theory on a four-dimensional hypercubic lattice and then, to utilize the maximum symmetry of the lattice theory, we described the discretization of this theory on a very special lattice called the A_4^* lattice.

The lattice formulation of the $\mathcal{N} = 4$ SYM theory retains an exact supersymmetry, even at non zero lattice spacing. But this is only one out of the sixteen continuum supersymmetric invariances. There is still a question of how much fine tuning would be required to take a continuum limit of this lattice theory targeting the usual $\mathcal{N} = 4$ theory. In this Chapter[1], we address this issue using both general arguments valid to all orders in perturbation theory and an explicit calculation of the renormalization of the lattice theory to one-loop order.

We can make a quite general argument that the symmetries of the lattice theory strongly constrain the possible counterterms that can arise as a result of quantum corrections. We will see that the only relevant operators that can be induced via radiative effects correspond to renormalizations of four marginal operators already present in the tree level theory. These operators correspond to kinetic terms in the bare action. We

[1]This Chapter is based on the work [49].

also show that no mass terms are induced, to all orders in perturbation theory, using a topological argument based on the exact lattice supersymmetry.

We then go on to ask what divergences can arise in the renormalization of these four bare couplings to address the remaining fine tuning question. On using lattice perturbation theory, we proceed to calculate these divergences at one-loop. The lattice structure of the theory, coming from the twisted supersymmetry, allows us to extract these leading divergences. We derive the Feynman rules governing the perturbative structure of the lattice theory and write down the diagrams needed to renormalize the theory at one-loop. We need only to examine the renormalization of the three types of twisted fermion propagators and a single propagator for an auxiliary bosonic field. We show that all these propagators exhibit a common logarithmic divergence at one-loop. The appearance of a single logarithmic divergence ensures that, at one-loop, only finite parts need to be fine tuned in order to regain full supersymmetry in the continuum limit. This is a huge advantage of this approach, as compared to earlier efforts at constructing supersymmetric lattice theories in four dimensions.

We also compute the partition function of the theory at one-loop and show that it is independent of any background fields, and, furthermore, that this is true to all orders in perturbation theory.

5.1 General analysis of renormalization

From power counting, we see that the four-dimensional $\mathcal{N} = 4$ theory in the continuum has an infinite number of superficially divergent Feynman diagrams occurring at all orders of perturbation theory. All of these potential divergences cancel between diagrams to render the quantum theory finite in the continuum. This perfect cancellation may not happen on the lattice, since the lattice theory does not possess all the supersymmetries of the continuum theory.

Before we proceed to the perturbative analysis of the lattice theory, let us check what kinds of counterterms are permitted by the lattice symmetries. The four-dimensional theory on an A_4^* lattice has the following set of symmetries:

i. The exact supersymmetry corresponding to the scalar supercharge $\mathcal{Q}$.

ii. Lattice gauge symmetry.

iii. The S_5 point group symmetry and discrete translations on the lattice.

If we take the gauge group to be $U(N)$, lattice gauge theory possesses an additional fermionic symmetry, given by

$$\eta(\boldsymbol{n}) \to \eta(\boldsymbol{n}) + \epsilon \mathbb{I}_N, \qquad \delta_\epsilon(\text{all other fields}) = 0 \ , \tag{5.1}$$

where ϵ is an infinitesimal Grassmann parameter. Thus, our list contains one more symmetry:

iv. Fermionic shift symmetry.

In this Chapter, we will change our conventions to hermitian basis for the generators of the gauge group satisfying Tr $(T^A T^B) = \frac{1}{2}\delta^{AB}$. We also explicitly indicate the dependence on the coupling parameter g. In terms of the complexified connections, the three types of covariant derivatives and field strengths take the form:

$$D_a \cdot \equiv \partial_a + ig[A_a, \ \cdot \ ], \quad F_{ab} \equiv -\frac{i}{g}[D_a, D_b] \ , \tag{5.2}$$

$$\mathcal{D}_a \cdot \equiv \partial_a + ig[\mathcal{A}_a, \ \cdot \ ], \quad \mathcal{F}_{ab} \equiv -\frac{i}{g}[\mathcal{D}_a, \mathcal{D}_b] \ , \tag{5.3}$$

$$\overline{\mathcal{D}}_a \cdot \equiv \partial_a + ig[\overline{\mathcal{A}}_a, \ \cdot \ ], \quad \overline{\mathcal{F}}_{ab} \equiv -\frac{i}{g}[\overline{\mathcal{D}}_a, \overline{\mathcal{D}}_b] \ . \tag{5.4}$$

The continuum action of the theory is:

$$\begin{aligned} S \ &= \ \int \mathrm{Tr}\, \Big(\overline{\mathcal{F}}_{ab}\mathcal{F}_{ab} + \frac{1}{2g^2}[\overline{\mathcal{D}}_a, \mathcal{D}_a]^2 - \chi_{ab}\mathcal{D}_{[a}\psi_{b]} - \eta\overline{\mathcal{D}}_a\psi_a \\ &\quad -\frac{1}{2}\epsilon_{abcde}\chi_{de}\overline{\mathcal{D}}_c\chi_{ab}\Big). \end{aligned} \tag{5.5}$$

We extract the coupling parameter dependence from the terms in the action by rescaling the fields $g\eta \to \eta$, $g\psi_a \to \psi_a$, $g\chi_{ab} \to \chi_{ab}$ and $g\mathcal{A}_a \to \mathcal{A}_a$:

$$\begin{aligned} S \ &= \ \frac{1}{g^2}\int \mathrm{Tr}\, \Big(-[\overline{\mathcal{D}}_a, \overline{\mathcal{D}}_b][\mathcal{D}_a, \mathcal{D}_b] + \frac{1}{2}[\overline{\mathcal{D}}_a, \mathcal{D}_a]^2 - \chi_{ab}\mathcal{D}_{[a}\psi_{b]} - \eta\overline{\mathcal{D}}_a\psi_a \\ &\quad - \frac{1}{2}\epsilon_{abcde}\chi_{de}\overline{\mathcal{D}}_c\chi_{ab}\Big). \end{aligned} \tag{5.6}$$

The lattice action is

$$\begin{aligned} S \ &= \ \frac{1}{g^2}\sum_{\boldsymbol{n}} \ \Big\{ \mathcal{Q}\ \mathrm{Tr}\, \Big[-i\chi_{ab}\mathcal{D}_a^{(+)}\mathcal{U}_b(\boldsymbol{n}) - \eta(\boldsymbol{n})\Big(i\mathcal{D}_a^{\dagger(-)}\mathcal{U}_a(\boldsymbol{n}) - \frac{1}{2}d(\boldsymbol{n})\Big)\Big] \\ &\quad -\frac{1}{2}\mathrm{Tr}\ \epsilon_{abcde}\chi_{de}(\boldsymbol{n} + \widehat{\boldsymbol{\mu}}_a + \widehat{\boldsymbol{\mu}}_b + \widehat{\boldsymbol{\mu}}_c)\mathcal{D}_c^{\dagger(-)}\chi_{ab}(\boldsymbol{n} + \widehat{\boldsymbol{\mu}}_c)\Big\} \ , \end{aligned} \tag{5.7}$$

where the lattice field strength is given by:

$$\begin{aligned} \mathcal{F}_{ab}(\boldsymbol{n}) \ &\equiv \ -\frac{i}{g}\mathcal{D}_a^{(+)}\mathcal{U}_b(\boldsymbol{n}) \\ &= \ -\frac{i}{g}\Big(\mathcal{U}_a(\boldsymbol{n})\mathcal{U}_b(\boldsymbol{n} + \widehat{\boldsymbol{\mu}}_a) - \mathcal{U}_b(\boldsymbol{n})\mathcal{U}_a(\boldsymbol{n} + \widehat{\boldsymbol{\mu}}_b)\Big). \end{aligned} \tag{5.8}$$

We are primarily interested in relevant or marginal operators - operators whose mass dimension is less than or equal to four - on the lattice. We will see that the set of relevant counterterms in the lattice theory is rather short. The lattice symmetries, gauge-invariance in particular, being extremely restrictive in comparison to the equivalent situation in the continuum. Invariance under $\mathcal{Q}$ restricts the possible counterterms to be either of a $\mathcal{Q}$-exact form, or of a $\mathcal{Q}$-closed form. There is only one $\mathcal{Q}$-closed operator permitted by the lattice symmetries, and it is already present in our bare lattice action. A possible renormalization of this fermion kinetic term is hence allowed. Beyond that, the exact lattice supersymmetry forces us to look at the set of $\mathcal{Q}$-exact counterterms.

The bosonic and fermionic fields have the following canonical dimensions:

$$[\mathcal{U}_a] = 1,\ [\Psi] = \tfrac{3}{2} \text{ and } [\mathcal{Q}] = \tfrac{1}{2}$$

where Ψ stands for any of the twisted fermion fields $(\lambda, \psi_a, \chi_{ab})$. Any counterterm we add to the action, which respects the lattice symmetries, must be of the form

$$\mathcal{O} = \mathcal{Q}\mathrm{Tr}\ (\Psi f(\mathcal{U}, \mathcal{U}^\dagger)).$$

There are, thus, no terms permitted by symmetries with a dimension less than two. In addition, gauge-invariance tells us that each term must correspond to the trace of a closed loop on the lattice. The smallest dimension gauge-invariant operator is then just $\mathcal{Q}(\mathrm{Tr}\ \psi_a \mathcal{U}_a^\dagger)$. But this vanishes identically, since both $\mathcal{U}_a^\dagger$ and ψ_a are singlets under $\mathcal{Q}$. No dimension $\frac{7}{2}$ operators can be constructed with this structure, and we are left with just dimension four counterterms. Notice, in particular, that lattice symmetries permit no simple fermion bi-linear mass terms. However, gauge-invariant fermion bi-linears with link field insertions are possible, and their effect should be accounted for carefully.

Thus, the set of possible dimension four operators is, schematically,

$$\begin{aligned} L_1 &= g^{-2}\mathcal{Q}\mathrm{Tr}\ (\chi_{ab}\mathcal{U}_a\mathcal{U}_b) \\ L_2 &= g^{-2}\mathcal{Q}\mathrm{Tr}\ (\eta\mathcal{D}_a^\dagger\mathcal{U}_a) \\ L_3 &= g^{-2}\mathcal{Q}\mathrm{Tr}\ (\eta\mathcal{U}_a\mathcal{U}_a^\dagger) \\ L_4 &= g^{-2}\mathcal{Q}\mathrm{Tr}\ (\eta)\mathrm{Tr}\ (\mathcal{U}_a\mathcal{U}_a^\dagger) \end{aligned} \tag{5.9}$$

The first operator can be simplified on account of the antisymmetry of χ_{ab} to simply $\mathcal{Q}(\chi_{ab}\mathcal{F}_{ab})$, which, again, is nothing but one of the continuum $\mathcal{Q}$-exact terms present in the bare action. The second term in (5.9) also corresponds to one of the $\mathcal{Q}$-exact terms in the bare action. However, the third term L_3 is a new operator not present in the bare Lagrangian and the same is true for the final double-trace operator L_4. Both of these operators transform non-trivially under the fermionic shift symmetry, but a linear combination of the two:

$$D = L_3 - \frac{1}{N}L_4 \tag{5.10}$$

is invariant under the shift symmetry with N the rank of the gauge group $U(N)$.

It is quite remarkable to see that these arguments lead to relevant counterterms corresponding to renormalizations of operators that are already present in the bare action together with D. Thus, the most general form for the renormalized lattice Lagrangian is:

$$\begin{aligned} \mathcal{L} = \sum_{\boldsymbol{n},a,b,c,d,e} & \Big\{\mathcal{Q}\ \mathrm{Tr}\Big[-i\alpha_1\chi_{ab}\mathcal{D}_a^{(+)}\mathcal{U}_b(\boldsymbol{n}) - i\alpha_2\eta(\boldsymbol{n})\mathcal{D}_a^{\dagger(-)}\mathcal{U}_a(\boldsymbol{n}) \\ & + \frac{\alpha_3}{2}\eta(\boldsymbol{n})d(\boldsymbol{n})\Big] - \frac{\alpha_4}{2}\mathrm{Tr}\ \epsilon_{abcde}\chi_{de}(\boldsymbol{n}+\widehat{\boldsymbol{\mu}}_a+\widehat{\boldsymbol{\mu}}_b+\widehat{\boldsymbol{\mu}}_c)\mathcal{D}_c^{\dagger(-)}\chi_{ab}(\boldsymbol{n}+\widehat{\boldsymbol{\mu}}_c)\Big\} \\ & + \mathcal{Q}\beta D\ , \end{aligned} \tag{5.11}$$

where $(\alpha_i, i = 1\ldots4)$ and β are dimensionless numbers taking values $(1,1,1,1)$ and 0 respectively in the classical lattice theory. Thus, it appears that, at most, four dimensionless ratios of these couplings might need to be tuned to approach $\mathcal{N} = 4$ Yang–Mills in the continuum limit. Furthermore, since these operators are dimension four, we expect this tuning to be, at worst, logarithmic in the cut-off.

In order to see the explicit form of the D operator close to the continuum limit, we expand the action around $\mathcal{U}_m(\boldsymbol{n}) = \frac{1}{a}\mathbb{I}$. The result is

$$L_4 \sim \frac{1}{a}\left[\text{Tr }\eta(\boldsymbol{n})(\sum_{m=1}^{5}\psi^m(\boldsymbol{n})) - \frac{1}{N}\text{Tr }\eta(\boldsymbol{n})\text{Tr }(\sum_{m=1}^{5}\psi^m(\boldsymbol{n}))+\right]\ldots \tag{5.12}$$

where ellipsis are dictated by supersymmetry. It is interesting to see that $(\sum_{a=1}^{5}\psi_a)$ is nothing but the S_5 (and twisted $SO(4)'$) singlet contained in the reducible representation ψ_a. It is the only field that could form a fermion mass term by pairing with η.

We conclude our exploration using general lattice symmetry arguments here. We now turn to a full perturbative analysis to determine how the couplings (α_i, β) evolve with the cut-off.

5.2 Deriving the lattice propagators and vertices

We begin our perturbative analysis of the lattice $\mathcal{N}=4$ SYM theory by deriving the boson and fermion propagators and the vertices connecting them.

The classical lattice action (5.7) is a combination of three parts - bosonic (S_B), fermionic (S_F) and $\mathcal{Q}$-closed terms (S_c). They are given below:

$$\begin{aligned}
S_B &= \frac{1}{g^2}\sum_{\boldsymbol{n},a,b}\text{Tr}\left[\left(\mathcal{D}_a^{(+)}\mathcal{U}_b(\boldsymbol{n})\right)^\dagger\left(\mathcal{D}_a^{(+)}\mathcal{U}_b(\boldsymbol{n})\right)+\frac{1}{2}\left(\mathcal{D}_a^{\dagger(-)}\mathcal{U}_a(\boldsymbol{n})\right)^2\right]\\
&= \frac{1}{g^2}\sum_{\boldsymbol{n},a,b}\text{Tr}\left[\left(\mathcal{U}_b^\dagger(\boldsymbol{n}+\widehat{\boldsymbol{\mu}}_a)\mathcal{U}_a^\dagger(\boldsymbol{n})-\mathcal{U}_a^\dagger(\boldsymbol{n}+\widehat{\boldsymbol{\mu}}_b)\mathcal{U}_b^\dagger(\boldsymbol{n})\right)\right.\\
&\quad\times\left(\mathcal{U}_a(\boldsymbol{n})\mathcal{U}_b(\boldsymbol{n}+\widehat{\boldsymbol{\mu}}_a)-\mathcal{U}_b(\boldsymbol{n})\mathcal{U}_a(\boldsymbol{n}+\widehat{\boldsymbol{\mu}}_b)\right)\\
&\quad\left.+\frac{1}{2}\left(\mathcal{U}_a(\boldsymbol{n})\mathcal{U}_a^\dagger(\boldsymbol{n})-\mathcal{U}_a^\dagger(\boldsymbol{n}-\widehat{\boldsymbol{\mu}}_a)\mathcal{U}_a(\boldsymbol{n}-\widehat{\boldsymbol{\mu}}_a)\right)^2\right],
\end{aligned}\tag{5.13}$$

$$\begin{aligned}
S_F &= -\frac{1}{g^2}\sum_{\boldsymbol{n},a,b,c,d}\text{Tr}\,\frac{1}{2}(\delta_{ac}\delta_{bd}-\delta_{ad}\delta_{bc})\Big[\chi_{ab}(\boldsymbol{n})\Big(\mathcal{U}_c(\boldsymbol{n})\psi_d(\boldsymbol{n}+\widehat{\boldsymbol{\mu}}_c)\\
&\quad-\psi_d(\boldsymbol{n})\mathcal{U}_c(\boldsymbol{n}+\widehat{\boldsymbol{\mu}}_d)\Big)\Big]+\eta(\boldsymbol{n})\Big(\psi_a(\boldsymbol{n})\mathcal{U}_a^\dagger(\boldsymbol{n})\\
&\quad-\mathcal{U}_a^\dagger(\boldsymbol{n}-\widehat{\boldsymbol{\mu}}_a)\psi_a(\boldsymbol{n}-\widehat{\boldsymbol{\mu}}_a)\Big),
\end{aligned}\tag{5.14}$$

and

$$\begin{aligned}
S_c &= -\frac{1}{2g^2}\sum_{\boldsymbol{n},a,b,c,d,e}\text{Tr}\,\epsilon_{abcde}\Big(\chi_{de}(\boldsymbol{n}+\widehat{\boldsymbol{\mu}}_a+\widehat{\boldsymbol{\mu}}_b+\widehat{\boldsymbol{\mu}}_c)\\
&\quad\times\Big[\chi_{ab}(\boldsymbol{n}+\widehat{\boldsymbol{\mu}}_c)\mathcal{U}_c^\dagger(\boldsymbol{n})-\mathcal{U}_c^\dagger(\boldsymbol{n}+\widehat{\boldsymbol{\mu}}_a+\widehat{\boldsymbol{\mu}}_b)\chi_{ab}(\boldsymbol{n})\Big]\Big),
\end{aligned}\tag{5.15}$$

where we have expressed the field strength and covariant derivatives in terms of the bosonic link fields $\mathcal{U}_a(\boldsymbol{n})$.

To proceed further, we expand the $\mathcal{U}_a(\boldsymbol{n})$ fields around unity

$$\mathcal{U}_a(\boldsymbol{n}) = \frac{1}{a}\mathbb{I}_N + i\mathcal{A}_a(\boldsymbol{n}) \ , \tag{5.16}$$

$$\mathcal{U}_a^\dagger(\boldsymbol{n}) = \frac{1}{a}\mathbb{I}_N - i\overline{\mathcal{A}}_a(\boldsymbol{n}) \ . \tag{5.17}$$

Notice that this expansion point is but one of an infinite number of classical vacuum solutions - the full moduli space of the lattice theory corresponds to the set of all bosonic field variables $\mathcal{U}_a(\boldsymbol{n})$ such that

$$\begin{aligned} 0 = \sum_{\boldsymbol{n},a,b} \mathrm{Tr}\ \Big[&\Big(\mathcal{U}_b^\dagger(\boldsymbol{n}+\widehat{\boldsymbol{\mu}}_a)\mathcal{U}_a^\dagger(\boldsymbol{n}) - \mathcal{U}_a^\dagger(\boldsymbol{n}+\widehat{\boldsymbol{\mu}}_b)\mathcal{U}_b^\dagger(\boldsymbol{n})\Big) \\ &\times\Big(\mathcal{U}_a(\boldsymbol{n})\mathcal{U}_b(\boldsymbol{n}+\widehat{\boldsymbol{\mu}}_a) - \mathcal{U}_b(\boldsymbol{n})\mathcal{U}_a(\boldsymbol{n}+\widehat{\boldsymbol{\mu}}_b)\Big) \\ &+\frac{1}{2}\Big(\mathcal{U}_a(\boldsymbol{n})\mathcal{U}_a^\dagger(\boldsymbol{n}) - \mathcal{U}_a^\dagger(\boldsymbol{n}-\widehat{\boldsymbol{\mu}}_a)\mathcal{U}_a(\boldsymbol{n}-\widehat{\boldsymbol{\mu}}_a)\Big)^2\Big]. \end{aligned} \tag{5.18}$$

These equations possess a large class of solutions corresponding to constant diagonal matrices modulo gauge transformations. We will use this additional freedom later when we compute the one-loop contribution to the effective action of the theory.

5.2.1 The bosonic propagators on the lattice

As usual it is easiest to compute the Feynman diagrams in momentum space. On the A_4^* lattice a generic field $\Phi(\mathbf{x})$ has Fourier expansion

$$\Phi(\mathbf{x}) = \frac{1}{(La)^4}\sum_{\mathbf{p}} e^{i\mathbf{p}\cdot\mathbf{x}}\Phi_{\mathbf{p}} \ , \tag{5.19}$$

where $\mathbf{x} = a\sum_{a=1}^4 n_a\widehat{\boldsymbol{e}}_a$ denotes the position on A_4^* and the momenta lie on the dual lattice given by $\mathbf{p} = \frac{2\pi}{La}\sum_{a=1}^4 m_a\widehat{\boldsymbol{g}}_a$ (for a lattice with spacing a and length L). The dual basis vectors $\widehat{\boldsymbol{g}}_a, a = 1\ldots 4$ satisfy

$$\widehat{\boldsymbol{e}}_a.\widehat{\boldsymbol{g}}_b = \delta_{ab} \ . \tag{5.20}$$

On an L^4 lattice both sets of lattice coordinates n_a, m_a take integer values in the range $-L/2+1,\ldots,L/2$. We will assume periodic boundary conditions in all directions in this Chapter. Eqn. 5.19 implies that fields are automatically invariant under translations by a lattice length in any direction and a field shifted by one of the basis vectors can be expressed as[2]

$$\Phi(\mathbf{x}+\widehat{\boldsymbol{e}}_a) = \sum_{\mathbf{p}} e^{ip_a}e^{i\mathbf{p}\cdot\mathbf{x}}\Phi_{\mathbf{p}} \ , \tag{5.21}$$

where $p_a = \frac{2\pi}{L}m_a$. The only remaining is the question of how to deal with shifts in the lattice action associated with the additional $\widehat{\boldsymbol{e}}_5$ vector. However, the solution is

[2]For simplicity we will adopt the convention that momentum sums $\sum_k$ automatically include the $1/(La)^4$ normalization factor.

simple: since $\sum_{a=1}^{5} \widehat{\boldsymbol{e}}_a = 0$ we simply replace any $\widehat{\boldsymbol{e}}_5$ shift encountered in the action by the equivalent shift $-\sum_{a=1}^{4} \widehat{\boldsymbol{e}}_a$. One might have worried about an apparent lack of rotational invariance associated with the naive continuum limit of terms in the action which resemble $\sum_{a=1}^{5} \sin^2 p_a$ However, putting $p_a = \mathbf{p}.\widehat{\boldsymbol{e}}_a$ and taking the naive continuum limit this becomes

$$\sum_{a=1}^{5} p_a^2 = \sum_{\mu,\nu}^{4} \sum_{a=1}^{5} p_\mu p_\nu \widehat{\boldsymbol{e}}_a^\mu \widehat{\boldsymbol{e}}_a^\nu = \sum_{\mu}^{4} p_\mu^2 \ , \tag{5.22}$$

which has the correct rotationally invariant form since the Greek indices refer to a Cartesian basis.

Using these ideas the bosonic action when expanded around (5.16) and (5.17) gives the following second-order term in Fourier space

$$\begin{aligned} S_B^{(2)} \ &\approx \ 2 \sum_{\mathbf{k},a,b} \mathrm{Tr} \, \Big(\overline{\mathcal{A}}_a(\mathbf{k}) \Big[\delta_{ab} f_c(\mathbf{k}) f_c^*(\mathbf{k}) - f_a^*(\mathbf{k}) f_b(\mathbf{k}) \Big] \mathcal{A}_b(-\mathbf{k}) \\ &\quad + B_a(\mathbf{k}) \, \Big[f_a^*(\mathbf{k}) f_b(\mathbf{k}) \Big] \, B_b(-\mathbf{k}) \Big) \ , \end{aligned} \tag{5.23}$$

where

$$f_a(\mathbf{k}) = (e^{ik_a} - 1) \ . \tag{5.24}$$

We need to gauge-fix the bosonic action before we derive the propagators. A natural gauge-fixing choice would be an obvious generalization of Lorentz gauge-fixing [18]

$$G(\boldsymbol{n}) = \sum_a \Big(\partial_a^{(-)} \mathcal{A}_a(\boldsymbol{n}) + \partial_a^{(-)} \overline{\mathcal{A}}_a(\boldsymbol{n}) \Big) \ . \tag{5.25}$$

This gauge-fixing choice adds the following term to the bosonic action at quadratic order

$$S_{GF} = \frac{1}{4\alpha} \sum_{\boldsymbol{n}} G^2(\boldsymbol{n}) = \frac{1}{\alpha} \sum_{\boldsymbol{n},a} \mathrm{Tr} \, (\partial_a^{(-)} A_a(\boldsymbol{n}))^2 \ , \tag{5.26}$$

where $\partial_a^{(-)} f(\boldsymbol{n}) = f(\boldsymbol{n}) - f(\boldsymbol{n} - \widehat{\boldsymbol{\mu}}_a)$. On using the relation

$$\sum_{\boldsymbol{n}} (\partial_a^{(+)} f(\boldsymbol{n})) g(\boldsymbol{n}) = - \sum_{\boldsymbol{n}} f(\boldsymbol{n}) \partial_a^{(-)} g(\boldsymbol{n}) \ ,$$

the gauge-fixing term becomes

$$S_{GF} = -\frac{1}{\alpha} \sum_{\boldsymbol{n},a,b} \mathrm{Tr} \, A_a(\boldsymbol{n}) \partial_a^{(+)} \partial_b^{(-)} A_b(\boldsymbol{n}) \ . \tag{5.27}$$

In momentum space it becomes

$$S_{GF} \ = \ \frac{1}{\alpha} \sum_{\mathbf{k},a,b} \mathrm{Tr} \, A_a(\mathbf{k}) f_a^*(\mathbf{k}) f_b(\mathbf{k}) A_b(-\mathbf{k}) \ . \tag{5.28}$$

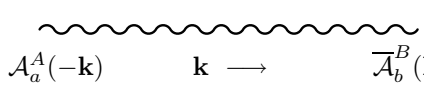

Figure 5.1: Bosonic propagators on the lattice.

Thus the gauge-fixed bosonic action to quadratic order is

$$\begin{aligned} S_B^{(2)} + S_{GF} &\approx 2\sum_{\mathbf{k},a,b,c} \mathrm{Tr}\,\Big(A_a(\mathbf{k})\,\Big[\delta_{ab}f_c(\mathbf{k})f_c^*(\mathbf{k}) - \Big(1-\frac{1}{2\alpha}\Big)f_a^*(\mathbf{k})f_b(\mathbf{k})\Big]\,A_b(-\mathbf{k}) \\ &\quad + B_a(\mathbf{k})\,\Big[\delta_{ab}f_c(\mathbf{k})f_c^*(\mathbf{k})\Big]\,B_b(-\mathbf{k})\Big)\ . \end{aligned} \tag{5.29}$$

The choice $\alpha = 1/2$ makes the above expression diagonal

$$\begin{aligned} S_B^{(2)} &\approx 2\sum_{\mathbf{k},a,b,c} \mathrm{Tr}\,\overline{\mathcal{A}}_a(\mathbf{k})\,[\delta_{ab}f_c(\mathbf{k})f_c^*(\mathbf{k})]\,\mathcal{A}_b(-\mathbf{k}) \\ &= 2\sum_{\mathbf{k},a,b} \mathrm{Tr}\,\Big[\overline{\mathcal{A}}_a(\mathbf{k})\delta_{ab}\Big(4\sum_c \sin^2\Big(\frac{k_c}{2}\Big)\Big)\mathcal{A}_b(-\mathbf{k})\Big]\ . \end{aligned} \tag{5.30}$$

Putting in the trace (using the convention $\mathrm{Tr}\,(T^AT^B) = \frac{1}{2}\delta_{AB}$) the quadratic bosonic action can be written as

$$S_B^{(2)} \approx \sum_{\mathbf{k},a,b} \overline{\mathcal{A}}_a^A(\mathbf{k})M_{ab}^{AB}(\mathbf{k})\mathcal{A}_b^B(-\mathbf{k})\ , \tag{5.31}$$

where $M_{ab}^{AB}(\mathbf{k}) = \widehat{\mathbf{k}}^2\delta_{ab}\delta_{AB}$, with $\widehat{\mathbf{k}}^2 = 4\sum_c \sin^2\Big(\frac{k_c}{2}\Big)$. Thus only the $\mathcal{A}\overline{\mathcal{A}}$ propagator is non-zero and it is given by (See figure 5.1.)

$$\langle \mathcal{A}_a^A(-\mathbf{k})\overline{\mathcal{A}}_b^B(\mathbf{k})\rangle = \delta_{ab}\delta_{AB}\frac{1}{\widehat{\mathbf{k}}^2}\ . \tag{5.32}$$

5.2.2 The fermionic propagators on the lattice

The fermionic part of the action has the following form on the lattice

$$\begin{aligned} S_F &= -\frac{1}{g^2}\sum_{\boldsymbol{n},a,b,c,d,e} \mathrm{Tr}\,\Big(\chi_{ab}(\boldsymbol{n})\mathcal{D}_{[a}^{(+)}\psi_{b]}(\boldsymbol{n}) + \eta(\boldsymbol{n})\mathcal{D}_a^{\dagger(-)}\psi_a(\boldsymbol{n}) \\ &\quad + \frac{1}{2}\epsilon_{abcde}\chi_{de}(\boldsymbol{n}+\widehat{\boldsymbol{\mu}}_a+\widehat{\boldsymbol{\mu}}_b+\widehat{\boldsymbol{\mu}}_c)\mathcal{D}_c^{\dagger(-)}\chi_{ab}(\boldsymbol{n}+\widehat{\boldsymbol{\mu}}_c)\Big)\ . \end{aligned} \tag{5.33}$$

When expanded up to second order in the fields using (5.16) and (5.17), it becomes

$$\begin{aligned} S_F^{(2)} &\approx \frac{1}{g^2}\sum_{\mathbf{k},a,b,c,d,e} \mathrm{Tr}\,\chi_{ab}(\mathbf{k})\Big[-f_a^*(\mathbf{k})\delta_{bc} + f_b^*(\mathbf{k})\delta_{ac}\Big]\psi_c(-\mathbf{k}) + \eta(\mathbf{k})f_c(\mathbf{k})\psi_c(-\mathbf{k}) \\ &\quad + \frac{1}{2}\epsilon_{abcde}\chi_{de}(\mathbf{k})e^{i(k_a+k_b)}f_c(\mathbf{k})\chi_{ab}(-\mathbf{k})\ . \end{aligned} \tag{5.34}$$

Upon restricting the sum and rescaling the field $2\chi_{ab} \to \chi_{ab}$ the fermionic action becomes

$$\begin{aligned} S_F^{(2)} &\approx \frac{1}{g^2}\sum_{\mathbf{k},a<b;c,d<e} \mathrm{Tr}\,\Big(\chi_{ab}(\mathbf{k})\Big[-f_a^*(\mathbf{k})\delta_{bc}+f_b^*(\mathbf{k})\delta_{ac}\Big]\psi_c(-\mathbf{k})+\eta(\mathbf{k})f_c(\mathbf{k})\psi_c(-\mathbf{k}) \\ &\quad +\frac{1}{2}\epsilon_{abcde}\chi_{de}(\mathbf{k})e^{i(k_a+k_b)}f_c(\mathbf{k})\chi_{ab}(-\mathbf{k})\Big)\ . \end{aligned} \tag{5.35}$$

We can then write this action in the form of a matrix product

$$\begin{aligned} S_F^{(2)} &\approx \frac{1}{g^2}\sum_{\mathbf{k}}(\Psi(\mathbf{k})\Psi(-\mathbf{k}))\left(\frac{1}{4}\right)\begin{pmatrix} 0 & M(\mathbf{k}) \\ -M^T(\mathbf{k}) & 0\end{pmatrix}\begin{pmatrix}\Psi(\mathbf{k})\\ \Psi(-\mathbf{k})\end{pmatrix} \\ &= \frac{1}{4g^2}\sum_{\mathbf{k}}\Phi(\mathbf{k})\mathcal{M}\Phi(\mathbf{k})\ . \end{aligned} \tag{5.36}$$

where $\Phi \equiv (\Psi(\mathbf{k}),\Psi(-\mathbf{k}))$ and $\Psi_i = (\eta,\psi_1,\ldots,\psi_5,\chi_{12},\ldots,\chi_{15},\ldots,\chi_{45})$ and $M(\mathbf{k})$ is given in block matrix form

$$(\eta\ \psi_a\ \chi_{de})(\mathbf{k})\begin{pmatrix} 0 & f_b(\mathbf{k}) & 0 \\ -f_a^*(\mathbf{k}) & 0 & f_g(\mathbf{k})\delta_{ha}-f_h(\mathbf{k})\delta_{ga} \\ 0 & -f_d^*(\mathbf{k})\delta_{eb}+f_e^*(\mathbf{k})\delta_{db} & \epsilon_{ghcde}q_{gh}f_c(\mathbf{k})\end{pmatrix}\begin{pmatrix}\eta\\ \psi_b\\ \chi_{gh}\end{pmatrix}(-\mathbf{k}).$$

where $q_{gh}=e^{i(k_g+k_h)}$. Notice that M has the properties $M^T(\mathbf{k})=-M^*(\mathbf{k})=-M(-\mathbf{k})$.

Using the property that $\sum_a \widehat{\boldsymbol{\mu}}_a = 0$, we can square the matrix to obtain

$$M^2(\mathbf{k}) = -\sum_{a=1}^{5}|e^{ik_a}-1|^2\mathbb{I}_{16} = -4\sum_{a=1}^{5}\sin^2\left(\frac{k_a}{2}\right)\mathbb{I}_{16} = -\widehat{\mathbf{k}}^2\mathbb{I}_{16}\ . \tag{5.37}$$

Thus,

$$M^{-1} = -\frac{1}{\widehat{\mathbf{k}}^2}M\ , \tag{5.38}$$

and the inverse of the full fermion matrix is:

$$\mathcal{M}^{-1} = -\frac{1}{\widehat{\mathbf{k}}^2}\begin{pmatrix} 0 & -M^T(\mathbf{k}) \\ M(\mathbf{k}) & 0\end{pmatrix}\ . \tag{5.39}$$

Then we can write the quadratic part of the fermionic action as:

$$\begin{aligned} S_F^{(2)} &= \frac{1}{4g^2}\sum_{\mathbf{k}}\mathrm{Tr}\,\left[\sum_{ij}\Phi_i(\mathbf{k})\mathcal{M}_{ij}(\mathbf{k})\Phi_j(\mathbf{k})\right] \\ &= \frac{1}{4g^2}\sum_{\mathbf{k}}\sum_{ij,A,B}\Phi_i^A(\mathbf{k})\mathcal{M}_{ij}(\mathbf{k})\Phi_j^B(\mathbf{k})\mathrm{Tr}\,(T^AT^B) \\ &= \frac{1}{8g^2}\sum_{\mathbf{k}}\sum_{ij,A,B}\Phi_i^A(\mathbf{k})\mathcal{M}_{ij}(\mathbf{k})\Phi_j^B(\mathbf{k})\delta_{AB}\ , \end{aligned} \tag{5.40}$$

where we have expanded the fermions as $\Phi=\Phi^AT^A$ and used $\mathrm{Tr}\,(T^AT^B)=\frac{1}{2}\delta_{AB}$. Thus, we write the propagators as:

$$\langle\Phi_i^A(\mathbf{k})\Phi_j^B(\mathbf{k})\rangle = 2\mathcal{M}_{ij}^{-1}(\mathbf{k})\delta_{AB}\ , \tag{5.41}$$

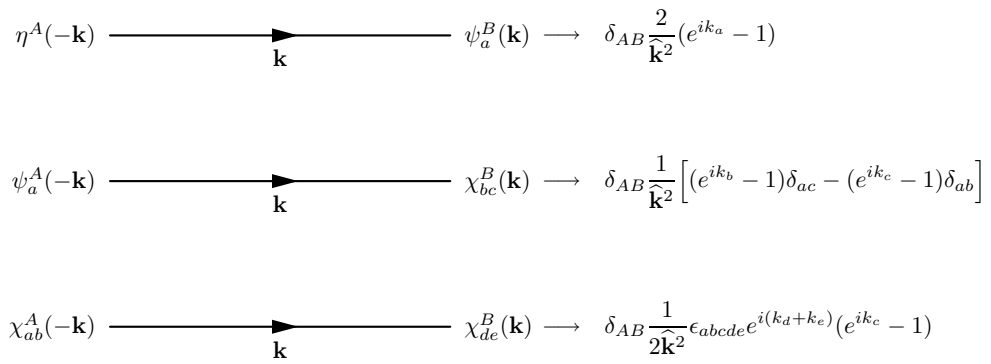

Figure 5.2: Fermionic propagators on the lattice.

or, alternatively,

$$\langle \Psi^A_i(\mathbf{k})\Psi^B_j(-\mathbf{k})\rangle = \frac{2}{\widehat{\mathbf{k}}^2}M^T_{ij}(\mathbf{k})\delta_{AB}\ . \tag{5.42}$$

Notice that by switching the fields (with some relabeling), we have

$$\begin{aligned}\langle \Psi^A_i(-\mathbf{k})\Psi^B_j(\mathbf{k})\rangle &= -\langle \Psi^B_j(\mathbf{k})\Psi^A_i(-\mathbf{k})\rangle \\ &= -\frac{2}{\widehat{\mathbf{k}}^2}M^T_{ji}(\mathbf{k})\delta_{BA} = -\frac{2}{\widehat{\mathbf{k}}^2}M_{ij}(\mathbf{k})\delta_{AB}\ .\end{aligned} \tag{5.43}$$

For a consistency check, we replace $\mathbf{k}$ with $-\mathbf{k}$ and get

$$\langle \Psi^A_i(-\mathbf{k})\Psi^B_j(\mathbf{k})\rangle = \frac{2}{\widehat{\mathbf{k}}^2}M^T_{ij}(-\mathbf{k})\delta_{AB} = -\frac{2}{\widehat{\mathbf{k}}^2}M_{ij}(\mathbf{k})\delta_{AB}\ . \tag{5.44}$$

We must also undo the earlier rescaling of the χ field, giving a factor of $\frac{1}{2}$ in the $\psi\chi$ propagators and a factor of $\frac{1}{4}$ in the $\chi\chi$ propagators. It is also important to note that if we switch the direction of fermion flow in the propagators, then we pick up an additional minus sign.

5.2.3 The vertices on the lattice

The expressions for vertices require additional trace contractions of the gauge group generators. So let us further fix our conventions on the trace algebra.

For the generators T^A of $U(N)$, one has

$$T^AT^B = \frac{1}{2}(d_{ABC} + if_{ABC})T^C\ , \tag{5.45}$$

where d_{ABC} and f_{ABC} are the symmetric and antisymmetric structure constants, respectively. This product formula is consistent with our previous trace convention Tr $(T^AT^B) =$

$\frac{1}{2}\delta_{AB}$ and, in addition, yields the results:

$$\begin{aligned}\mathrm{Tr}\,(T^A T^B T^C) &= \mathrm{Tr}\,\left(\frac{1}{2}(d_{ABD}+if_{ABD})T^D T^C\right) \\ &= \frac{1}{2}(d_{ABD}+if_{ABD})\mathrm{Tr}\,[T^D T^C] \\ &= \frac{1}{2}(d_{ABD}+if_{ABD})\frac{1}{2}\delta_{DC} \\ &= \frac{1}{4}(d_{ABC}+if_{ABC}) = \frac{1}{4}\lambda_{ABC}\ .\end{aligned} \tag{5.46}$$

Since f_{ABC} is antisymmetric and d_{ABC} is symmetric, it follows that

$$\lambda_{ACB} = \overline{\lambda}_{ABC}\ . \tag{5.47}$$

To extract expressions for the vertices, we now return to the original gauge-fixed action for the theory given by

$$\begin{aligned}S &= \frac{1}{g^2}\sum_{\boldsymbol{n}}\mathrm{Tr}\,\Big[\Big(\mathcal{D}_a^{(+)}\mathcal{U}_b(\boldsymbol{n})\Big)^\dagger\Big(\mathcal{D}_a^{(+)}\mathcal{U}_b(\boldsymbol{n})\Big)+\frac{1}{2}\Big(\mathcal{D}_a^{\dagger(-)}\mathcal{U}_a(\boldsymbol{n})\Big)^2 \\ &\quad + 2A_a(\boldsymbol{n})\partial_a^{(+)}\partial_b^{(-)}A_b(\boldsymbol{n}) - \Big(\chi_{ab}(\boldsymbol{n})\mathcal{D}_{[a}^{(+)}\psi_{b]}(\boldsymbol{n})+\eta(\boldsymbol{n})\mathcal{D}_a^{\dagger(-)}\psi_a(\boldsymbol{n}) \\ &\quad + \frac{1}{2}\epsilon_{abcde}\chi_{de}(\boldsymbol{n}+\widehat{\boldsymbol{\mu}}_a+\widehat{\boldsymbol{\mu}}_b+\widehat{\boldsymbol{\mu}}_c)\mathcal{D}_c^{\dagger(-)}\chi_{ab}(\boldsymbol{n}+\widehat{\boldsymbol{\mu}}_c)\Big)\Big]\ .\end{aligned} \tag{5.48}$$

The last three terms of the action give rise to vertices between varying number of $\mathcal{A}$'s and the fermions η, ψ_a, and χ_{ab}. There are three vertices that arise at linear order in $\mathcal{A}$:

The $\psi\overline{\mathcal{A}}\eta$ vertex

$$\begin{aligned}V_{\psi\overline{\mathcal{A}}\eta} &= -\sum_{\boldsymbol{n},a}\mathrm{Tr}\,\Big(\eta(\boldsymbol{n})\mathcal{D}_a^{\dagger(-)}\psi_a(\boldsymbol{n})\Big) \\ &= -\sum_{\boldsymbol{n},a}\mathrm{Tr}\,\Big(\eta(\boldsymbol{n})\psi_a(\boldsymbol{n})\mathcal{U}_a^\dagger(\boldsymbol{n})-\eta(\boldsymbol{n})\mathcal{U}_a^\dagger(\boldsymbol{n}-\widehat{\boldsymbol{\mu}}_a)\psi_a(\boldsymbol{n}-\widehat{\boldsymbol{\mu}}_a)\Big) \\ &= -\sum_{\boldsymbol{n},\mathbf{k},\mathbf{q},\mathbf{p},a}\mathrm{Tr}\;\; e^{i(\mathbf{k}+\mathbf{q}+\mathbf{p})\cdot\boldsymbol{n}}\Big(\eta(\mathbf{k})\psi_a(\mathbf{q})(-i)\overline{\mathcal{A}}_a(\mathbf{p}) \\ &\quad -\eta(\mathbf{k})(-i)\overline{\mathcal{A}}_a(\mathbf{p})e^{ip_a}\psi_a(\mathbf{q})e^{iq_a}\Big) \\ &= \sum_{\mathbf{k},\mathbf{q},\mathbf{p}}\delta_{-\mathbf{k},\mathbf{q}+\mathbf{p}}\eta^C(\mathbf{k})\overline{\mathcal{A}}_b^B(\mathbf{p})\psi_a^A(\mathbf{q})\left(\frac{i}{4}\right)\delta_{ab}[\lambda_{ABC}-\overline{\lambda}_{ABC}e^{-i(p_a+q_a)}]\ .\end{aligned} \tag{5.49}$$

Thus, the Feynman diagram contribution for this vertex is (add a minus since it comes from the first order term of e^{-S}):

$$V_{\eta\overline{\mathcal{A}}\psi} = -\frac{i}{4}\delta_{ab}[\lambda_{ABC}-\overline{\lambda}_{ABC}e^{-i(p_a+q_a)}]\ . \tag{5.50}$$

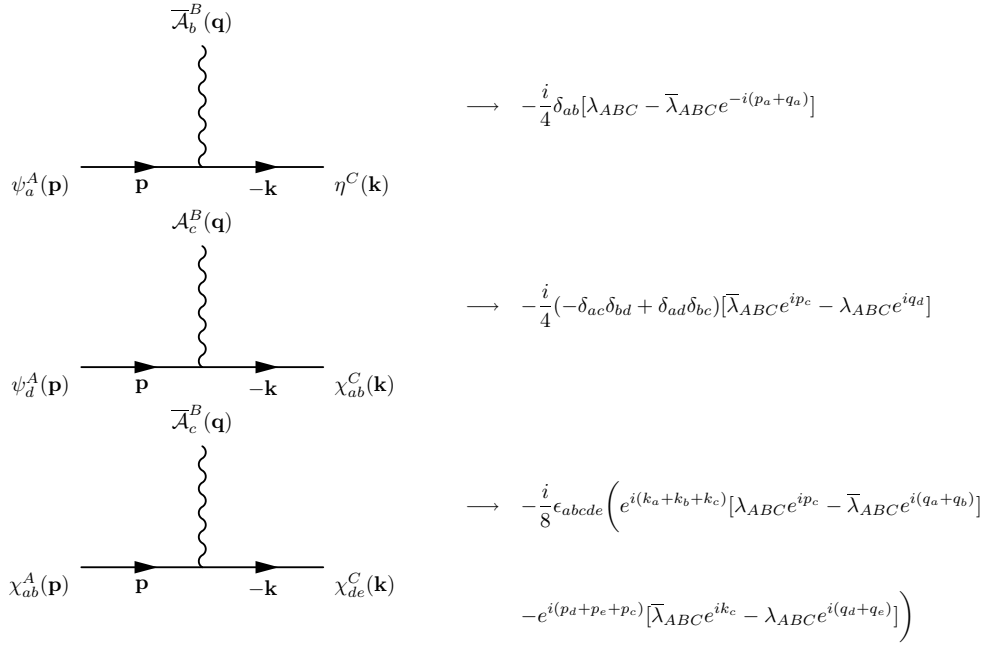

Figure 5.3: Boson-fermion vertices on the lattice.

The $\psi\mathcal{A}\chi$ vertex

$$
\begin{aligned}
V_{\psi\mathcal{A}\chi} &= -\sum_{\boldsymbol{n},a,b} \mathrm{Tr}\; \chi_{ab}(\boldsymbol{n})\mathcal{D}^{(+)}_{[a}\psi_{b]}(\boldsymbol{n}) \\
&= \sum_{\boldsymbol{n},a,b} \mathrm{Tr}\; \Big(-\chi_{ab}(\boldsymbol{n})\mathcal{D}^{(+)}_{a}\psi_{b}(\boldsymbol{n}) + \chi_{ab}(\boldsymbol{n})\mathcal{D}^{(+)}_{b}\psi_{a}(\boldsymbol{n})\Big) \\
&= \sum_{\boldsymbol{n},a,b,c,d} (-\delta_{ac}\delta_{bd} + \delta_{ad}\delta_{bc})\mathrm{Tr}\; \Big[\chi_{ab}(\boldsymbol{n})\Big(\mathcal{U}_c(\boldsymbol{n})\psi_d(\boldsymbol{n}+\widehat{\boldsymbol{\mu}}_c) - \psi_d(\boldsymbol{n})\mathcal{U}_c(\boldsymbol{n}+\widehat{\boldsymbol{\mu}}_d)\Big)\Big] \\
&= \sum_{\mathbf{k},\mathbf{q},\mathbf{p},a,b,c,d} \delta_{-\mathbf{k},\mathbf{q}+\mathbf{p}}(-\delta_{ac}\delta_{bd} + \delta_{ad}\delta_{bc})\chi^C_{ab}(\mathbf{k})\mathcal{A}^B_c(\mathbf{q})\psi^A_d(\mathbf{p}) \\
&\quad \times\frac{i}{4}[\overline{\lambda}_{ABC}e^{ip_c} - \lambda_{ABC}e^{iq_d}]\;. \qquad (5.51)
\end{aligned}
$$

The vertex is given by

$$
V_{\chi\mathcal{A}\psi} = -\frac{i}{4}(-\delta_{ac}\delta_{bd} + \delta_{ad}\delta_{bc})[\overline{\lambda}_{ABC}e^{ip_c} - \lambda_{ABC}e^{iq_d}]\;. \qquad (5.52)
$$

The $\chi\overline{\mathcal{A}}\chi$ vertex

$$\begin{aligned}
V_{\chi\overline{\mathcal{A}}\chi} &= -\frac{1}{2}\sum_{\boldsymbol{n},a,b,c,d,e} \mathrm{Tr}\ \epsilon_{abcde}\chi_{de}(\boldsymbol{n}+\widehat{\boldsymbol{\mu}}_a+\widehat{\boldsymbol{\mu}}_b+\widehat{\boldsymbol{\mu}}_c)\mathcal{D}_c^{\dagger(-)}\chi_{ab}(\boldsymbol{n}+\widehat{\boldsymbol{\mu}}_c) \\
&= -\frac{1}{2}\sum_{\boldsymbol{n},a,b,c,d,e} \mathrm{Tr}\ \epsilon_{abcde}\chi_{de}(\boldsymbol{n}+\widehat{\boldsymbol{\mu}}_a+\widehat{\boldsymbol{\mu}}_b+\widehat{\boldsymbol{\mu}}_c)\Big(\chi_{ab}(\boldsymbol{n}+\widehat{\boldsymbol{\mu}}_c)\mathcal{U}_c^{\dagger}(\boldsymbol{n}) \\
&\quad -\mathcal{U}_c^{\dagger}(\boldsymbol{n}+\widehat{\boldsymbol{\mu}}_a+\widehat{\boldsymbol{\mu}}_b)\chi_{ab}(\boldsymbol{n})\Big) \\
&= \frac{1}{2}\sum_{\mathbf{k},\mathbf{p},\mathbf{q},a,b,c,d,e} \delta_{-\mathbf{k},\mathbf{q}+\mathbf{p}}\epsilon_{abcde}\chi_{de}^{C}(\mathbf{k})\overline{\mathcal{A}}_c^{B}(\mathbf{q})\chi_{ab}^{A}(\mathbf{p}) \\
&\quad \Bigg(e^{i(k_a+k_b+k_c)}\frac{i}{4}[\lambda_{ABC}e^{ip_c}-\overline{\lambda}_{ABC}e^{i(q_a+q_b)}] \\
&\quad -e^{i(p_d+p_e+p_c)}\frac{i}{4}[\overline{\lambda}_{ABC}e^{ik_c}-\lambda_{ABC}e^{i(q_d+q_e)}]\Bigg)\ .
\end{aligned}$$

The vertex is given by (taking into account both possible contractions with external propagators):

$$\begin{aligned}
V_{\chi\overline{\mathcal{A}}\chi} &= -\frac{i}{8}\epsilon_{abcde}\Bigg(e^{i(k_a+k_b+k_c)}[\lambda_{ABC}e^{ip_c}-\overline{\lambda}_{ABC}e^{i(q_a+q_b)}] \\
&\quad -e^{i(p_d+p_e+p_c)}[\overline{\lambda}_{ABC}e^{ik_c}-\lambda_{ABC}e^{i(q_d+q_e)}]\Bigg)\ . \qquad (5.53)
\end{aligned}$$

5.3 One-loop diagrams for the renormalized fermion propagators

It is straightforward to see that we can construct four different *amputated* diagrams using these propagators and vertices. The renormalized fermion propagators receive contributions from these amputated diagrams. We write down these diagrams below. In Appendix A, we show the simplification of these diagrams.

- The amputated $\eta\psi$ diagram.

  We have an $\overline{\mathcal{A}}\mathcal{A}$ propagator, a $\psi\chi$ propagator, an $\eta\overline{\mathcal{A}}\psi$ vertex, and a $\chi\mathcal{A}\psi$ vertex. Using the expressions above, we have:

$$\begin{aligned}
I_{\eta\psi}(\mathbf{p}) &= \sum_{\mathbf{k},\mathbf{q}}\sum_{BC}\sum_{abc}\delta_{-\mathbf{p},\mathbf{k}+\mathbf{q}}\Big[\frac{1}{\widehat{\mathbf{k}}^2}[(e^{ik_b}-1)\delta_{ac}-(e^{ik_c}-1)\delta_{ab}]\Big]\cdot\Big[\frac{1}{\widehat{\mathbf{q}}^2}\Big] \\
&\quad \cdot\Big[\frac{i}{4}[\lambda_{ABC}-\overline{\lambda}_{ABC}e^{i(k_a+q_a)}]\Big] \\
&\quad \cdot\Big[\frac{i}{4}(-\delta_{ba}\delta_{cd}+\delta_{bd}\delta_{ca})[\overline{\lambda}_{BCD}e^{-ip_a}-\lambda_{BCD}e^{iq_d}]\Big]\ . \qquad (5.54)
\end{aligned}$$

- The first amputated $\psi\chi$ diagram.

  We have an $\mathcal{A}\overline{\mathcal{A}}$ propagator, a $\chi\chi$ propagator, a $\psi\mathcal{A}\chi$ vertex, and a $\chi\overline{\mathcal{A}}\chi$ vertex.

$$\begin{aligned} I^1_{\psi\chi}(\mathbf{p}) &= \sum_{\mathbf{k},\mathbf{q}} \sum_{bcdefm} \sum_{BC} \Big[\frac{1}{2\widehat{\mathbf{k}}^2}\epsilon_{bcmef} e^{i(k_e+k_f)}(e^{ik_m}-1)\Big] \\ &\quad \cdot\Big[\frac{1}{\widehat{\mathbf{q}}^2}\Big]\cdot\Big[-\frac{i}{4}(-\delta_{bd}\delta_{ca}+\delta_{ba}\delta_{cd})[\overline{\lambda}_{ACB}e^{ip_d}-\lambda_{ACB}e^{-iq_a}]\Big] \\ &\quad \cdot\Big[\frac{i}{8}\epsilon_{efdgh}\Big(e^{ik_{(d+g+h)}}[\overline{\lambda}_{BCD}e^{-ip_d}-\lambda_{BCD}e^{i(q_g+q_h)}]\Big] \\ &\quad -e^{-ip_{(d+e+f)}}[\lambda_{BCD}e^{ik_d}-\overline{\lambda}_{BCD}e^{i(q_e+q_f)}]\Big)\Big] \ . \end{aligned} \tag{5.55}$$

- The second amputated $\psi\chi$ diagram.

  It has an $\overline{\mathcal{A}}\mathcal{A}$ propagator, an $\eta\psi$ propagator, a $\psi\overline{\mathcal{A}}\eta$ vertex, and a $\psi\mathcal{A}\chi$ vertex. This yields:

$$\begin{aligned} I^2_{\psi\chi}(\mathbf{p}) &= \sum_{\mathbf{k},\mathbf{q}} \sum_{bc} \sum_{BC} \Big[\frac{2}{\widehat{\mathbf{k}}^2}(e^{ik_c}-1)\Big]\cdot\Big[\frac{1}{\widehat{\mathbf{q}}^2}\Big]\cdot\delta_{ab}\Big[-\frac{i}{4}[\lambda_{ACB}-\overline{\lambda}_{ACB}e^{-i(p_a-q_a)}]\Big] \\ &\quad \cdot\Big[-\frac{i}{4}(-\delta_{db}\delta_{ec}+\delta_{dc}\delta_{eb})[\lambda_{DCB}e^{ik_b}-\overline{\lambda}_{DCB}e^{iq_c}]\Big] \ . \end{aligned} \tag{5.56}$$

- The amputated $\chi\chi$ diagram.

  It has a $\overline{\mathcal{A}}\mathcal{A}$ propagator, a $\chi\psi$ propagator, a $\chi\overline{\mathcal{A}}\chi$ vertex, and a $\psi\mathcal{A}\chi$.

$$\begin{aligned} I_{\chi\chi}(\mathbf{p}) &= \sum_{\mathbf{k},\mathbf{q}} \sum_{cdef} \sum_{BC} \delta_{\mathbf{k}+\mathbf{q}-\mathbf{p},0}\Big[\frac{1}{\widehat{\mathbf{k}}^2}[(e^{-ik_e}-1)\delta_{fd}-(e^{-ik_d}-1)\delta_{fe}]\Big]\cdot\Big[\frac{1}{\widehat{\mathbf{q}}^2}\Big] \\ &\quad \cdot\Big[-\frac{i}{8}\epsilon_{abcde}\Big(e^{-ik_{(a+b+c)}}[\lambda_{ACB}e^{ip_c}-\overline{\lambda}_{ACB}e^{-i(q_a+q_b)}] \\ &\quad -e^{ip_{(c+d+e)}}[\overline{\lambda}_{ACB}e^{-ik_c}-\lambda_{ACB}e^{-i(q_d+q_e)}]\Big)\Big] \\ &\quad \cdot\Big[-\frac{i}{4}(-\delta_{gc}\delta_{hf}+\delta_{gf}\delta_{hc})[\overline{\lambda}_{BCD}e^{ik_c}-\lambda_{BCD}e^{iq_f}]\Big] \ . \end{aligned} \tag{5.57}$$

The contributions of these diagrams all vanish in the limit $p \to 0$, indicating that mass counterterms are absent in the lattice theory at one-loop. We show the details of this calculation in Appendix B. In our general argument of section 5.1, we argued that the only dangerous mass term involved a coupling of η and ψ_a. We now see that this term does not arise at one-loop. In the next section, we will show that this feature persists to all orders and, thus, our general conclusion will be that *no mass counterterms are needed at any finite order of perturbation theory.*

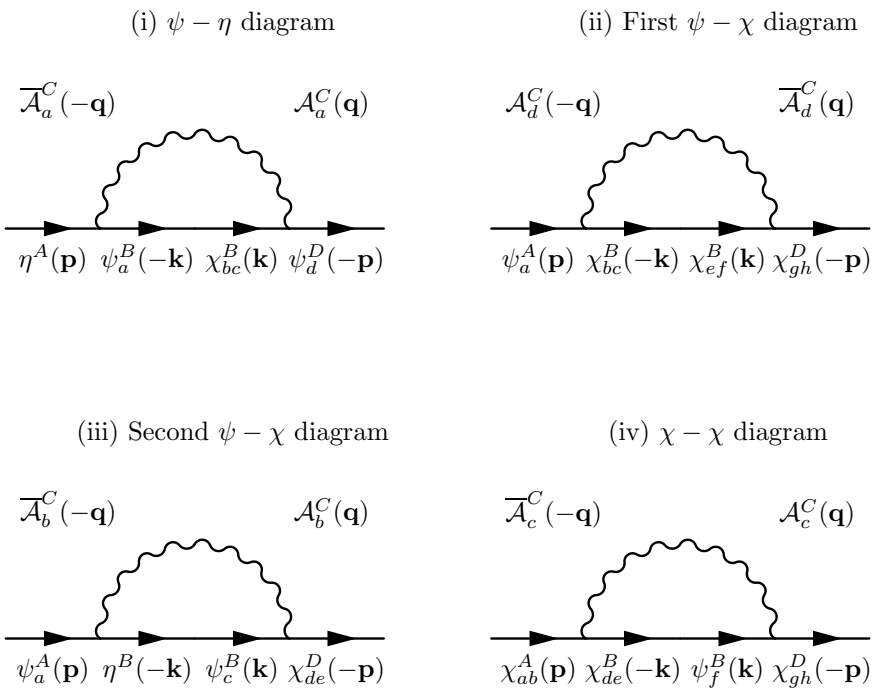

Figure 5.4: One-loop diagrams of fermions and complexified gauge fields.

5.4 The effective action

In this section, we will compute the partition function of the lattice theory in one-loop order around an arbitrary classical vacuum state in which the fermions vanish and the bosonic fields correspond to constant commuting matrices. To start, we expand the fields around such a constant commuting background,

$$\mathcal{U}_a(\boldsymbol{n}) = \mathcal{U}_a + i\mathcal{A}_a(\boldsymbol{n}), \quad \mathcal{U}_a^\dagger(\boldsymbol{n}) = \mathcal{U}_a^\dagger - i\overline{\mathcal{A}}_a(\boldsymbol{n}) \ . \tag{5.58}$$

Choosing the gauge $\alpha = 1/2$, the quadratic part of the bosonic action then takes the form

$$S_B = -2 \sum_{\boldsymbol{n},a,b} \mathrm{Tr}\ \mathcal{A}_b(\boldsymbol{n}) \mathcal{D}_a^{\dagger(-)} \mathcal{D}_a^{(+)} \mathcal{A}_b(\boldsymbol{n}) \ . \tag{5.59}$$

Here the covariant derivatives depend on the constant commuting classical background $[\mathcal{U}_a, \mathcal{U}_a^\dagger] = 0$. After integration over the fluctuations in the bosonic fields, we find that the bosonic contribution to the one-loop partition function is given by

$$\det{}^{-5}(\mathcal{D}_a^{\dagger(-)} \mathcal{D}_a^{(+)}) \ . \tag{5.60}$$

The gauge-fixing functional (5.25) leads to the quadratic ghost action:

$$S_G = \sum_{\boldsymbol{n},a} \mathrm{Tr}\ \overline{c}\, \mathcal{D}_a^{\dagger(-)} \mathcal{D}_a^{(+)} c \ . \tag{5.61}$$

The quadratic fermionic part of the action is given by the corresponding terms in (5.7), except that now the covariant derivatives depend only on the background fields.

Since the background is constant, we can pass to momentum space in which the action separates into terms for each mode $\mathbf{k}$. The 16×16 fermion matrix $M(\mathbf{k})$ for the mode $\mathbf{k}$ then can be shown (using MAPLE to compute the determinant) to satisfy

$$\det M(\mathbf{k}) = \det(\mathcal{D}_a^{\dagger(-)}(\mathbf{k})\mathcal{D}_a^{(+)}(\mathbf{k}))^8 \ . \tag{5.62}$$

Going back to position space, and taking into account the fact that there is a double counting of modes in the matrix form (5.36), we obtain

$$\mathrm{Pf}(\mathcal{M}) = \det{}^4(\mathcal{D}_a^{\dagger(-)}\mathcal{D}_a^{(+)}) \ . \tag{5.63}$$

The ghosts add another factor of $\det(\overline{\mathcal{D}}_a^{\dagger(-)}\mathcal{D}_a^{(+)})$, which is just what is needed to cancel the bosonic contribution given earlier.

In conclusion, we have shown that the one-loop effective action of the lattice theory obtained by expanding about an arbitrary point in the classical moduli space is identically zero. Thus, as for the continuum, the moduli space is not lifted in this analysis and, hence, there can be no boson or fermion masses at one-loop. Furthermore, we expect that we can extend this analysis to all loops since the partition function of the lattice theory is a topological invariant and, hence, can be computed exactly in the semi-classical approximation (see Appendix C). Indeed, Matsuura uses similar arguments to show that the vacuum energy of supersymmetric lattice theories with four and eight supercharges remains zero to all orders in the coupling [50]. The calculation presented here extends this to the case of sixteen supercharges[3]. Thus, we conclude that boson and scalar masses remain zero to all orders in the coupling constant. This implies that the fermions also remain massless, which is consistent with our explicit one-loop calculation.

At this point, we have derived expressions for the amputated one-loop diagrams that contribute to the renormalization of the three twisted fermion propagators. This is sufficient to calculate α_1, α_2 and α_4 that appear in the general action:

$$\begin{aligned}\mathcal{L} \ = \ & \frac{1}{g^2}\sum_{\boldsymbol{n},a,b,c,d,e}\Big\{\mathcal{Q}\ \mathrm{Tr}\Big[-i\alpha_1\chi_{ab}\mathcal{D}_a^{(+)}\mathcal{U}_b(\boldsymbol{n}) - i\alpha_2\eta(\boldsymbol{n})\mathcal{D}_a^{\dagger(-)}\mathcal{U}_a(\boldsymbol{n}) + \frac{\alpha_3}{2}\eta(\boldsymbol{n})d(\boldsymbol{n})\Big] \\ & -\frac{\alpha_4}{2}\mathrm{Tr}\ \epsilon_{abcde}\chi_{de}(\boldsymbol{n}+\widehat{\boldsymbol{\mu}}_a+\widehat{\boldsymbol{\mu}}_b+\widehat{\boldsymbol{\mu}}_c)\mathcal{D}_c^{\dagger(-)}\chi_{ab}(\boldsymbol{n}+\widehat{\boldsymbol{\mu}}_c)\Big\} \ .\end{aligned} \tag{5.64}$$

However the coefficient α_3 requires further work. One simple way to extract it is via a computation of the renormalized auxiliary boson propagator that we turn to in the next section.

[3]Notice that in this calculation we have not included any mass terms that would guarantee the stability of the initial classical vacuum state we have chosen to expand around. We have also ignored a potential sign problem associated with the replacement of a Pfaffian with a square root of a determinant. Nevertheless, we expect the result to be robust; the existence of an exact supersymmetry should ensure that the object we are computing is a lattice regularized Witten index and hence independent of both coupling constant and background field.

5.5 One-loop diagrams for the auxiliary field propagator

We have shown that the off-shell form of the bosonic action is given by

$$S_B = \sum_{\boldsymbol{n},a,b} \mathrm{Tr}\,\left(\mathcal{F}^\dagger_{ab}(\boldsymbol{n})\mathcal{F}_{ab}(\boldsymbol{n}) - \frac{i}{g}d(\boldsymbol{n})\mathcal{D}^{\dagger(-)}_a\mathcal{U}_a(\boldsymbol{n}) + \frac{1}{2}d^2(\boldsymbol{n})\right)\,, \tag{5.65}$$

where $\mathcal{F}_{ab}(\boldsymbol{n}) = -\frac{i}{g}\mathcal{D}^{(+)}_a\mathcal{U}_b(\boldsymbol{n})$.

In our previous computation of the fermion diagrams, we integrated out the field d to give an on-shell action defined just in terms of the complex gauge link fields $\mathcal{U}_a$ and $\mathcal{U}^\dagger_a$. In this section we will not do this but, instead, focus on a computation of the renormalized propagator for the d field. The Feynman rules for the fermions will be identical to our previous scheme, but the boson propagators will change and so we need to recompute those propagators in this off-shell scheme. We proceed in the standard fashion by expanding the link field $\mathcal{U}_a(\boldsymbol{n})$:

$$\mathcal{U}_a(\boldsymbol{n}) = \mathbf{1} + ig\mathcal{A}_a(\boldsymbol{n}),\;\; \mathcal{U}^\dagger_a(\boldsymbol{n}) = \mathbf{1} - ig\overline{\mathcal{A}}_a(\boldsymbol{n}). \tag{5.66}$$

and using the same lattice gauge-fixing term as before

$$S_{GF}[A] = -\frac{1}{\alpha}\sum_{\boldsymbol{n},a}\mathrm{Tr}\,(\partial^{(-)}_a A_a(\boldsymbol{n}))^2, \tag{5.67}$$

we find the momentum space form:

$$S_{GF}[A] = \frac{1}{\alpha}\sum_{\mathbf{k},a,b}\mathrm{Tr}\,A_a(\mathbf{k})f^*_a(\mathbf{k})f_b(\mathbf{k})A_b(-\mathbf{k})\;. \tag{5.68}$$

It is convenient in this calculation to work with the real and imaginary parts of the complex gauge field explicitly, thus,

$$\mathcal{A}_a = A_a + iB_a\;. \tag{5.69}$$

The gauge-fixed bosonic action on the lattice to quadratic order in fields, with the choice $\alpha = \frac{1}{2}$, is then

$$\begin{aligned} S^{(2)}_B \;=\; & \sum_{\mathbf{k},a,b}\mathrm{Tr}\,2A_a(\mathbf{k})\Big[\delta_{ab}f_c(\mathbf{k})f^*_c(\mathbf{k})\Big]A_b(-\mathbf{k}) \\ & +2B_a(\mathbf{k})\Big[\delta_{ab}f_c(\mathbf{k})f^*_c(\mathbf{k}) - f^*_a(\mathbf{k})f_b(\mathbf{k})\Big]B_b(-\mathbf{k}) \\ & -2id(\mathbf{k})f_a(\mathbf{k})B_a(-\mathbf{k}) + \frac{1}{2}d(\mathbf{k})d(-\mathbf{k})\;. \end{aligned} \tag{5.70}$$

We see that the $d - B_a$ system decouples from A_a to this order. Its action is given by

$$\begin{aligned} S^{(2)}_B[d,B_a] \;\sim\; & \sum_{\mathbf{k},a,b}\mathrm{Tr}\,2B_a(\mathbf{k})\Big[\delta_{ab}f^*_c(\mathbf{k})f_c(\mathbf{k}) - f^*_a(\mathbf{k})f_b(\mathbf{k})\Big]B_b(-\mathbf{k}) \\ & -2id(\mathbf{k})f_a(\mathbf{k})B_a(-\mathbf{k}) + \frac{1}{2}d(\mathbf{k})d(-\mathbf{k})\;. \end{aligned} \tag{5.71}$$

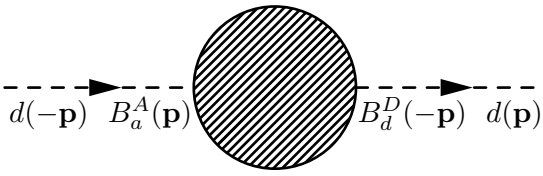

Figure 5.5: The generic diagram contributing to renormalized d propagator

or in matrix form

$$\left(\begin{array}{cc} d & B_a \end{array} \right)(\mathbf{k}) \left(\begin{array}{cc} \frac{1}{2} & -if_b(\mathbf{k}) \\ -if_a^*(\mathbf{k}) & M_{ab}(\mathbf{k}) \end{array} \right) \left(\begin{array}{c} d \\ B_b \end{array} \right)(-\mathbf{k}) \; , \tag{5.72}$$

where $M_{ab}(\mathbf{k}) = 2[\delta_{ab} \sum_c f_c(\mathbf{k}) f_c^*(\mathbf{k}) - f_a^*(\mathbf{k}) f_b(\mathbf{k})]$. Using standard identities for the inverse of a partitioned matrix, we find

$$M^{-1} = \left(\begin{array}{cc} \frac{1}{2} & -if_b(\mathbf{k}) \\ -if_a^*(\mathbf{k}) & M_{ab}(\mathbf{k}) \end{array} \right)^{-1} = \frac{1}{\sum_c f_c(\mathbf{k}) f_c^*(\mathbf{k})} \left(\begin{array}{cc} 0 & if_b(\mathbf{k}) \\ if_a^*(\mathbf{k}) & \frac{1}{2}\mathbf{1}_5 \end{array} \right) \; . \tag{5.73}$$

We have $\sum_c f_c(\mathbf{k}) f_c^*(\mathbf{k}) = 4 \sum_c \sin^2\left(\frac{\mathbf{k}_c}{2}\right)$ and, as before, we define $\widehat{\mathbf{k}}^2 \equiv 4 \sum_c \sin^2\left(\frac{\mathbf{k}_c}{2}\right)$. Thus the lattice propagators are

$$\langle d^A(\mathbf{k}) d^B(-\mathbf{k}) \rangle = 0 \; , \tag{5.74}$$

$$\langle d^A(\mathbf{k}) B_a^B(-\mathbf{k}) \rangle = i\delta_{AB} \frac{(e^{-ik_a} - 1)}{\widehat{\mathbf{k}}^2} \; , \tag{5.75}$$

$$\langle B_a^A(\mathbf{k}) B_b^B(-\mathbf{k}) \rangle = \delta_{ab}\delta_{AB} \frac{1}{2\widehat{\mathbf{k}}^2} \; . \tag{5.76}$$

From (5.70) the propagator for the A field is also

$$\langle A_a^A(\mathbf{k}) A_b^B(-\mathbf{k}) \rangle = \delta_{ab}\delta_{AB} \frac{1}{2\widehat{\mathbf{k}}^2} \; . \tag{5.77}$$

Notice that the field d is non-propagating at tree level. Using these propagators and those derived earlier for the bosons and fermions, we can now write down the generic Feynman diagram contributing to a renormalization of the auxiliary boson propagator. It is shown in figure 5.5 and represents the set of amputated diagrams possessing two external B field legs. These combine with the external $\langle dB \rangle$ propagators derived above to yield the renormalized propagator for the auxiliary field d. Notice that the vanishing of the tree level $\langle dd \rangle$ propagators ensures that no amputated diagrams with 2 d field external legs contribute. The set of all such lattice Feynman diagrams is shown below and corresponds to a subset of the B field vacuum polarization diagrams. It is important to notice that almost all these diagrams appear in the continuum off-shell twisted theory. The exceptions are just the diagrams containing a BBd vertex that corresponds to the lattice vertex

$$V_{dBB} = \langle d^A(-\mathbf{k}-\mathbf{q}) B_a^B(\mathbf{k}) B_b^C(\mathbf{q}) \rangle = \frac{i}{2}\delta_{ab}(\lambda_{ABC} + \overline{\lambda}_{ABC})(1 - e^{-i(k_a+q_a)}) \; . \tag{5.78}$$

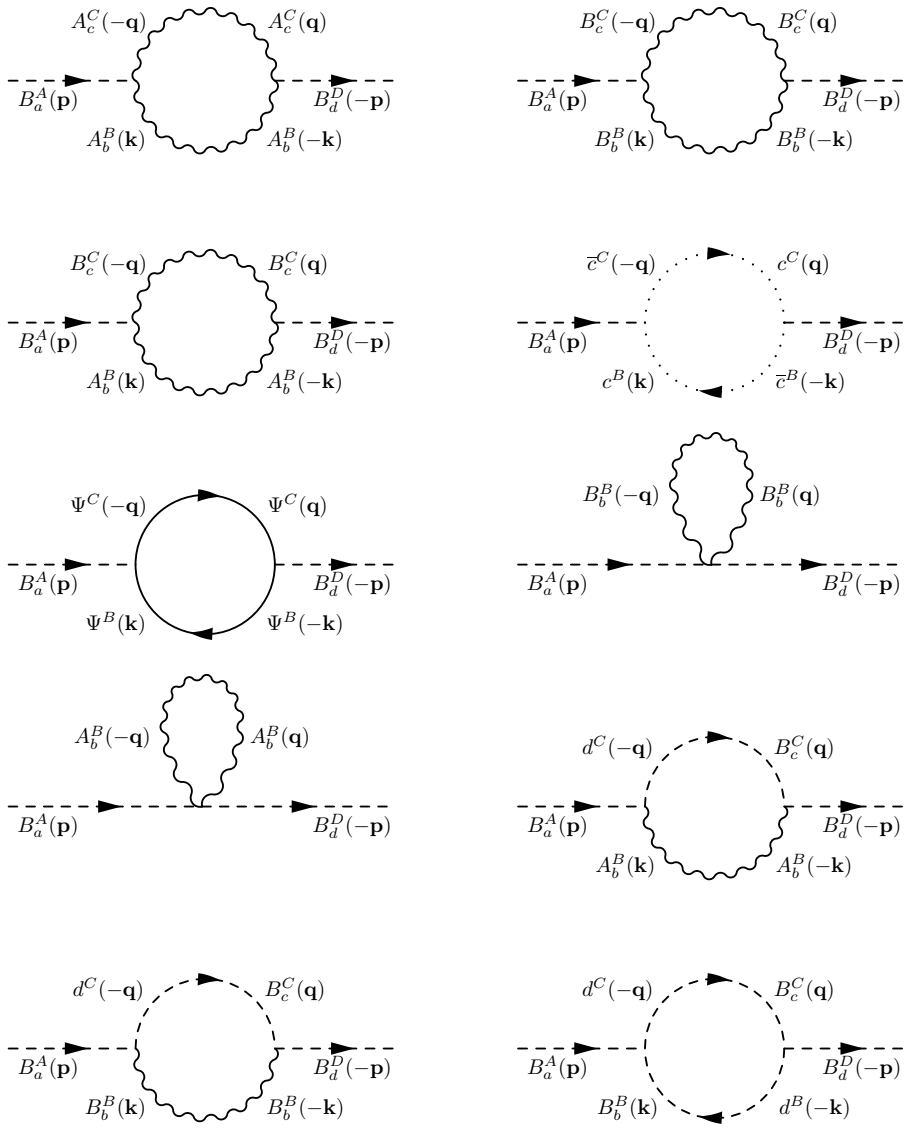

Figure 5.6: Set of all lattice amputated Feynman diagrams contributing the renormalized d propagator.

Clearly, this vertex vanishes as the lattice spacing is sent to zero and, hence, this diagram does not contribute to the divergent piece in the $\langle dd \rangle$ propagator at this order of perturbation theory.

Hence, we are left with a set of diagrams that correspond to those of the equivalent continuum theory at one-loop order. This fact can be exploited later to allow us to argue that the leading logarithmic divergences of the lattice theory are shared with the continuum theory. Anticipating this, we will not write down explicit expressions for these amputated lattice diagrams in this section.

5.6 Divergence structure of the one-loop diagrams

At this point, we have derived expressions for the amputated one-loop diagrams that determine the renormalization of three fermion propagators and also the set of Feynman graphs needed to renormalize the auxiliary bosonic field propagator. In principle, this input will allow us to determine all four coefficients α_i appearing in the renormalized action (5.11). Of course, the question of how much fine tuning is required to regain full supersymmetry is determined by the parts of these expressions that diverge as the lattice spacing is sent to zero. We must, therefore, evaluate the expressions for the one-loop integrals as the lattice spacing tends to zero.

First, let us discuss the diagrams contributing to the fermion propagators. We have shown in Appendix B that the one-loop fermion propagators all vanish for vanishing external momentum, which is consistent with our effective action computation showing that no fermionic mass terms can be generated perturbatively. Reisz's power counting theorem [51]-[54] shows us that we cannot simply take the naive continuum limit of the expressions for the amputated one-loop diagrams as they have a naive degree of divergence of 1. However, we can use a trick due to [55] and detailed in [56] to extract the leading divergences.

We split the integral $I(\mathbf{p})$ into two pieces as follows:

$$\begin{aligned} \lim_{a\to 0} I(\mathbf{p}) &= \lim_{a\to 0}\left[I(\mathbf{p}) - I(\mathbf{0}) - \sum_b p_b \frac{\partial I}{\partial p_b}\Big|_{\mathbf{p}=\mathbf{0}} \right] \\ &\quad + \lim_{a\to 0}\left[I(\mathbf{0}) + \sum_b p_b \frac{\partial I}{\partial p_b}\Big|_{\mathbf{p}=\mathbf{0}} \right] . \end{aligned} \tag{5.79}$$

The first term in square brackets can now be evaluated in the naive continuum limit and contains no divergence. The second term contains the divergence but contains no external momenta in the integrand, which simplifies its evaluation on the lattice. In addition we know that $I(\mathbf{0})$ vanishes for each of our diagrams so the calculation becomes simpler still.

We will find that the resulting expressions have logarithmic divergences of the form $\log \mu a$, where μ is a small mass parameter used to regulate the behavior of the integrand close to the origin of momentum space and a the lattice spacing[4].

[4]We will only consider the case of infinite lattice size which reduces all lattice sums in momentum space to integrals.

One obvious way to proceed is simply to numerically evaluate the integral for a variety of regulator masses μ and extract the logarithmic divergence and any constant contributions using a fitting procedure. However, if we are only interested in the leading log divergences, there is a simpler approach detailed in the next section in which a naive continuum limit can be taken and the expressions evaluated using, for example, dimensional regularization.

In the next section, we give an example of this procedure for the amputated $\eta\psi$ diagram and show how to extract similar results for the remaining fermion self-energy diagrams. We will also see that the same procedure allows us to argue that the leading log divergent contribution to α_3 is also equal to its value in the continuum theory.

5.6.1 The amputated fermion diagrams

We start with our simplified expression for $I_{\eta\psi_d}(\mathbf{p})$ given in Appendix A

$$\begin{aligned} I_{\eta\psi_d}(\mathbf{p}) &= \int \frac{d^4\mathbf{q}}{(2\pi)^4} \sum_{BC} \left[\frac{(1-e^{i(p-q)_d})}{8\widehat{(\mathbf{p}-\mathbf{q})}^2 \widehat{\mathbf{q}}^2} \right] \Big[-\sum_{a\neq d} \big[d_{ABC} d_{BCD} \\ &\quad \times (e^{-ip_a} - e^{iq_d} - 1 + e^{ip_a+iq_d}) \\ &\quad + f_{ABC} f_{BCD} (e^{-ip_a} + e^{iq_d} + 1 + e^{ip_a+iq_d}) \big] \Big] \, . \end{aligned} \tag{5.80}$$

As a first step we need to calculate the derivative of the diagram (re-inserting the lattice spacing a and the infra-red cutoff μ)

$$\begin{aligned} \left. \frac{\partial I_{\eta\psi_d}(\mathbf{p})}{\partial p_b} \right|_{\mathbf{p}=\mathbf{0}} &= \int_{\frac{-\pi}{a}}^{\frac{\pi}{a}} \frac{d^4\mathbf{q}}{(2\pi)^4} \frac{-2a^4 \sin aq_b}{(\widehat{\mathbf{q}}^2 + \mu^2 a^2)^3} (1-e^{-iaq_d}) f_{ABC} f_{BCD} (1+e^{iaq_d}) \\ &\quad + \int_{\frac{-\pi}{a}}^{\frac{\pi}{a}} \frac{d^4\mathbf{q}}{(2\pi)^4} \frac{-a^3}{(\widehat{\mathbf{q}}^2 + \mu^2 a^2)^2} (-ia\delta_{db} e^{-iaq_d}) f_{ABC} f_{BCD} (1+e^{iaq_d}) \\ &\quad + \int_{\frac{-\pi}{a}}^{\frac{\pi}{a}} \frac{d^4\mathbf{q}}{(2\pi)^4} \frac{-a^3}{8(\widehat{\mathbf{q}}^2 + \mu^2 a^2)^2} (1-e^{-iaq_d}) \\ &\quad \times \sum_{a\neq d} (d_{ABC} d_{BCD} + f_{ABC} f_{BCD}) \delta_{ab} (-ia)(1-e^{iaq_d}) \, . \end{aligned} \tag{5.81}$$

A further simplification now occurs. If we are only interested in the leading $\log \mu a$ coefficient, we can evaluate this integral in a small q region around zero. This is because the contribution of the integrand to the $\log \mu a$ coefficient comes only from small q. Furthermore, in the region $q \to 0$, the propagators and vertices inside the integral will approach their continuum counterparts and, hence, the logarithmic divergence can be extracted by replacing the lattice integrals by their naive continuum limit. Note that this only works for the coefficient of the log - we must evaluate the integral numerically (and then fit) in order to extract the constant terms.

Thus, we find:

$$\lim_{a\to 0}\left.\frac{\partial I_{\eta\psi_d}(\mathbf{p})}{\partial p_b}\right|_{\mathbf{p}=\mathbf{0}} \sim \int_{-\infty}^{\infty}\frac{d^4\mathbf{q}}{(2\pi)^4}\frac{-4iq_bq_d}{(q^2+\mu^2)^3}f_{ABC}f_{BCD} + \int_{-\infty}^{\infty}\frac{d^4\mathbf{q}}{(2\pi)^4}\frac{2i\delta_{db}}{(q^2+\mu^2)^2}f_{ABC}f_{BCD}\ . \tag{5.82}$$

Note that we cannot just set the first term in this expression to zero as $\widehat{e}_d$ and $\widehat{e}_b$ are not orthogonal to each other; instead, we have:

$$\begin{aligned}\int d^d\mathbf{q}\frac{q_bq_d}{(q^2+\mu^2)^3} &= e_b^\mu e_d^\nu\int d^d\mathbf{q}\frac{q^\mu q^\nu}{(q^2+\mu^2)^3}\\ &= \widehat{e}_b\cdot\widehat{e}_d\int d^d\mathbf{q}\frac{q^2}{d(q^2+\mu^2)^3}\ .\end{aligned} \tag{5.83}$$

Then $\widehat{e}_b\cdot\widehat{e}_d=\delta_{bd}-\frac{1}{5}$. We use dimensional regularization and the fact that $\sum_b p_b=0$ to evaluate the resulting integrals getting

$$\begin{aligned}I_{\eta\psi_d}(\mathbf{p}) &\sim \sum_b p_b\left.\frac{\partial I_{\eta\psi_d}(\mathbf{p})}{\partial p_b}\right|_{\mathbf{p}=\mathbf{0}}\\ &\sim -\frac{i}{8\pi^2}p_d f_{ABC}f_{BCD}\log\mu a\ .\end{aligned} \tag{5.84}$$

Note that we have inserted the cutoff $\frac{1}{a}$ inside the logarithm to ensure that it is dimensionless.

Since all the Feynman graphs we need to evaluate are logarithmically divergent and in one-to-one correspondence with continuum diagrams, the resulting logarithmic divergences can all be extracted by following a similar procedure i.e. taking the naive continuum limit of the relevant $I(\mathbf{p})$.

$$\begin{aligned}\lim_{a\to 0}I^{(1)}_{\psi_a\chi_{gh}}(\mathbf{p}) &\sim \int\frac{d^4\mathbf{q}}{(2\pi)^4}\sum_m\frac{-i(p-q)_m}{2(q^2+\mu^2)((\mathbf{p}-\mathbf{q})^2+\mu^2)}\\ &\quad\times\left(3\delta_{ag}\delta_{mh}-3\delta_{ah}\delta_{mg}\right)f_{ABC}f_{BCD}\\ &\sim \frac{3i}{32\pi^2}f_{ABC}f_{BCD}\left(\delta_{ag}p_h-\delta_{ah}p_g\right)\log\mu a\ .\end{aligned} \tag{5.85}$$

$$\begin{aligned}\lim_{a\to 0}I^{(2)}_{\psi_a\chi_{de}}(\mathbf{p}) &\sim \int\frac{d^4\mathbf{q}}{(2\pi)^4}\sum_c\frac{-i(p-q)_c}{2(q^2+\mu^2)((\mathbf{p}-\mathbf{q})^2+\mu^2)}\\ &\quad\times(\delta_{da}\delta_{ec}-\delta_{dc}\delta_{ea})f_{ABC}f_{BCD}\\ &\sim \frac{i}{32\pi^2}f_{ABC}f_{BCD}(\delta_{da}p_e-\delta_{ea}p_d)\log\mu a\ .\end{aligned} \tag{5.86}$$

This obviously leads us to define $I_{\psi_a\chi_{de}}(\mathbf{p})=I^{(1)}_{\psi_a\chi_{de}}(\mathbf{p})+I^{(2)}_{\psi_a\chi_{de}}(\mathbf{p})$ and therefore

$$I_{\psi_a\chi_{de}}(\mathbf{p}) \sim \frac{i}{8\pi^2}f_{ABC}f_{BCD}(\delta_{da}p_e-\delta_{ea}p_d) \tag{5.87}$$

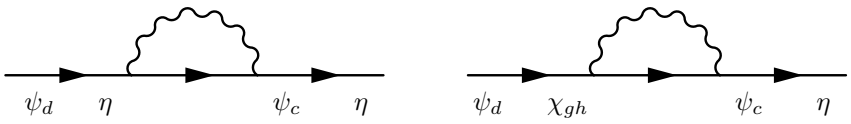

Figure 5.7: Full $\eta\psi$ propagators.

$$\begin{aligned}\lim_{a\to 0} I_{\chi_{ab}\chi_{gh}}(\mathbf{p}) &\sim \int \frac{d^4\mathbf{q}}{(2\pi)^4}\sum_d \frac{i(p-q)_d}{2(q^2+\mu^2)((\mathbf{p}-\mathbf{q})^2+\mu^2)}\epsilon_{abdgh}f_{ABC}f_{BCD} \\ &\quad -(h\leftrightarrow g) \\ &\sim -\frac{i}{16\pi^2}f_{ABC}f_{BCD}\sum_d \epsilon_{abdgh}p_d \log\mu a \ . \end{aligned} \tag{5.88}$$

Note that these calculations of the log terms for the other diagrams have also been verified by numerical evaluation and fitting of the resulting lattice integrals.

5.6.2 The auxiliary field diagram

Since the amputated divergent diagrams for the lattice d propagator are log divergent, we can extract the sum of these logarithmic divergences using the same tricks we used for the fermions, evaluating the diagram in the naive continuum limit. The sum of all these diagrams, contracted with external dB propagators, will then yield a log divergent term of the form

$$C_{dd} = cf_{ACB}f_{DCB}\log(\mu a) \ , \tag{5.89}$$

where c is a constant to be determined by explicitly evaluating the diagrams. However, we will argue in the next section that it is not necessary to evaluate these diagrams, even in the continuum, to determine α_3 – the requirement that the continuum theory preserve full supersymmetry will automatically determine α_3 in terms of the other α_i corresponding to the fermion propagator renormalization.

5.6.3 From amputated diagrams to renormalized propagators

The leading logarithmic divergences appearing in the renormalized propagators are obtained by combining the (divergent parts of) the individual amputated diagrams we have just computed. In principle, several of the amputated fermion diagrams can appear as internal bubbles when correcting a given fermion propagator. As an example, consider the $\psi\eta$ diagram shown in Figure 5.7. Naively, we see that three of our amputated diagrams contribute to the renormalization of this propagator. However, we find that (at least in the case of the log divergences) the Lorentz structure of the propagators and integrals means that only the $\eta\psi$ amputated diagram contributes to the renormalization of the $\eta\psi$ propagator.

We demonstrate this through explicit calculation. Denoting the full diagrams by C and noting that, as we are dealing with only the divergent part, we can approximate the

lattice propagators by their continuum analogues we find

$$\begin{aligned} C_{\psi_d\eta} &= \frac{2ip_d}{p^2}\sum_c I_{\eta\psi_c}(\mathbf{p})\frac{2ip_c}{p^2} + \sum_{c,g,h}\frac{ip_g\delta_{dh} - ip_h\delta_{dg}}{p^2} I_{\chi_{gh}\psi_c}(\mathbf{p})\frac{2ip_c}{p^2} \\ &\sim -\frac{2ip_d}{p^2}\frac{i}{8\pi^2}f_{ABC}f_{BCD}\sum_c p_c\frac{2ip_c}{p^2}\log\mu a \\ &\sim \frac{1}{4\pi^2}f_{ABC}f_{BCD}\frac{2ip_d}{p^2}\log\mu a\ . \end{aligned} \tag{5.90}$$

The second term disappears as

$$\begin{aligned} \sum_{c,g,h}(p_g\delta_{dh} - p_h\delta_{dg})(\delta_{cg}p_h - \delta_{ch}p_g)p_c &= \sum_c (p_cp_d - p^2\delta_{cd} - p^2\delta_{dc} + p_cp_d)p_c \\ &= 0\ . \end{aligned} \tag{5.91}$$

We can similarly show that only $I_{\psi\chi}$ contributes to $C_{\psi\chi}$ and $I_{\chi\chi}$ to $C_{\chi\chi}$. Note, however, that this analysis strictly only applies to the logarithmically divergent piece in C.

$$\begin{aligned} C_{\psi_a\chi_{de}} &= \frac{i}{8\pi^2}f_{ABC}f_{BCD}\sum_{g,h,c}\frac{ip_g\delta_{ah} - ip_h\delta_{ag}}{p^2}(\delta_{gc}p_h - \delta_{hc}p_g) \\ &\quad\times\frac{ip_d\delta_{ce} - ip_e\delta_{cd}}{p^2}\log\mu a \\ &= \frac{1}{4\pi^2}f_{ABC}f_{BCD}\frac{ip_d\delta_{ae} - ip_e\delta_{ad}}{p^2}\ \log\mu a\ . \end{aligned} \tag{5.92}$$

In calculating $C_{\chi\chi}$ we must take into account that the internal propagator in $I_{\chi\chi}$ can be a $\psi\chi$ or $\chi\psi$. This contributes another factor of 2 to $C_{\chi\chi}$.

$$\begin{aligned} C_{\chi_{ab}\chi_{de}} &= -\frac{i}{8\pi^2}f_{ABC}f_{BCD}\log\mu a\sum_{c,f,g,i,h,j,k}\epsilon_{abcfg}\frac{ip_c}{2p^2}\epsilon_{fgihj}p_i\epsilon_{hjkde}\frac{ip_k}{2p^2} \\ &= -\frac{i}{2\pi^2}f_{ABC}f_{BCD}\log\mu a\sum_{c,i,k}\frac{ip_c}{2p^2}p_i\frac{ip_k}{2p^2} \\ &\quad\times(\delta_{ai}\epsilon_{bckde} + \delta_{bi}\epsilon_{cakde} + \delta_{ci}\epsilon_{abkde}) \\ &= \frac{1}{4\pi^2}f_{ABC}f_{BCD}\log\mu a\sum_k\frac{ip_k}{2p^2}\epsilon_{abkde}\ . \end{aligned} \tag{5.93}$$

The coefficients α_i are now determined by the coefficient of the propagator in the renormalized propagator amplitudes C. Explicitly, we find

$$\alpha_i = 1 + b_i\log\mu a \quad i = 1, 2, 4\ , \tag{5.94}$$

where

$$b_i = b = \frac{g^2N}{4\pi^2}. \tag{5.95}$$

Note that we have used $f_{ABC}f_{BCD} = N\delta_{AD}$. This is required, as the color structure of any counterterms must match the tree propagators. However, this is strictly only true for $SU(N)$ as $f_{ABC}f_{BCD} = N(\delta_{AD} - \delta_{A0}\delta_{D0})$ for $U(N)$. This does not matter in the continuum, as the $U(1)$ trace piece simply decouples from the rest of the system and can be ignored. When doing lattice simulations, we might imagine achieving a similar result by giving the $U(1)$ mode a large mass of the order of the cut-off that will serve to decouple it from the $SU(N)$ modes at finite lattice spacing. The breaking of supersymmetry in this sector may then be removed by sending this $U(1)$ mass to zero *after* taking the continuum limit.

While naively one might have expected the coefficients b_i to be all different, our results indicate that, in fact, the log divergent parts of b_i and, hence, α_i are actually all equal. This fact can be understood quite simply; to untwist the continuum theory into a theory with four Majorana spinors requires that the continuum twisted fermions exhibit a common wavefunction renormalization. This just follows from the fact that the individual components of the spinors mix the different twisted fermions together. To achieve this requires that the corresponding renormalization constants of the kinetic terms α_i should all be equal – just as we find. Furthermore, since the leading log behavior of the lattice theory is the same as the continuum, we should expect that the log divergent part of the lattice couplings behave in the same way. Thus, a single wavefunction renormalization of the twisted lattice fermions is all that is needed to render the renormalized theory finite. The common anomalous dimension of the fermions in this twisted scheme is then given by

$$\gamma = \frac{g^2 N}{8\pi^2}. \tag{5.96}$$

In the case of the $\langle dd \rangle$ propagator, the leading log divergent contribution can be computed from the naive continuum limit of the corresponding continuum expression for the sum of the BB bubble diagrams given in diagram 5.6. Combined with the fact that the tree level $\langle dB \rangle$ propagators required on the outside of these BB amputated diagrams are the same as the continuum to $\mathcal{O}(a)$, we find that the log divergence in the mass renormalization of the d field must be the same on the lattice as in the continuum. Using this fact we can argue that the log divergent part of α_3 must actually be equal to that of the fermions, α_1, for example. This follows from the fact that the bosonic action for general α_i can be rewritten as

$$\alpha_1\Big(\overline{\mathcal{F}}_{ab}\mathcal{F}_{ab}\Big) + \frac{\alpha_2^2}{\alpha_3}\Big(\frac{1}{2}[\overline{\mathcal{D}}_a, \mathcal{D}_a]^2\Big)\ . \tag{5.97}$$

Only for $\alpha_3 = \alpha_2 = \alpha_1$ can this renormalized bosonic action be untwisted to yield the conventional gauge field plus scalar action in the continuum limit. But, since the continuum twisted theory possesses full supersymmetry, this must be true. And our general arguments then tell us the log divergence of α_3 on the lattice must satisfy the same property.

To summarize: we find that the log divergent parts of the coefficients $\alpha_i, i = 1 \ldots 4$ must all be equal to one-loop order in the lattice theory. This implies that a common wavefunction renormalization of both twisted fermions and bosons is sufficient to render the renormalized theory finite at one-loop with all fields acquiring an anomalous

dimension (in this scheme) given by $\gamma = \frac{g^2 N}{8\pi^2}$. Physically, the equality of the couplings $\alpha_i, i = 1 \ldots 4$ means that *no* logarithmic fine tuning is required at weak coupling for the lattice theory to exhibit full supersymmetry as the lattice spacing is sent to zero.

Chapter 6

Simulating Lattice SYM Theories

The unique geometric structure of the twisted SYM theories calls for a special class of algorithms to simulate them on the lattice. Fortunately, we are equipped with the right tools to perform the simulations and, thus, extract some interesting results. We will present some interesting results in the case of two-dimensional sixteen supercharge Yang-Mills theory in the next Chapter. In this Chapter, we briefly describe the simulation algorithms and architectures needed to simulate the above mentioned twisted SYM theories.

6.1 Hybrid Monte Carlo algorithm

We begin with the case of conventional lattice QCD. To compute an observable Ω in a theory with a set of bosonic fields Φ and fermionic fields $\overline{\psi}$, ψ, we use the path integral

$$\langle\Omega\rangle = \frac{1}{Z}\int [d\Phi] e^{-S_B[\Phi]}\ [\det \mathcal{M}(\Phi)]^{\alpha}\Omega(\Phi)\ , \tag{6.1}$$

where we have integrated out the fermionic fields to get the determinant, Z is the partition function

$$Z = \int [d\Phi] e^{-S_B[\Phi]}\ [\det \mathcal{M}(\Phi)]^{\alpha}\ , \tag{6.2}$$

with the parameter α depending on the number of the fermion species, and the operator $\mathcal{M} \equiv M^{\dagger}M$ with M the discretized Dirac operator.

The parameter α takes integer values in conventional theories and, when $\alpha = 1$, we use the well known Hybrid Monte Carlo (HMC) algorithm [57]. Later we see that we can, in fact, define a theory (the twisted SYM theories belong to such class) with an arbitrary number of fermions if we are willing to allow a non-integer α. The HMC algorithm fails in such cases because there is no prescription to evaluate directly either the action or its variation with respect to the bosonic fields to evaluate the forces, so we are in need of an enhanced HMC algorithm.

Let us try to understand the HMC algorithm first before we move on to an alternative algorithm to simulate the twisted SYM theories. HMC algorithm is the *de facto* algorithm for fermion theories where $\alpha = 1$. Here we rewrite the fermion determinant in terms of pseudo-fermions F [58]

$$\det \mathcal{M} = \int [dF^\dagger][dF]\ e^{-F^\dagger \mathcal{M}^{-1} F} = \int [dF^\dagger][dF]\ e^{-S_{pf}}\ . \tag{6.3}$$

We then introduce fictitious momentum fields p_Φ and p_F, conjugate to the fields Φ and F, respectively[1], whose values are drawn from a Gaussian distribution, and define a Hamiltonian

$$H = \frac{1}{2}p_\Phi^2 + \frac{1}{2}p_F^2 + S_B + S_{pf}. \tag{6.4}$$

The basic idea of HMC algorithm is to use the fact that the Hamiltonian is a constant of classical dynamics to update the fields. The field variables are now promoted to be variables of a new Monte Carlo "time" τ[2].

Now that the Hamiltonian is defined, we can evolve the fields through integrating Hamilton's equations of motion. The resulting fields will have the desired probability distribution,

$$\mathcal{P}(\Phi, F) = \frac{1}{Z} e^{-S_B - S_{pf}}\ . \tag{6.5}$$

We refresh the momenta periodically, once per trajectory, to ensure ergodicity of the algorithm.

We discretize the fictitious time dimension τ and employ a numerical integration scheme with step-size $\delta\tau$ to evolve the fields by integrating Hamilton's equations. This process introduces an $\mathcal{O}(\delta\tau^k)$ error to the field distribution, where k is equal to the order of the integration scheme used. We can use the Metropolis acceptance test at the end of each trajectory to stochastically correct this error. The Metropolis test requires detailed balance. This requirement places two constraints on the integration scheme chosen: the integration process should be reversible and area preserving. Symmetric symplectic integrators respect these constraints and the most simple of these is the second order leapfrog integrator. Thus, the HMC algorithm is an exact algorithm and the results obtained are independent of the step-size if the step-size is chosen to give a reasonable acceptance rate[3].

We summarize the steps involved in the HMC algorithm below:

1. Choose a starting bosonic field configuration Φ.

2. Choose the momentum p_Φ from a Gaussian ensemble with Boltzmann factor $\exp(-\frac{1}{2}p_\Phi^2)$.

[1] Introducing conjugate momenta in the Hamiltonian will not affect the measured expectation values of observables.

[2] This should not be confused with the Euclidean time direction in the theory.

[3] There exist integration schemes in HMC with multiple time scales to evolve bosonic and fermionic field variables independently to optimize the algorithm.

3. Choose ξ to be a field of Gaussian noise and calculate

$$F = M^{\dagger}(\Phi)\xi. \tag{6.6}$$

4. Evolve fields and momenta to get the corresponding updated configurations.

5. At the end of the trajectory[4], accept the new configuration with probability

$$P_{acc} = \min(1, e^{-\delta H}). \tag{6.7}$$

6. Save the new configuration generated, or the old configuration, depending on the outcome of the Metropolis test.

7. Return to 3.

6.2 Rational Hybrid Monte Carlo algorithm

The simulations of twisted SYM theories calls for an algorithm that takes care of non-integer α values. The best alternative is the Rational Hybrid Monte Carlo (RHMC) algorithm [59]. We briefly describe the algorithm below.

We rewrite the determinant in terms of pseudo-fermions, but now replace the fermion operator in the bilinear by a rational approximation,

$$\det \mathcal{M}^{\alpha} = \int [dF^{\dagger}][dF] e^{-F^{\dagger}\mathcal{M}^{-\alpha}F} \approx \int [dF^{\dagger}][dF] e^{-F^{\dagger}r^2(\mathcal{M})F} \ , \tag{6.8}$$

with $r(\mathcal{M}) = \mathcal{M}^{-\alpha/2}$.

The rational approximation has far superior convergence properties. We can use Remez algorithm to generate optimal rational approximations. The roots and poles of such approximations are, in general, real. The poles are also always positive for $|\alpha| < 1$, which are the functions of our interest. We write $r(\mathcal{M})$ in partial fraction form:

$$r(\mathcal{M}) = \sum_{k=1}^{m} \frac{\alpha_k}{\mathcal{M} + \beta_k} \ , \tag{6.9}$$

and then evaluate using a multi-shift solver [60]. The cost of evaluating a rational function is essentially the same as a single matrix inversion and the precision is independent of the cost to first order. For $|\alpha| < 1$, the α_k coefficients are in general all the same sign and so the evaluation of rational functions using partial fractions is numerically stable.

We summarize the steps involved in the RHMC algorithm below:

1. Choose a starting bosonic field configuration Φ.

2. Choose the momentum p_Φ from a Gaussian ensemble with Boltzmann factor $\exp(-\frac{1}{2}p_\Phi^2)$.

[4]The trajectory has $\tau/\delta\tau$ steps.

3. Choose ξ to be a field of Gaussian noise and calculate

$$F = r(\mathcal{M})^{-1}\xi. \tag{6.10}$$

4. Evolve fields and momenta to get the corresponding updated configurations.

5. At the end of the trajectory, accept the new configuration with probability

$$P_{acc} = \min(1, e^{-\delta H}).$$

6. Save the new configuration generated, or the old configuration, depending on the outcome of the Metropolis test.

7. Return to 3.

In the case of twisted SYM theories we integrate out the fermions to produce a Pfaffian, which is in turn represented by the square root of a determinant[5] and can be simulated using the RHMC algorithm.

If we denote the set of twisted fermions by the field $\Psi = (\eta, \psi_\mu, \chi_{\mu\nu})$, we first introduce a parallel pseudo-fermion field Φ with action:

$$S_{\rm PF} = \Phi^\dagger (M^\dagger M)^{-\frac{1}{4}} \Phi \ , \tag{6.11}$$

where $M = M(\mathcal{U},\mathcal{U}^\dagger)$ is the antisymmetric twisted lattice fermion operator[6].

Integrating over the fields Φ will then yield (up to a possible phase) the Pfaffian of the operator $M(\mathcal{U},\mathcal{U}^\dagger)$ as required. The fractional power is approximated by the partial fraction expansion:

$$\frac{1}{(M^\dagger M)^{\frac{1}{4}}} = \alpha_0 + \sum_{i=1}^{P} \frac{\alpha_i}{M^\dagger M + \beta_i} \ , \tag{6.12}$$

where the coefficients $\{\alpha_i, \beta_i\}$ are evaluated offline using the Remez algorithm to minimize the error in some interval (ϵ, A). Typically, we have used $P = 15$ which yields a fractional error of 0.00001 for the interval $0.0000001 \to 1000.0$, which conservatively covers the range we are interested in.

Following the standard procedure, we introduce momenta $(p_{\mathcal{U}}, p_F)$ conjugate to the coordinates $(\mathcal{U}, \Phi)$, and evolve the coupled system using a discrete time leapfrog algorithm according to the classical Hamiltonian

$$H = S_B + S_{\rm PF} + p_{\mathcal{U}}\bar{p}_{\mathcal{U}} + p_\Phi \bar{p}_\Phi. \tag{6.13}$$

The bosonic action is real, positive semi-definite in all these theories even on the lattice.

[5]This ignores a possible sign ambiguity in the fermionic determinant.

[6]The antisymmetry is guaranteed if the fermion action is rewritten as the sum of the original terms plus their lattice transposes.

One step of the discrete time update is given by:

$$\begin{aligned}
\delta p_{\mathcal{U}} &= \frac{\delta t}{2} \bar{f}_{\mathcal{U}} && (6.14)\\
\delta p_{\Phi} &= \frac{\delta t}{2} \bar{f}_{\Phi} && (6.15)\\
\delta \mathcal{U} &= \left(e^{\delta t p_{\mathcal{U}}} - I\right) \mathcal{U} && (6.16)\\
\delta \Phi &= \delta t p_{\Phi} && (6.17)\\
\delta p_{\mathcal{U}} &= \frac{\delta t}{2} \bar{f}_{\mathcal{U}} && (6.18)\\
\delta p_{\Phi} &= \frac{\delta t}{2} \bar{f}_{\Phi} && (6.19)
\end{aligned}$$

where the forces $f_{\mathcal{U}}$ and f_{Φ} are given by:

$$\begin{aligned}
f_{\mathcal{U}} &= -\frac{\delta S}{\delta \mathcal{U}} && (6.20)\\
f_{\Phi} &= -\frac{\delta S}{\delta \Phi} && (6.21)
\end{aligned}$$

and the bar denotes complex conjugation. Using the partial fraction expansion given in (6.12) these forces take the form:

$$f_{\mathcal{U}} = \sum_{i=1}^{P} \alpha_i \left[\bar{t}_i \frac{\delta M}{\delta \mathcal{U}} s_i + \overline{\left(\bar{t}_i \frac{\delta M}{\delta \bar{\mathcal{U}}} s_i \right)} \right] \qquad (6.22)$$

$$f_{\Phi} = -\alpha_0 \bar{\Phi} - \sum_{i=1}^{P} \alpha_i \bar{s}_i \qquad (6.23)$$

where

$$(M^{\dagger} M + \beta_i) s_i = \Phi \qquad (6.24)$$

$$t_i = M s_i \qquad (6.25)$$

The latter set of sparse linear equations is solved using a multimass CG-solver [61], which allows for the simultaneous solution of all P systems in a single CG solve.

At the end of one such classical trajectory the final configuration is subjected to a standard Metropolis test based on the Hamiltonian H. The symplectic and reversible nature of the discrete time update is then sufficient to allow for detailed balance to be satisfied and hence expectation values are independent of δt. After each such trajectory, the momenta are refreshed from the appropriate Gaussian distribution as determined by H, which renders the simulation ergodic.

The forces are derived below:

$$
\begin{aligned}
f_{\mathcal{U}_m} &= \frac{\partial S_{pf}}{\partial \mathcal{U}_m} = \sum_{i=1}^{P} \alpha_i F^\dagger \frac{-1}{(M^\dagger M+\beta_i)^2} \frac{\partial}{\partial \mathcal{U}_m}(M^\dagger M) F \\
&= -\sum_{i=1}^{P} \alpha_i \Big(\frac{F}{(M^\dagger M+\beta_i)}\Big)^\dagger \frac{\partial}{\partial \mathcal{U}_m}(M^\dagger M) \Big(\frac{F}{(M^\dagger M+\beta_i)}\Big) \\
&= -\sum_{i=1}^{P} \alpha_i \Big(\frac{F}{(M^\dagger M+\beta_i)}\Big)^\dagger \Big(M^\dagger \frac{\partial M}{\partial \mathcal{U}_m} + \frac{\partial M^\dagger}{\partial \mathcal{U}_m} M\Big) \Big(\frac{F}{(M^\dagger M+\beta_i)}\Big) \\
&= -\sum_{i=1}^{P} \alpha_i \Big[\Big(M \frac{F}{(M^\dagger M+\beta_i)}\Big)^\dagger \frac{\partial M}{\partial \mathcal{U}_m} \Big(\frac{F}{(M^\dagger M+\beta_i)}\Big) \\
&\quad + \Big(\frac{F}{(M^\dagger M+\beta_i)}\Big)^\dagger \frac{\partial M^\dagger}{\partial \mathcal{U}_m} \Big(M \frac{F}{(M^\dagger M+\beta_i)}\Big)\Big] \\
&= -\sum_{i=1}^{P} \alpha_i \Big[t_i^\dagger \frac{\partial M}{\partial \mathcal{U}_m} s_i + s_i^\dagger \frac{\partial M^\dagger}{\partial \mathcal{U}_m} t_i\Big] \ . \qquad (6.26)
\end{aligned}
$$

$$
\begin{aligned}
f_F &= \frac{\partial S_{pf}}{\partial F} \\
&= \alpha_0 \frac{\partial}{\partial F}(F^\dagger F) + \sum_{i=1}^{P} \alpha_i \frac{\partial}{\partial F}\Big(F^\dagger \Big[(M^\dagger M+\beta_i)^{-1} F\Big]\Big) \\
&= \alpha_0 F^\dagger + \sum_{i=1}^{P} \alpha_i s_i^\dagger \ . \qquad (6.27)
\end{aligned}
$$

6.3 Overall structure of the C++ code

We focus on implementing the SYM theories on hypercubic lattices. For a p-dimensional hypercubic lattice there are p orthogonal basis vectors $\widehat{\boldsymbol{\mu}}_1, \cdots, \widehat{\boldsymbol{\mu}}_p$. In the case of $\mathcal{N}=4$ in four dimensions, we have to augment this set with one additional body diagonal lattice link. We introduce the `Lattice_Vector` class to store the coordinates of the lattice sites and also the vector between sites. Such lattice vectors can be added or subtracted by overloading the '+' or '−' operators. These operations also respect the lattice boundary conditions.

The bosonic and pseudo-fermionic fields are stored in various objects belonging to the classes corresponding to them. We define various classes such as `Umatrix`, `Gauge_Field`, `Twist_Fermion`, `Site_Field`, `Link_Field`, `Plaq_Field`, `Body_Field`, etc., in `utilities.h`.

Let us briefly describe how the code works. The general organizational structure of the code is given in figure 3. We begin with `sym.cpp`. It reads the input parameters, such as number of sweeps (`SWEEPS`), number of thermalization steps (`THERM`), gap in measurements (`GAP`), the 't Hooft coupling (`LAMBDA`), etc., using functions contained in the file `read_param.cpp`. It can also read in previously generated field configurations using

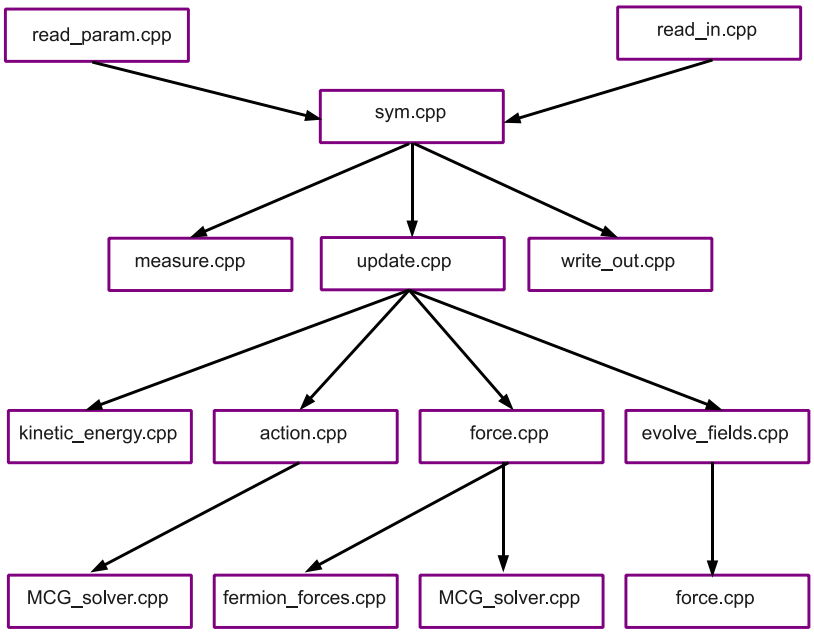

Figure 6.1: The organizational structure of the C++ code that generates and measures field configurations.

`read_in.cpp`.

The code `sym.cpp` performs three major tasks:

1. Update the field configurations as the simulation time progresses. This is accomplished by calling the function `update(U,F)` contained in `update.cpp`

2. Save the field configurations after some number of Monte Carlo sweeps and then a Metropolis test. (using the functions in `write_out.cpp`)

3. Measure the observables in the theory. This is done by function calls within (`measure.cpp`)

Let us focus on the task of updating field configurations first. After reading the initial parameters and field configurations, `update()` is called. Here, we refresh the momenta `p_U` and `p_F` (at the beginning from a Gaussian distribution) and then go to `kinetic_energy.cpp` to compute the kinetic energy

```
Adj(p_U)*p_U + Cjg(p_F)*p_F.
```

Compare this with the first two terms in the classical Hamiltonian (6.13):

$$\overline{p}_{\mathcal{U}} p_{\mathcal{U}} + \overline{p}_F p_F$$

After computing kinetic energy, the boson and pseudo-fermion actions (6.13) are computed with a call to `action()`.

The computation of the bosonic action S_B is straightforward. In the code, it is accomplished with the line:

```
KAPPA*[0.5*Tr(DmuUmu*DmuUmu) + 2.0*Tr(Fmunu*Adj(Fmunu))]  .
```

Here `KAPPA` is the dimensionless lattice coupling. It is defined in `read_param.cpp` and depends on the number of dimensions (`D`), size of the lattice (`LX`, `LY`, `LZ`, `T`) and number of colors (`NCOLOR`). The terms in the bosonic action can easily be identified with those of the lattice action. We have

```
DmuUmu(x) → Umu(x)*Udagmu(x)-Udagmu(x-e_mu)*Umu(x-e_mu)
Fmunu(x) → Umu(x)*Unu(x+e_mu)-Unu(x)*Umu(x+e_nu)
```

The fermionic part of the action is computed by taking the real part of

$$\texttt{S\_F = ampdeg*(Cjg(F)*F) + } \sum_{\texttt{n=0}}^{\texttt{DEGREE}} \texttt{amp[n]*(Cjg(F)*sol[n])} \ ,$$

where `n` runs from `0` to `DEGREE` (which is equal to number of terms in the Remez approximation P), `ampdeg` corresponds to α_0, `F` the twisted pseudo-fermion F, `Cjg(F)` is $F^\dagger$, `amp[n]` is α_i and `sol[n]` corresponds to $s_i \equiv (M^\dagger M + \beta_i)^{-1} F$.

Compare this pseudo-fermion action with

$$S_{pf} = \alpha_0 F^\dagger F + \sum_{i=1}^{P} \alpha_i F^\dagger \Big[(M^\dagger M + \beta_i)^{-1} F \Big].$$

We invoke a multimass conjugate gradient (MCG) solver `MCG_solver`, provided in `MCG_solver.cpp`, to help compute the terms needed in the fermionic action. The MCG solver can return solution to $(M^\dagger M + \beta_i) s_i = F$ for all shifts β_i.

Once the Hamiltonian is computed, we evolve the fields along a classical trajectory. This is handled by the function `evolve_fields`. The evolution of the fields and momenta are achieved through a leapfrog algorithm. In the first half step we have:

```
p_Umu  →  p_Umu + 0.5*DT*f_Umu
  p_F  →  p_F + 0.5*DT*f_F
  Umu  →  Umu + exp(DT*p_Umu)
    F  →  F + DT*p_F
```

Immediately after computing the change in fields (`Umu` and `F`) and momenta (`p_Umu` and `p_F`), we update the forces by calling `force()`. The bosonic force contribution to `f_Umu` is given by:

```
f_Umu(x)  →  f_Umu(x)+Umu(x)*Udagmu(x)*DmuUmu(x)
             -Umu(x)*DmuUmu(x+e_mu)*Udagmu(x)
             +2.0*Umu(x)*Unu(x+e_mu)*Adj(Fmunu(x))
             -2.0*Umu(x)*Adj(Fmunu(x-e_nu))*Unu(x-e_nu)
```

The computation of the fermionic force `f_F` requires first a call to the MCG solver `MCG_solver`(). We find

$$\texttt{f\_F = -ampdeg*Cjg(F) - } \sum_{\texttt{n=0}}^{\texttt{DEGREE}} \texttt{amp[n]*Cjg(sol[n])}$$

Once we have this solution an additional contribution to the gauge force coming from the pseudo-fermions is gotten by a call to the function `fermion_forces()`. Each fermionic term in the action yields a contribution. We provide a part of this code in figure 4. In the second half step of the leapfrog algorithm, the momenta `p_U` and `p_F` are again updated with the new forces. These final forces are then saved for the next iteration.

In practice it is important to use a multi-time step integrator for this evolution [62]. In this case, while the fermions are with a time step of `DT`, the bosons are integrated with the time step `DT/MSTEP`. Provided the boson force is substantially larger than the fermionic contribution, this can result in fewer costly fermion inversions for a fixed acceptance rate. In practice, the parameter `MSTEPS` can be tuned to optimize the update.

Finally, control returns to `update()` and the updated Hamiltonian `H_new` is computed. A simple Metropolis test is used to accept or reject the field configuration at the end of the trajectory.

```
#include "fermion_forces.h"

void fermion_forces(const Gauge_Field &U, Gauge_Field &f_U,
        const Twist_Fermion &s, const Twist_Fermion &p)
{
  Lattice_Vector x, e_mu;
  int sites, mu, a, b;
  Umatrix tmp;
  Gauge_Field Udag;

  Udag=Adj(U);
  f_U=Gauge_Field();
  //contribution to f_U from psi_muDb_mu(U)eta term
    sites=0;
    while(loop_over_lattice(x,sites))
    {
      for(mu=0;mu<NUMLINK;mu++)
      {e_mu=Lattice_Vector(mu);
      tmp=Umatrix();
        for(a=0;a<NUMGEN;a++)
        {
          for(b=0;b<NUMGEN;b++)
          {tmp=tmp+conjug(p.getS().get(x).get(a))*s.getL().get(x,mu).get(b)
          *Lambda[a]*Lambda[b]*Udag.get(x,mu)-conjug(p.getS().get(x+e_mu).get(a))
          *BC(x,e_mu)*s.getL().get(x,mu).get(b)*Lambda[b]*Lambda[a]*Udag.get(x,mu);}
        }
        f_U.set(x,mu,f_U.get(x,mu)-0.5*Adj(tmp));}
    }
    sites=0;
    while(loop_over_lattice(x,sites))
    {
      for(mu=0;mu<NUMLINK;mu++)
      {e_mu=Lattice_Vector(mu);
      tmp=Umatrix();
        for(a=0;a<NUMGEN;a++)
        {
          for(b=0;b<NUMGEN;b++)
          {tmp=tmp+conjug(p.getL().get(x,mu).get(a))*s.getS().get(x+e_mu).get(b)
          *BC(x,e_mu)*Lambda[a]*Lambda[b]*Udag.get(x,mu)-
          conjug(p.getL().get(x,mu).get(a))*s.getS().get(x).get(b)
          *Lambda[b]*Lambda[a]*Udag.get(x,mu);}
        }
        f_U.set(x,mu,f_U.get(x,mu)-0.5*Adj(tmp));}
    }
    sites=0;
    while(loop_over_lattice(x,sites))
    {for(mu=0;mu<NUMLINK;mu++){f_U.set(x,mu,-1.0*Adj(f_U.get(x,mu)));}}
return;
}
```

Figure 6.2: A part of the C++ code to compute the fermion force contribution.

Chapter 7

D1-brane Thermodynamics from Lattice Super Yang–Mills

In this Chapter[1], we investigate the phase structure of the two-dimensional lattice SYM theory with sixteen supercharges using Monte Carlo simulations described in Chapter 6. The two-dimensional theory is obtained by the dimensional reduction of the $\mathcal{N} = 4$, $d = 4$ SYM theory. We write down the lattice version of the theory using the twisted formulation and study the possible large N transitions between spatially confined and deconfined phases of the theory as revealed by behavior of the spatial Polyakov line. This theory has a supergravity dual; we also investigate the possible transitions between certain black holes in the dual supergravity theory.

The holographic duality conjecture connects supersymmetric gauge theories with string theories in certain background. According to this conjecture, type II superstring theory in $AdS_{d+1} \times M$ space, where M is a compact manifold with positive curvature, should be equivalent to a superconformal field theory living on the d-dimensional boundary of AdS_{d+1}. In recent years the holographic principle between supersymmetric gauge theories and supergravity theories [65] has been explored using a series of numerical studies. So far, these studies have been confined to the case when the super Yang–Mills theory is one-dimensional and the dual gravitational theory describes the low energy dynamics of D0-branes [66, 67, 68, 69, 70, 71, 72, 73] or the $\mathcal{N} = 4$ theory compactified on $S^3 \times \mathbb{R}$ [74, 75, 76].

In this Chapter, we extend these calculations to the case of N coincident D1-branes wrapped on a spatial circle, which, in the decoupling limit, is described by a two-dimensional maximally SYM theory on a circle [65, 77]. This two-dimensional Yang–Mills system possesses a richer structure at large N than its one-dimensional counterpart. The reason is that there is a new dimensionless coupling in the theory that can be varied in addition to the temperature when the spatial direction is compactified on a circle.

[1]This Chapter is based on the work [63, 64].

Arguments from a high temperature limit and also from strong coupling, using a dual supergravity description, indicate that the system should possess an interesting phase structure in the two-dimensional parameter space spanned by the temperature and this new coupling in the large N limit [77, 78]. A large N transition between confined and deconfined phases with respect to the spatial Polyakov line is expected, which interpolates between the high temperature region and the strongly coupled region. In particular, for the strongly coupled region, the dual D1-brane system can be described by certain black holes in supergravity, with a compact spatial circle. Then arguments from the dual gravity model indicate a first order Gregory-Laflamme (GL) [79, 80] phase transition between the black hole solutions localized on the circle and uniform black hole solutions which wrap the circle [77, 78, 81, 82, 83, 84, 85, 86]. Translating back to the SYM, the dual gravity model predicts the parametric dependence of the transition temperature against dimensionless circle coupling – a dependence that seemingly cannot be deduced by simple SYM considerations. Interestingly, since the relevant gravity solutions have not been constructed yet (analog solutions are known, but not in the correct dimension [87, 88, 89]), the precise coefficient in this relation is not known, and determining it in SYM yields a prediction for the phase transition temperature that could be tested in the future when the gravity solutions are constructed – a classical, but, nonetheless, rather non-trivial gravitational problem.

The numerical results appear to confirm the expected deconfinement phase transition in the two-dimensional sixteen supercharge SYM theory. At strong coupling, the position of the observed critical line agrees with the parametric dependence on couplings predicted by the dual gravity analysis. In particular, we can give an estimate of the coefficient in this relation and, hence, derive a prediction for the GL phase transition temperature for the dual black holes theory.

In the next section we review the theoretical background to the conjectured two-dimensional Yang–Mills/D1-brane duality when the theories are compactified on a circle and describe the expected phase structure in certain limits.

7.1 Theoretical background

We are interested in studying large N thermal two-dimensional maximally supersymmetric (16 supercharge) $SU(N)$ Yang–Mills theory, in the 't Hooft limit, with coupling $\lambda = Ng_{YM}^2$, with the spatial direction compactified. Continuing the theory to Euclidean time, this implies the Yang–Mills theory is defined on a rectangular 2-torus, with time cycle size β, and space cycle size R. The fermion boundary conditions distinguish the two cycles, being anti-periodic on the time cycle so that β has the interpretation of inverse temperature, and periodic boundary conditions on the space cycle. The action may then be written as:

$$\begin{aligned} S &= \frac{N}{\lambda}\int_{T^2} d\tau dx \mathrm{Tr}\Big[\tfrac{1}{4}F_{\mu\nu}^2 + \tfrac{1}{2}\sum_I [D_\mu\phi^I, D^\mu\phi^I]^2 - \tfrac{1}{4}\sum_{I,J}[\phi^I,\phi^J]^2 \\ &\quad +\text{fermions}\Big] , \end{aligned} \tag{7.1}$$

where $I, J = 1, \ldots, 8$ and ϕ^I are the 8 adjoint scalars, and τ is the coordinate on the time circle, and x the coordinate on the space circle. Since λ, β and R are dimensionful, it is convenient to work with the two dimensionless couplings:

$$r_\tau = \sqrt{\lambda}\,\beta \quad \text{and} \quad r_x = \sqrt{\lambda}\,R, \tag{7.2}$$

which give the dimensionless radii of the time and space circles, respectively, measured in units of the 't Hooft coupling. We will be interested in the expectation values of the trace of the Polyakov loops on the time and space circles,

$$P_\tau = \frac{1}{N}\Big\langle \Big| \mathrm{Tr}\,(P\exp(i\oint A_\tau))\Big|\Big\rangle, \quad P_x = \frac{1}{N}\Big\langle \Big| \mathrm{Tr}\,(P\exp(i\oint A_x))\Big|\Big\rangle\,, \tag{7.3}$$

as at large N, these give order parameters for confinement/deconfinement (or center symmetry breaking) phase transitions which we will discuss below.

As discussed in [77, 78] there are several interesting limits for the theory. In the large torus limit, $1 \ll r_x, r_\tau$ the string theory dual may be described by supergravity. For the weak coupling limit, $r_x, r_\tau \ll 1$, or asymmetric torus limits $r_\tau \ll r_x^3$ and $r_x \ll r_\tau^3$, we will find the dynamics are captured by a lower dimensional YM theory. Let us now review these cases and their predictions.

7.1.1 Large torus limits and IIB and IIA supergravity duals

When the torus becomes large in units of the 't Hooft coupling, one finds that in certain regimes, the dual D1-branes in string theory can be well described by supergravities [65] as we shall now briefly review. Having a supergravity description of the full string theory dual allows certain behaviors of the theory to be studied using simple semi-classical gravity reasoning, which allows powerful predictions to be inferred for the dual SYM.

The dual IIB string theory is given by the 'decoupling limit' of N coincident D1-branes [65]. This decoupling limit is where one considers finite energy excitations of the D1-branes while taking the limit,

$$g_{YM}^2 = \frac{1}{2\pi}\frac{g_s}{\alpha'} = \text{fixed}, \quad \alpha' \to 0, \tag{7.4}$$

where g_s is the string coupling and α' determines the string tension. Since the Euclidean SYM is defined on a torus, the string dual is too, being at finite temperature and having one spatial direction compactified into a circle of radius R with periodic fermion boundary conditions.

One finds that for $1 \ll r_\tau \ll r_x^2$, this string theory can be described effectively by its supergravity sector. String oscillator and winding mode corrections to this supergravity description are small in this limit. The IIB supergravity solution describing the thermal vacuum is a black hole, carrying electric D1-brane charge. The D1-brane charge is string like, (i.e., its field strength tensor is a 3-form), and the appropriate configuration is to take the charge to wrap over the compact space circle. The solution preserves translational invariance around the space circle direction and is thought to be stable to small perturbations.

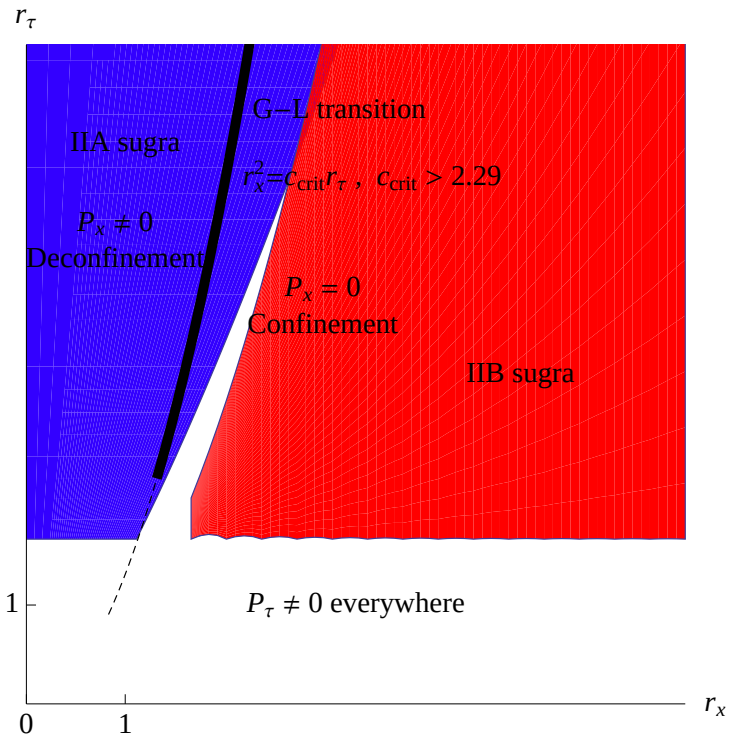

Figure 7.1: Figure indicating the regions of coupling space where, at large N, the dual string theory may be approximated by (red) IIB supergravity and (blue) IIA supergravity. In these regions, the SYM thermodynamics is dual to the thermodynamics of certain black holes in the corresponding supergravity. The IIA region predicts a large N first order phase transition (the Gregory-Laflamme phase transition) between black holes localized on the spatial circle, and wrapping over the circle. The phase transition is known to occur along the curve $r_x^2 = c_{crit} r_\tau$ where c_{crit} is a constant, not yet determined, but known to be order one and $c_{crit} > 2.29$. The SYM transition is thought to be a deconfinement transition of the spatial Polyakov loop.

However, there is a second supergravity description of the theory which is valid in a partly overlapping and partly complementary range $1 \ll r_\tau$ and $r_x^{4/3} \ll r_\tau$, obtained by performing a T-duality transformation on the compact spatial circle of the IIB string theory [77, 78]. Roughly speaking, such a T-duality exchanges winding and momentum modes of the string on this spatial circle, and exchanges the IIB string theory for a IIA string theory. In our case, the N D1-branes now get exchanged with N D0-branes in the IIA theory. Since the D0-branes are point like, rather than string like, they have freedom to distribute their electric charge over the circle in various ways - it may be uniformly distributed, non-uniformly distributed, or fully localized on the circle, the latter two choices breaking the translational symmetry along the space circle direction. It is then a dynamical question which case is preferred.

It is thought [77] that there are 3 types of black hole solution that indeed realize these 3 choices. The uniform black hole solution exists for all temperatures, but it is known to have a dynamical perturbative instability of the Gregory-Laflamme type [79, 80] for low temperatures $r_x^2 \leq 2.29\, r_\tau$ [77]. For higher temperatures it is thought to be dynamically stable. However, at a higher temperature than the instability point, so that $r_x^2 = c_{crit}\, r_\tau$ for some constant c_{crit} with $c_{crit} > 2.29$, the uniform black hole is thought to become globally thermodynamically less favored than the localized black hole solution. The actual transition temperature that governs the constant c_{crit} is not yet known, as the localized black hole solutions have not yet been constructed in the correct context to be embedded in the supergravity dual. The line $r_x^2 = c_{crit}\, r_\tau$ represents a first order thermal phase transition between the uniform and localized solutions, with uniform favored for higher temperature $r_x^2 > c_{crit}\, r_\tau$ and localized favored for lower temperature $r_x^2 < c_{crit}\, r_\tau$[2]. We term this the GL phase transition and emphasize that this is distinct from the GL dynamical instability. Whilst there is a non-uniform black hole solution it is never thermally dominant. For reviews on the GL dynamical instability, phase transition and uniform, non-uniform and localized black hole solutions, see [90, 91, 92].

According to the duality hypothesis, a Polyakov loop about the time/space circle in the Euclidean SYM is computed in the leading large N limit by considering whether a two-dimensional minimal area surface (the classical string worldsheet) that asymptotically wraps the time/space circle exists. If the time/space circle is contractible in the interior of the gravity solution, a minimal area solution for the string worldsheet will exist and then the correspondence states that $P_{\tau/x} \sim O(1)$. However, if the circle is not contractible, there cannot exist a minimal surface that gives a finite action for the string worldsheet, and the correspondence states that $P_{\tau/x} \sim O(1/N)$ and hence $P_{\tau/x} = 0$ in the large N limit. It is a standard result of Euclidean gravity that black hole solutions have contractible time circles in the interior of the solution, and in fact the time circle contracts precisely at the horizon. The contractability of the spatial circle however depends on the type of black hole. In the IIB supergravity solution the space circle is non-contractible. The IIA uniform (and non-uniform) solutions have non-contractible space circles, whereas the localized solution has a contractible circle. In fact, the eigenvalues of the SYM spatial

[2]The region $r_x^2 < \alpha\, r_\tau$ for $2.29 < \alpha < c_{crit}$ is the region where the localized solution dominates the canonical ensemble, but the uniform phase could in principle be constructed as a metastable supercooled state (although here we will only be concerned with equilibrium thermodynamics).

Polyakov loop (which are phases, and hence live on a circle) are thought to correspond to the positions of these D0-branes on the space circle in the IIA dual. Hence, the GL phase transition can physically be thought of as a thermal instability associated with the clumping of D0-branes, breaking the $U(1)$ circle translation symmetry. In the large N SYM, this symmetry breaking is the spontaneous breaking of center symmetry Z_N, where for large N, $U(1) \simeq Z_N$.

Let us summarize our predictions for the large torus. We learn that in the IIB regime, $1 \ll r_\tau \ll r_x^2$, we expect $P_\tau \neq 0$ but $P_x = 0$. In the IIA regime, where $1 \ll r_\tau$ and $r_x^{4/3} \ll r_\tau$, we have $P_\tau \neq 0$, and $P_x \neq 0$ for $r_x^2 \leq c_{crit}\, r_\tau$ and $P_x = 0$ for $r_x^2 > c_{crit}\, r_\tau$, with c_{crit} an order one constant with $c_{crit} > 2.29$. We note that, in the regime where both IIA and IIB apply, they give consistent results. Thus, in the large torus, supergravity regimes, the SYM is always deconfined in the time direction, and there is a first order deconfinement/confinement transition in the space direction at $r_x^2 = c_{crit}\, r_\tau$.

7.1.2 Dimensional reduction

Consider the toy model scalar theory defined on the 2-torus:

$$S = \frac{1}{\lambda} \int_{T^2} d\tau dx \left((\partial_\mu \phi)^2 + \phi^4 \right) \ . \tag{7.5}$$

First we change to angular coordinates $\theta_\tau = \tau/\beta$ and $\theta_x = x/R$ with unit radius, so $\theta_{\tau,x} \sim \theta_{\tau,x} + 1$, and then define the dimensionless scalar variable $\tilde{\phi} = (\beta R/\lambda)^{1/4}\, \phi$. The action can now be written as:

$$S = \int_0^{2\pi} d\theta_\tau d\theta_x \left(\tilde{\phi}^4 + \sqrt{\frac{r_x}{r_\tau^3}} (\partial_{\theta_\tau} \tilde{\phi})^2 + \sqrt{\frac{r_\tau}{r_x^3}} (\partial_{\theta_x} \tilde{\phi})^2 \right) \ , \tag{7.6}$$

and we see that the dimensionless couplings r_x/r_τ^3 and r_τ/r_x^3 determine the masses of the non-constant modes of the field ϕ on the torus. There are three interesting limits. When $r_x \sim r_\tau \ll 1$, then the non-constant modes of the scalar become very massive and, hence, weakly coupled and one may integrate these out to arrive simply at the quartic integral governing the constant modes. If only $1 \ll r_x/r_\tau^3$, then the non-constant modes on the time circle are weakly coupled and one may integrate these out to obtain the dimensional reduction, which now lives only on the space circle. Likewise, if $1 \ll r_\tau/r_x^3$, one may dimensionally reduce to obtain a theory only on the time circle.

The structure of this toy example is such that precisely the same phenomenon occurs with the full SYM on a 2-torus, as discussed in [78]. One difference is that, due to the anti-periodic boundary conditions on the time circle, the Fourier decomposition of the fermions contain only non-constant modes in the time direction. Another difference is that, under a reduction, the constant component of the gauge field in the direction of reduction yields a scalar field, similar to the scalars ϕ^I, in the reduced theory. This scalar in the reduced theory corresponds to the Polyakov loop about the cycle that has been reduced on. Since the expectation value of the eigenvalue distribution of the scalar in the reduced theory will have a non trivial profile, this implies that center symmetry is

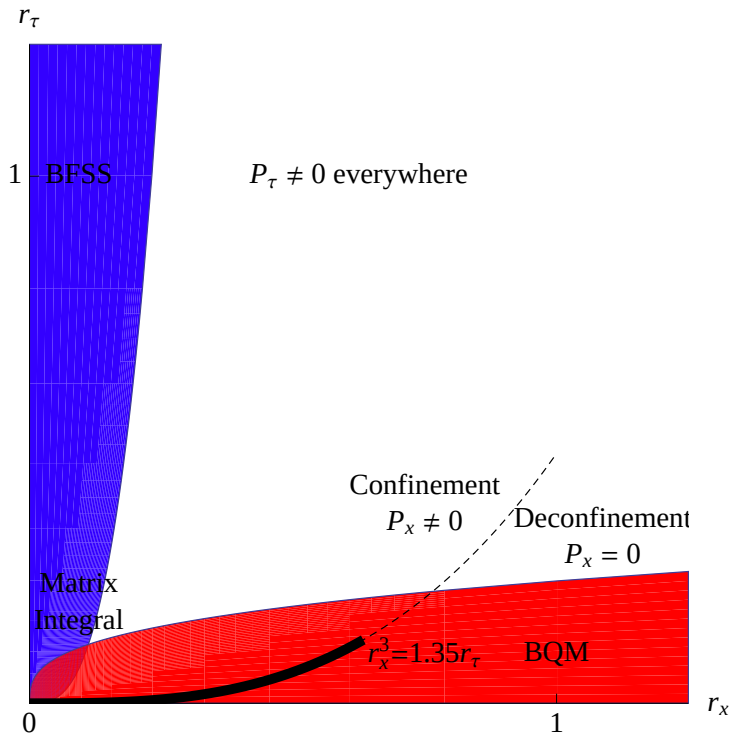

Figure 7.2: Figure showing the regions of coupling space where the SYM may be dimensionally reduced on the time and/or space circles. The blue region indicates where reduction on the space circle gives a good approximation, yielding a supersymmetric quantum mechanics theory, the BFSS model. The red region indicates where reduction on the space circle to a bosonic quantum mechanics (BQM) is a good approximation. This latter reduction predicts a large N deconfinement phase transition in the spatial Polyakov loop for $r_x^3 = 1.35 r_\tau$ and this curve is shown.

broken in the Polyakov loop about the reduced cycle[3].

There are, again, 3 regimes. For $r_x \sim r_\tau \ll 1$, one may reduce on both time and space to just give the zero modes of the theory, and arrive at a bosonic Yang–Mills matrix integral, since, in reducing on the time circle one loses the fermions that have no zero modes. Such a reduction indicates that, in this limit, the two-dimensional SYM should have $P_\tau, P_x \neq 0$.

For $r_x^3 \ll r_\tau$, the theory may be dimensionally reduced on the space circle to give the thermal supersymmetric matrix quantum mechanics living on the time circle with radius β. The spatial Polyakov loop is then given in terms of one of the 9 scalars of the BFSS model, and, since these scalars have localized eigenvalues, the two-dimensional SYM should be deconfined in the space direction with $P_x \neq 0$. This theory is precisely the BFSS theory [94], and recently this has been numerically simulated in the 't Hooft limit [67, 68, 69], and indeed, the results obtained are consistent with the theory always being deconfined, so $P_\tau \neq 0$. The coupling of this quantum mechanics is given by $r_\tau/(r_x)^{1/3}$ and, when this is large, we know from our arguments above that we are in a regime where a dual IIA supergravity description exists, and the dynamics are given by the localized black hole solution, which is indeed consistent with $P_\tau, P_x \neq 0$.

For $r_\tau^3 \ll r_x$ one may again perform a dimensional reduction, now on the time circle. Thus, in the two-dimensional theory, we expect $P_\tau \neq 0$. Since there are no fermion zero modes on the time circle, the resulting one-dimensional theory is a bosonic quantum mechanics (BQM) defined on a circle radius R and with dimensionless coupling r_x^3/r_τ. Numerical [77, 78, 95] and analytic study [96] indicate that this theory has a large N confinement/deconfinement transition at $r_x^3/r_\tau \simeq 1.35$ of second order. There is also thought to be a third order Gross-Witten [97, 98] transition very nearby at $r_x^3/r_\tau \simeq 1.49$ [95, 96].

7.1.3 Expectations for large N phase diagram

We conclude by putting together the above discussions. The simplest picture is then that the Gregory-Laflamme first order phase transition, $r_x^2 = c_{crit}\, r_\tau$ for $1 \ll r_\tau$ (recall $c_{crit} > 2.29$), and the second order transition $r_\tau^3 \ll r_x$ and $r_x^3 = 1.35\, r_\tau$ in the time reduced BQM are two ends of the same spatial Polyakov loop confinement/deconfinement phase transition line. At some point in-between, the order presumably changes, and here the new third order Gross-Witten phase transition emerges, although this is not measured by center symmetry breaking, but by more detailed information about the spatial Polyakov loop eigenvalue distribution. It is interesting [84, 77, 85] that the new phase at small r_x also exists for $1 \ll r_x$ in the form of non-uniform IIA black strings, but, unlike at weak coupling, these are never thermally dominant in the IIA supergravity region. In figure 7.3, we summarize the expected phase diagram for the spatial confinement/deconfinement transition.

[3]This is to be contrasted with the Eguchi-Kawai reduction [93] where quite the opposite occurs; one can only reduce on a direction if center symmetry is unbroken.

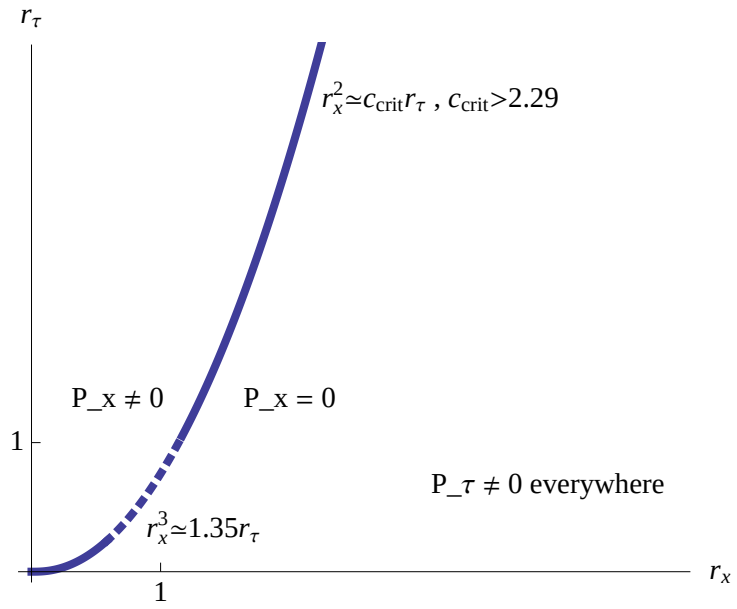

Figure 7.3: Cartoon of the expected large N, spatial Polyakov loop deconfinement transition line in coupling space. Pictured is the simplest possibility, namely that the spatial deconfinement transition interpolates between the strong coupling Gregory-Laflamme transition parametric behavior $r_x^2 \sim r_\tau$, and the high temperature reduction deconfinement transition behavior $r_x^3 = 1.35 r_\tau$.

7.2 Sixteen supercharge theory on the lattice

In Chapter 4, we have written down the lattice version of the sixteen supercharge theory in four dimensions (the $\mathcal{N} = d = 4$ SYM theory). We need to dimensionally reduce this theory down to two dimensions to obtain the sixteen supercharge theory of our interest[4]. We saw that a better choice in four dimensions is the A_4^* lattice, which retains a higher point group symmetry than the hypercubic lattice. It is not necessary for two dimensions, and, indeed would complicate the calculation of Polyakov lines.

We dimensionally reduce the four-dimensional supersymmetric lattice action

$$\begin{aligned} S &= \frac{1}{g_{YM}^2}\sum_{\boldsymbol{n}} \mathrm{Tr}\ \left(\mathcal{F}_{ab}^\dagger \mathcal{F}_{ab} + \frac{1}{2}\left(\overline{\mathcal{D}}_a^{(-)}\mathcal{U}_a\right)^2 - \chi_{ab}\mathcal{D}_{[a}^{(+)}\psi_{b]} - \eta\overline{\mathcal{D}}_a^{(-)}\psi_a \right) \\ &\quad + S_{\text{closed}} \ , \end{aligned} \tag{7.7}$$

where

$$S_{\text{closed}} = -\frac{1}{8g_{YM}^2}\sum_{\boldsymbol{n}} \mathrm{Tr}\ \epsilon_{mnpqr}\chi_{qr}(\boldsymbol{n}+\widehat{\boldsymbol{\mu}}_m+\widehat{\boldsymbol{\mu}}_n+\widehat{\boldsymbol{\mu}}_p)\overline{\mathcal{D}}_p^{(-)}\chi_{mn}(\boldsymbol{n}+\widehat{\boldsymbol{\mu}}_p) \ , \tag{7.8}$$

along two lattice directions using periodic boundary conditions to obtain the two-dimensional theory. The resultant lattice action corresponds in the naive continuum limit to the target $\mathcal{Q} = 16$ YM theory in two dimensions. In this limit, its exact supersymmetry is enhanced to correspond to 4 continuum supercharges corresponding to the four scalar fermions that now appear in the dimensionally reduced theory [35].

We will be interested in this theory large N limit with 't Hooft coupling

$$\lambda = N g_{YM}^2 \ . \tag{7.9}$$

The lattice theory is then governed by the coupling

$$\kappa = \frac{NLT}{2r_\tau^2} \ , \tag{7.10}$$

where L and T denote the number of lattice sites in the spatial and temporal directions.

We have used periodic boundary conditions for the fields on the remaining spatial circle and anti-periodic boundary conditions for fermions in the temporal direction in order to access the thermal theory. Simulations were carried out using the RHMC algorithm, which is described in detail in [99].

It has been shown that the existence of a noncompact moduli space in the theory renders the thermal partition function divergent [72]. In order to regulate this divergence we have additionally introduced a mass term for the scalar fields appearing in the lattice action with a dimensionless mass parameter $m = m_{\text{phys}}\beta$.

$$S_m = \frac{m^2}{g_{YM}^2}\sum_x \left[\mathcal{U}_\mu^\dagger\mathcal{U}_\mu + \left(\mathcal{U}_\mu^\dagger\mathcal{U}_\mu\right)^{-1} - 2\right] \ . \tag{7.11}$$

[4]We assume an anti-hermitian basis for all fields, which take their values in the adjoint representation of the $SU(N)$ gauge group.

The form of this term is effective at suppressing arbitrarily large fluctuations of the exponentiated scalar fields and reduces to a simple mass term for small fluctuations characterizing the continuum limit. Notice that this infrared regulator term breaks supersymmetry softly and lifts the quantum moduli space of the theory. The simulations are then performed for a range of the parameter m in order to allow for an extrapolation $m \to 0$.

7.3 Simulation results

The numerical simulations of this theory focus on the Polyakov lines for both the thermal and spatial circle. These are defined on the lattice in the usual way

$$P_x = \frac{1}{N}\left\langle \left| \text{Tr } \Pi_{a_x=0}^{L-1} U_{a_x} \right| \right\rangle, \quad P_\tau = \frac{1}{N}\left\langle \left| \text{Tr } \Pi_{a_\tau=0}^{T-1} U_{a_\tau} \right| \right\rangle \ , \tag{7.12}$$

where the unitary piece of the complexified link $\mathcal{U}_\mu$ is extracted to compute these expressions. The values of spatial and temporal Polyakov lines are evaluated as a function of r_τ for two different lattices with the same aspect ratio, a 2×8 lattice and a 3×12 lattice, for $N = 3$ and with values of the infrared regulator $m = 0.05, 0.10$ and 0.20. The use of two different lattices with the same aspect ratio would allow to test for and quantify finite lattice spacing effects. The simulations are performed for values of the dimensionless time circle radius in the range $0.02 \leq r_\tau \leq 1.0$. Figure 7.4 shows the numerical results.

Notice that the temporal Polyakov remains close to unity over a wide range of r_τ. This indicates the theory is (temporally) deconfined and is consistent with expectations for the limits discussed in section 7.1 – the asymmetric torus limits, and the strong coupling regions, where there is a dual supergravity description in terms of black holes. However, the spatial Polyakov line has a different behavior taking values close to unity for small r_τ while falling rapidly to plateau at much smaller values for large r_τ. It is tempting to see the rather rapid crossover around $r_\tau \sim 0.2$ as a signal for a would be thermal phase transition as the number of colors is increased. This conjecture is seen to be consistent with the data: in figure 7.5 we show the Polyakov lines for $N = 2, 3, 4$ on 2×8 lattices as a function of r_τ. The plateau evident at large r_τ falls with increasing N and the crossover sharpens. This is consistent with the system developing a sharp phase transition in the large N limit.

Notice that in the data shown here, the results do not depend on the scalar mass. Indeed, for the length of Monte Carlo associated with the simulation time, it appears that m can be set to zero for $r_\tau < 2$ without fear of encountering the thermal divergence discussed in [72]. This stability in the scalar sector can be seen in figure 7.6, which shows the Monte Carlo time series for the eigenvalues of $\mathcal{U}_\mu^\dagger \mathcal{U}_\mu \sim e^{2\phi}$ at two different r_τ's with dimensionless mass parameter m = 0.05 and gauge group $SU(3)$. There is no evidence of a divergence over thousands of Monte Carlo sweeps. Furthermore, one sees that the eigenvalues of the scalar fields (rendered dimensionless using the lattice spacing) cluster with small separation for this range of r_τ.

The observations indicate that the $m = 0$ model does exhibit the same thermal instability observed in the case of supersymmetric quantum mechanics for sufficiently low temperature $r_\tau >> 1$ in agreement with the general arguments given in [72].

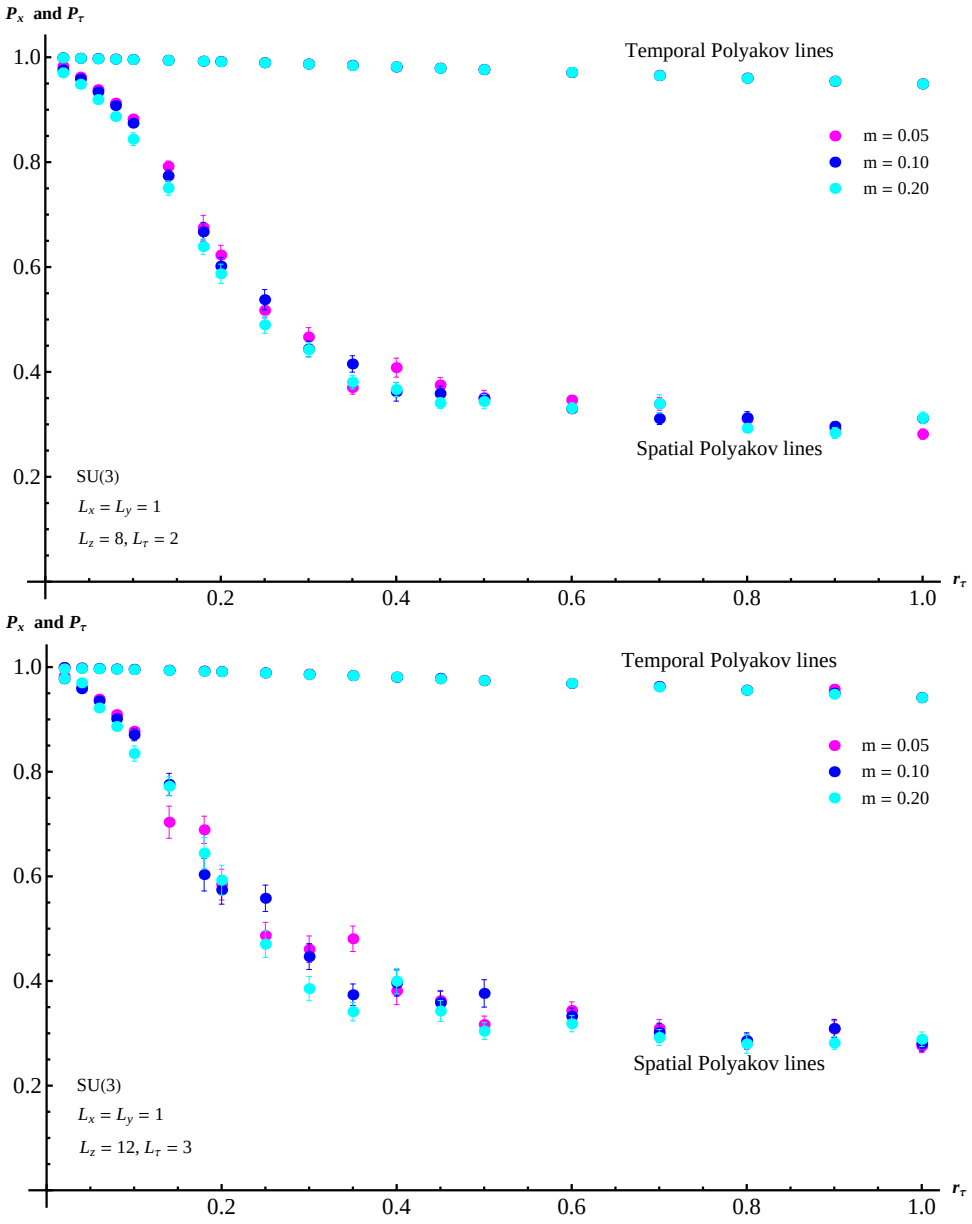

Figure 7.4: Spatial and temporal Polyakov lines (P_x and P_τ) against dimensionless time circle radius r_τ for maximally supersymmetric $SU(3)$ Yang–Mills on 2×8 and 3×12 lattices using different values of the infrared regulator m.

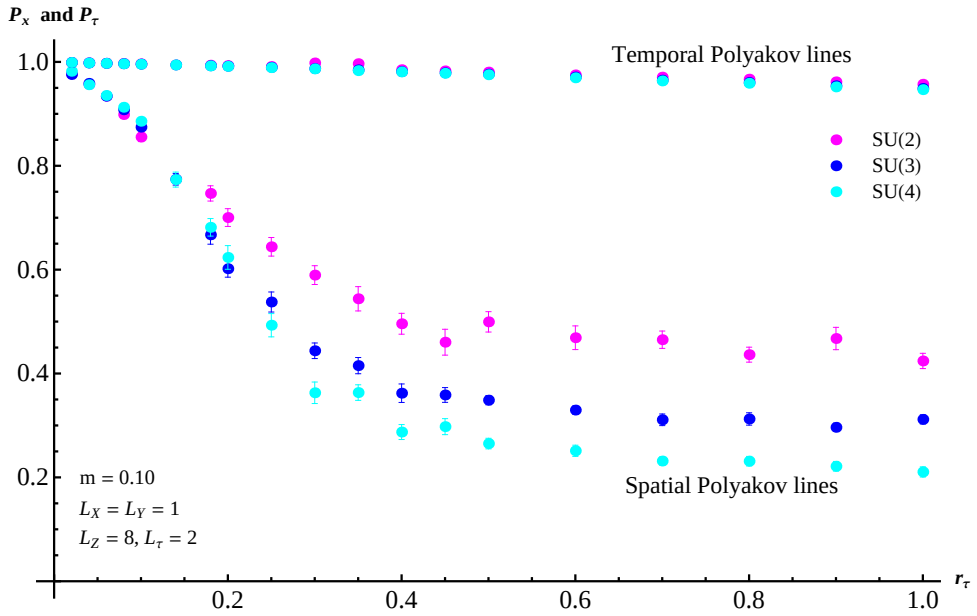

Figure 7.5: Plot of the absolute values of the spatial and temporal Polyakov lines (P_x and P_τ) against the dimensionless time circle radius r_τ for maximally supersymmetric $SU(N)$ Yang–Mills on a 2×8 lattice for $N = 2, 3, 4$, using the value of the infrared regulator m $= 0.10$.

Putting together several lattice aspect ratios for $N = 3, 4$, we can plot the spatial Polyakov loop as a function of r_s and r_τ, where data are available. This is done in figure 7.7. The three contours $P_x = 0.4, 0.5, 0.6$ are shown. We see that the contours for $SU(4)$ are closer together than those for $SU(3)$, as we expect for a large N transition. From these data we can try to assess where the large N transition in P_x may occur. In the detailed studies of the dimensionally reduced bosonic quantum mechanics [77], it was found that the large N transition occurred very close to $P_x \simeq 0.5$. Thus from the contours of the $SU(3)$ and $SU(4)$ data, we could take the $P_x = 0.5$ curves to give an estimate for the large N phase transition line. Another estimate is to plot the function

$$f_N \equiv P_x(SU(N)) - P_x(SU(N-1)) \ , \tag{7.13}$$

that measures the difference between the Polyakov lines for $SU(N)$ and $SU(N-1)$. At strong coupling, where we expect the large N transition is first order, the simplest situation is to have $f_N < 0$ in the confined region (where $P_x = 0$ for $N \to \infty$), and, correspondingly, $f_N > 0$ in the deconfined region as $N \to \infty$. Then plotting the boundary of the positive (or negative) region of f_4 calculated from the simulation data also gives an estimate of the critical line. Neither method can give a precise determination, and they should not be considered as a replacement for calculations at larger N than we have been able to reach here. However, in the absence of such large N data, we plot the $P_x = 0.5$ contours for $SU(4)$ and $SU(3)$ in figure 7.7, and, in addition, the region where f_4 is positive. We note that the $SU(3)$ and $SU(4)$ $P_x = 0.5$ contours are remarkably consistent with each other, which provides evidence that they are indeed a reasonable approximation to the large N transition curve. Whilst the f_4 data are rather noisy, and,

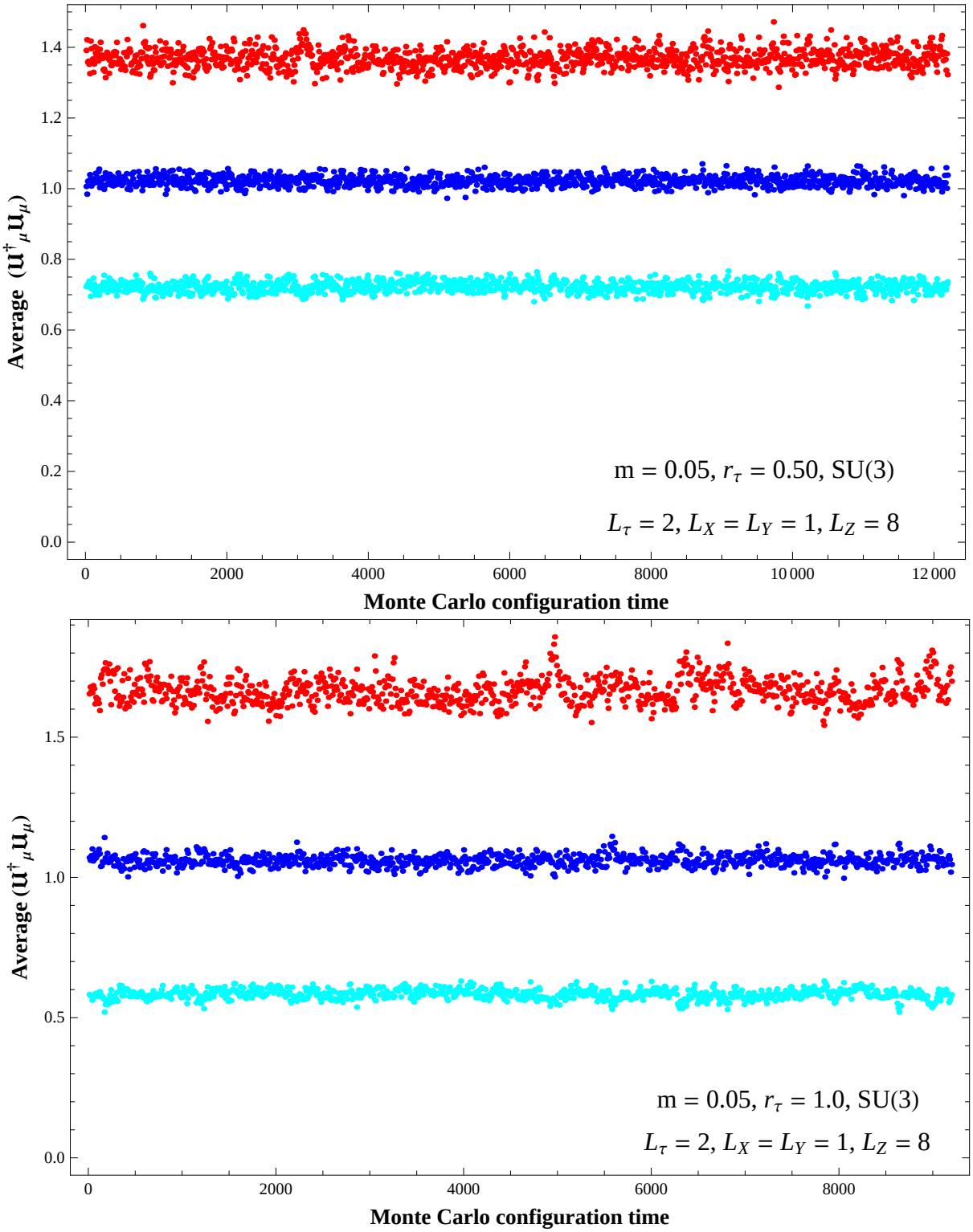

Figure 7.6: Plots of the average scalar eigenvalues against Monte Carlo configuration time step, for $N = 3$ on a 2×8 lattice with $r_\tau = 0.5$ and 1.0. Note that the spread between eigenvalues reduces as r_τ is decreased. We have used the dimensionless mass parameter $\mathrm{m} = 0.05$.

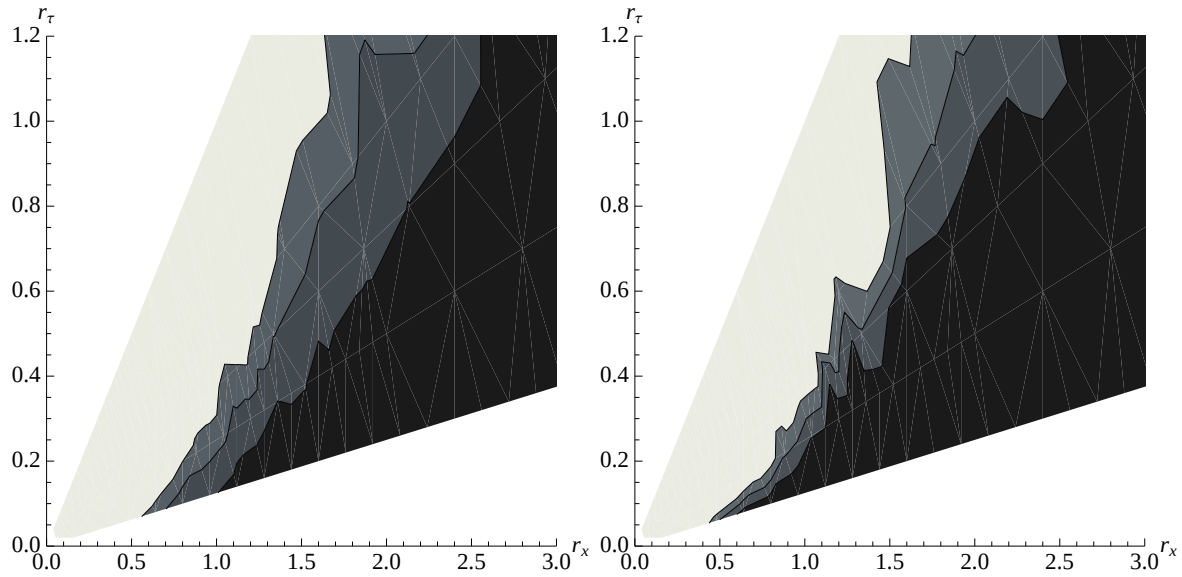

Figure 7.7: Plot of contours of the expectation of the spatial Polyakov line P_x over the r_x, r_τ plane. The left frame shows $SU(3)$, and the right $SU(4)$. The three contours plotted are $0.4, 0.5, 0.6$, and the simulation data collates and interpolates runs made on lattices 2×16, 2×8, 3×8, 4×4 and 4×8 therefore giving a variety of aspect ratios r_τ / r_x.

hence, the positive f_4 region has 'holes' in it, the function is positive only to left of the $P_x = 0.5$ curves, and, furthermore, extends right up to these curves. The curve $r_x^2 = 3.5 r_\tau$ is plotted on this graph and matches the contours $P_x = 0.5$, and the boundary of the positive f_4 region very well in the strong coupling region. This can be taken to indicate that the gravity prediction for the parametric behavior $r_x^2 = c_{crit} r_\tau$ is consistent with the simulation data. The estimated value turns out to be $c_{crit} \simeq 3.5$, which indeed obeys the gravity prediction that c_{crit} is order one and $c_{crit} > 2.29$. Furthermore, we see that the contours $P_x = 0.5$ also appear to be consistent with the high temperature prediction $r_x^3 = 1.35 r_\tau$ as well.

The value of the ratio

$$\alpha \equiv c_{crit} / 2.29 \tag{7.14}$$

gives the ratio of the GL thermal phase transition temperature to the GL dynamical instability temperature (the minimum temperature to which uniform strings can be supercooled), so

$$\alpha = T_{GL\, phase} / T_{GL\, instab}. \tag{7.15}$$

Whilst the GL instability temperature is known [77] (corresponding to the behavior $r_x^2 = 2.29 r_\tau$ at strong coupling), the GL phase transition temperature is not known in the gravity theory, as the localized solutions have not been constructed. In fact, the near extremal D0-charged black holes are simply related to vacuum solutions of pure gravity with $\mathbb{R}^{1,8} \times S^1$ asymptotics [77, 85]. Such localized black hole solutions have been constructed for asymptotics $\mathbb{R}^{1,3} \times S^1$ and $\mathbb{R}^{1,4} \times S^1$, using numerical techniques [100, 87, 89]. Extending these methods to the case of interest here, $\mathbb{R}^{1,8} \times S^1$, is obviously an interesting future

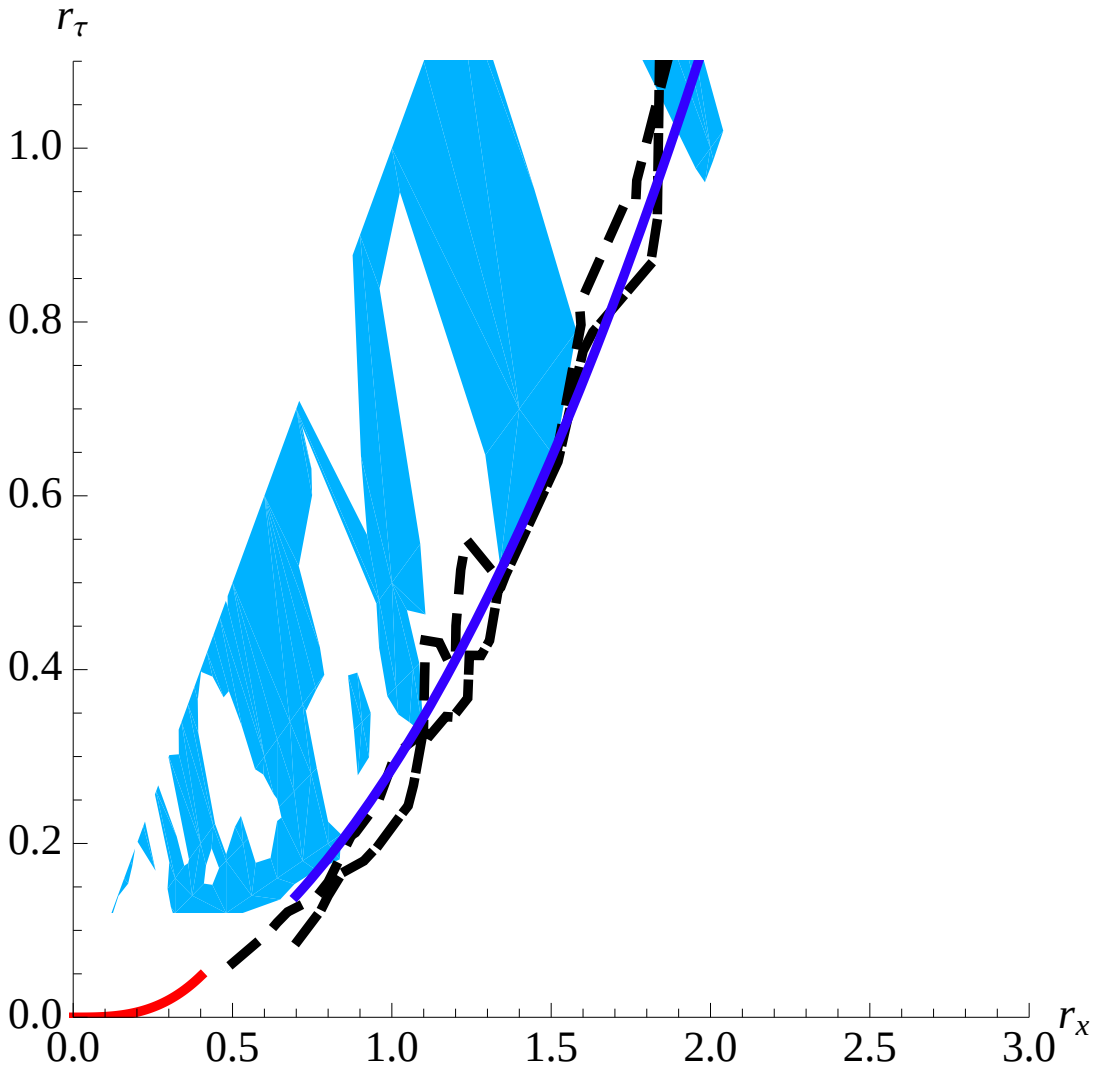

Figure 7.8: Plot showing a superposition of the $P_x = 0.5$ contours for $SU(3)$ and $SU(4)$ as dashed black lines. Also shown is the region (blue) where the $SU(4)$ loop P_x is greater than the $SU(3)$ loop, which is expected to estimate the large N deconfined region for a first order transition (which gravity suggests at strong coupling). 'Holes' in this blue region are due to statistical errors. We see the boundary of this region (ignoring 'holes') matches well the $P_x = 0.5$ contours, and represents our guess for where the large N transition resides. This figure should be compared to the previous figure 7.3 giving a sketch of the expected phase structure. Plotted on the figure is the high temperature prediction for the transition ($r_x^3 = 1.35 r_\tau$, red curve). We note that the estimated large N transition curve fits well both this high temperature prediction and also the strong coupling dual gravity predicted parametric behavior $r_x^2 = c_{crit} r_\tau$. The data obtained through simulations suggests $c_{crit} \simeq 3.5$ (plotted as blue curve), which obeys the constraint from gravity $c_{crit} > 2.29$.

direction. It is worth emphasizing that whilst finding localized solutions in the gravity theory only involves solving the classical Einstein equations, in practice, even phrasing the Einstein equations in a manner amenable to numerical solution, has presented a challenge [89] and then solving the resulting coupled partial differential equations is a serious numerical undertaking.[5] The lattice estimation, $\alpha \simeq 1.5$, obtained through the analysis performed above provides a prediction for the thermal behavior of the gravity solutions. This is the first time a prediction about the properties of non-trivial classical gravity solutions has been made from the Yang–Mills side of a holographic correspondence.

[5]Such solutions can be constructed perturbatively [101, 102, 103, 104] in a small radius limit (compared to the circle size) but the GL phase transition occurs for black holes with radius of order the circle size, and, hence, it is unclear how accurate perturbative methods are for a prediction of $T_{GL\ phase}/T_{GL\ instab}$.

Conclusions

In this dissertation, we have investigated the sixteen supercharge Yang–Mills theories in two and four dimensions on the lattice. We have given lattice constructions of these theories that preserve one exact supersymmetry. The lattice theories are also local, free of doublers and possess exact lattice gauge-invariance.

The lattice version of the four-dimensional $\mathcal{N} = 4$ SYM theory is investigated at one-loop using perturbation theory. We found that the exact symmetries of the classical lattice theory, namely, gauge-invariance, a single exact supersymmetry $\mathcal{Q}$ and the (large) point group symmetry of the lattice strongly constrain the possible counterterms induced by quantum corrections. Indeed, with one exception, the only relevant counterterms correspond to renormalizations of existing terms in the action. We furthermore show, by a computation of the effective action, that the one new operator that cannot be excluded in the general renormalization analysis actually makes no appearance in all orders in perturbation theory.

We have written down the renormalized action in terms of 4 coupling constants α_i that take the value unity in the classical lattice action. We evaluate the renormalization of these couplings at one-loop using lattice perturbation theory. Three of the couplings can be computed by examining the renormalization of the three twisted fermion propagators. The final coupling is most easily read off from a one-loop contribution to the propagator for a bosonic auxiliary field. The relevant propagators and vertices are derived and the amputated one-loop diagrams are constructed. All these diagrams possess identical logarithmic divergences of the form $\log \mu a$, where a is the lattice spacing and μ is a mass scale introduced to regulate the small momentum behavior of the integrands. This divergence can be absorbed by a common wavefunction renormalization of the twisted fermions and bosons.

The simplest way to understand this rather surprising result is to realize that the coefficient of the logarithmic divergence of some one-loop diagram in the lattice theory can be extracted by taking a naive continuum limit of the diagram, since the log divergence comes from the small loop momentum region of the integral. Provided that the lattice diagrams correspond one-to-one with equivalent continuum diagrams, and that all lattice propagators and vertices reduce to their continuum counterparts for small momenta, this means that the log divergences of the lattice theory are equal to the same divergences in

the continuum theory. Furthermore, since the twisted continuum theory is equivalent to the usual $\mathcal{N} = 4$ theory in flat space, it must possess the full $\mathcal{Q} = 16$ supersymmetry. This fact ensures that all divergences present in the twisted continuum fermion self-energies must be equal – which is indeed what we find. And this structure is necessarily inherited by the log divergent parts of the lattice theory at one-loop. This is what leads to the main result: that only a one-time tuning of the finite parts of the wavefunction renormalization needs to be performed at one-loop in order to restore the full supersymmetry.

This similarity between the divergence structure of the lattice theory and the continuum theory is strongly suggestive that the beta function of the lattice theory will also vanish at weak coupling. First, note that the calculation of the beta function requires the evaluation of one-loop vertex diagrams in the lattice theory. Preliminary calculations suggest that the set of relevant lattice vertex diagrams correspond one-to-one to continuum vertex diagrams and remain only logarithmically divergent. They may, thus, be evaluated in the continuum theory. The coefficient of this log divergence is then combined with the wavefunction renormalizations determined above to yield the one-loop beta function in the usual manner. However, we already know the result of this computation for the continuum theory: the beta function vanishes. We, hence, expect a similar result to hold at one-loop in the lattice theory. Thus, for weak coupling, we expect the lattice theory to possess a line of fixed points parametrized by the bare coupling constant, just as for the continuum theory. However, our calculations do not reveal whether this feature survives in the lattice theory to strong coupling. At two or more loops, the divergences of the lattice Feynman diagrams will not be equal to the those of the continuum theory and, hence, we cannot use the latter to infer the divergence structure of the lattice theory. To understand how to take the continuum limit in this regime will then require a mixture of two-loop and numerical calculations.

We also investigate the strongly coupled dynamics of the two-dimensional maximally supersymmetric $SU(N)$ Yang–Mills theory using the method of twisted lattice supersymmetry. Numerical simulations have been performed on the lattice to study the phase structure of the theory at finite temperature and compactified on a circle. The spatial Polyakov line serves as an order parameter for a large N deconfining phase transition in the theory. The simulations are consistent with the existence of a single transition curve in the two-dimensional parameter space spanned by the two dimensionless couplings (r_x and r_τ), which give the size of the thermal and spatial circle in units of the YM coupling.

At high temperature, $r_\tau^3 \ll r_x$, the simulations are consistent with the previously predicted behavior that the transition curve goes as $r_x^3 = 1.35 r_\tau$. At strong coupling, $1 \ll r_\tau$, the transition is conjectured to be the holographic dual of a first order Gregory-Laflamme phase transition, with the transition curve going a $r_x^2 = c_{crit} r_\tau$, with c_{crit}, an order one constant obeying the constraint $c_{crit} > 2.29$. The simulations are consistent with this parametric behavior. The $N = 3, 4$ data can be used to estimate the position of the large N transition, determining $c_{crit} \simeq 3.5$. This gives the ratio of the Gregory-Laflamme phase transition and dynamical instability temperatures to be $T_{GLphase}/T_{GLinstability} \simeq 1.5$. Since the dual localized black hole solutions have not been constructed, this constitutes a prediction for these non-trivial gravity solutions.

Appendix A

Simplification of the one-loop diagrams

We show the details of arriving at the simplified expressions given in (5.54)-(5.57). We use the following identities for the easy evaluation of the diagram:

$$\sum_{B,C} \lambda_{ABC}\lambda_{BCD} = \sum_{B,C} d_{ABC}d_{BCD} - f_{ABC}f_{BCD} \ , \tag{A.1}$$

$$\overline{\lambda}_{ABC} = \lambda_{ACB} \ . \tag{A.2}$$

These relations among structure constants imply

$$\begin{aligned}(\mathbf{A}\lambda_{ABC} - \mathbf{B}\overline{\lambda}_{ABC})(\mathbf{C}\lambda_{BCD} - \mathbf{D}\overline{\lambda}_{BCD}) \\ = d_{ABC}d_{BCD}(\mathbf{AC} - \mathbf{AD} - \mathbf{BC} + \mathbf{BD}) \\ - f_{ABC}f_{BCD}(\mathbf{AC} + \mathbf{AD} + \mathbf{BC} + \mathbf{BD}) \ .\end{aligned} \tag{A.3}$$

We look at the diagram $I_{\eta\psi}(\mathbf{p})$:

$$\begin{aligned}
I_{\eta\psi_d}(\mathbf{p}) &= \int \frac{d^4\mathbf{q}}{(2\pi)^4}\sum_{a,b,c}\sum_{BC}\Big(\frac{1}{16\widehat{(\mathbf{p}-\mathbf{q})}^2\widehat{\mathbf{q}}^2}\Big)(\lambda_{ABC}-\overline{\lambda}_{ABC}e^{ip_a}) \\
&\quad\times(\overline{\lambda}_{BCD}e^{-ip_a}-\lambda_{BCD}e^{iq_d}) \\
&\quad\Big[(1-e^{i(p-q)_b})\delta_{ca}(\delta_{ba}\delta_{cd}-\delta_{bd}\delta_{ca}) \\
&\quad-(1-e^{i(p-q)_c})(\delta_{ba}\delta_{cd}-\delta_{bd}\delta_{ca})\delta_{ba}\Big] \\
&= \int \frac{d^4\mathbf{q}}{(2\pi)^4}\sum_{a,b}\sum_{BC}\Big(\frac{1}{8\widehat{(\mathbf{p}-\mathbf{q})}^2\widehat{\mathbf{q}}^2}\Big) \\
&\quad\Big(d_{ABC}d_{BCD}(e^{-ip_a}-e^{iq_d}-1+e^{ip_a+iq_d}) \\
&\quad+f_{ABC}f_{BCD}(e^{-ip_a}+e^{iq_d}+1+e^{ip_a+iq_d})\Big) \\
&\quad\times(1-e^{i(p-q)_b})(\delta_{ba}\delta_{ad}-\delta_{bd}\delta_{aa})
\end{aligned}$$

That is

$$\begin{aligned}
I_{\eta\psi_d}(\mathbf{p}) &= \int \frac{d^4\mathbf{q}}{(2\pi)^4}\sum_{a}\sum_{BC}\left[\frac{1}{8\widehat{(\mathbf{p}-\mathbf{q})}^2\widehat{\mathbf{q}}^2}\right]\Big[\big[d_{ABC}d_{BCD}(e^{-ip_a}-e^{iq_d}-1+e^{ip_a+iq_d}) \\
&\quad+f_{ABC}f_{BCD}(e^{-ip_a}+e^{iq_d}+1+e^{ip_a+iq_d})\big](1-e^{i(p-q)_a})\delta_{ad} \\
&\quad-\big[d_{ABC}d_{BCD}(e^{-ip_a}-e^{iq_d}-1+e^{ip_a+iq_d}) \\
&\quad+f_{ABC}f_{BCD}(e^{-ip_a}+e^{iq_d}+1+e^{ip_a+iq_d})\big](1-e^{i(p-q)_d})\Big] \\
&= \int \frac{d^4\mathbf{q}}{(2\pi)^4}\sum_{BC}\left[\frac{1}{8\widehat{(\mathbf{p}-\mathbf{q})}^2\widehat{\mathbf{q}}^2}(1-e^{i(p-q)_d})\right] \\
&\quad\times\Big[\big[d_{ABC}d_{BCD}(e^{-ip_d}-e^{iq_d}-1+e^{i(p+q)_d}) \\
&\quad+f_{ABC}f_{BCD}(e^{-ip_d}+e^{iq_d}+1+e^{i(p+q)_d})\big] \\
&\quad-\sum_a\big[d_{ABC}d_{BCD}(e^{-ip_a}-e^{iq_d}-1+e^{ip_a+iq_d}) \\
&\quad+f_{ABC}f_{BCD}(e^{-ip_a}+e^{iq_d}+1+e^{ip_a+iq_d})\big]\Big]
\end{aligned}$$

On further simplification

$$\begin{aligned}
I_{\eta\psi_d}(\mathbf{p}) &= \int \frac{d^4\mathbf{q}}{(2\pi)^4}\sum_{BC}\left[\frac{(1-e^{i(p-q)_d})}{8\widehat{(\mathbf{p}-\mathbf{q})}^2\widehat{\mathbf{q}}^2}\right]\Big[-\sum_{a\neq d}\big[d_{ABC}d_{BCD}(e^{-ip_a}-e^{iq_d} \\
&\quad-1+e^{ip_a+iq_d})+f_{ABC}f_{BCD}(e^{-ip_a}+e^{iq_d}+1+e^{ip_a+iq_d})\big]\Big] \qquad \text{(A.4)}
\end{aligned}$$

Now $I^{(1)}_{\psi_a\chi_{gh}}$:

$$\begin{aligned}
I^{(1)}_{\psi_a\chi_{gh}}(\mathbf{p}) &= \int \frac{d^4\mathbf{q}}{(2\pi)^4} \sum_{b,c,d,e,m,f} \sum_{B,C} \frac{(-1)}{64\widehat{\mathbf{q}}^2(\widehat{\mathbf{p}-\mathbf{q}})^2} \epsilon_{bcmef}\epsilon_{ghdef} e^{i(p-q)_{(e+f)}} \\
&\quad (e^{i(p-q)_m}-1)(\delta_{bd}\delta_{ca}-\delta_{ba}\delta_{cd}) \\
&\quad \times \left(\lambda_{ABC}e^{ip_d} - \overline{\lambda}_{ABC}e^{-iq_a}\right)\Big(e^{-ip_{(d+e+f)}}\left(\overline{\lambda}_{BCD}e^{iq_{(e+f)}} - \lambda_{BCD}e^{i(p-q)_d}\right) \\
&\quad -e^{i(p-q)_{(d+g+h)}}\left(\lambda_{BCD}e^{iq_{(g+h)}} - \overline{\lambda}_{BCD}e^{-ip_d}\right)\Big) \\
&= \int \frac{d^4\mathbf{q}}{(2\pi)^4} \sum_{d,e,m,f} \sum_{B,C} \frac{1}{16\widehat{\mathbf{q}}^2(\widehat{\mathbf{p}-\mathbf{q}})^2} \epsilon_{admef}\epsilon_{ghdef}(e^{i(p-q)_m}-1) \\
&\quad \times\big(-d_{ABC}d_{BCD}(e^{i(p_d+q_{(g+h)})} - 1 - e^{iq_{(g+h-a)}} + e^{-i(p_d+q_a)}) \\
&\quad +f_{ABC}f_{BCD}(e^{i(p_d+q_{(g+h)})} + 1 + e^{iq_{(g+h-a)}} + e^{-i(p_d+q_a)})\big)
\end{aligned}$$

That is

$$\begin{aligned}
I^{(1)}_{\psi_a\chi_{gh}}(\mathbf{p}) &= \int \frac{d^4\mathbf{q}}{(2\pi)^4} \sum_{d,m} \sum_{B,C} \frac{1}{8\widehat{\mathbf{q}}^2(\widehat{\mathbf{p}-\mathbf{q}})^2} (e^{i(p-q)_m}-1) \\
&\quad \times (\delta_{ag}\delta_{mh}+\delta_{ah}\delta_{md}\delta_{dg}+\delta_{ad}\delta_{mg}\delta_{dh}-\delta_{ah}\delta_{mg}-\delta_{ag}\delta_{md}\delta_{dh}-\delta_{ad}\delta_{mh}\delta_{dg}) \\
&\quad \times\big(d_{ABC}d_{BCD}(e^{i(p_d+q_{(g+h)})} - 1 - e^{iq_{(g+h-a)}} + e^{-i(p_d+q_a)}) \\
&\quad -f_{ABC}f_{BCD}(e^{i(p_d+q_{(g+h)})} + 1 + e^{iq_{(g+h-a)}} + e^{-i(p_d+q_a)})\big) \qquad \text{(A.5)}
\end{aligned}$$

Looking at the second $\psi\chi$ diagram we have:

$$\begin{aligned}
I^{(2)}_{\psi_a\chi_{de}}(\mathbf{p}) &= \int \frac{d^4\mathbf{q}}{(2\pi)^4} \sum_{b,c,B,C} \frac{1}{8\widehat{\mathbf{q}}^2(\widehat{\mathbf{p}-\mathbf{q}})^2} (e^{i(p-q)_c}-1)\delta_{ab}(\delta_{db}\delta_{ec}-\delta_{dc}\delta_{eb}) \\
&\quad \times(\lambda_{ABC}e^{-i(p-q)_a} - \overline{\lambda}_{ABC})(\lambda_{BCD}e^{iq_c} - \overline{\lambda}_{BCD}e^{i(p-q)_b}) \\
&= \int \frac{d^4\mathbf{q}}{(2\pi)^4} \sum_{c,B,C} \frac{1}{8\widehat{\mathbf{q}}^2(\widehat{\mathbf{p}-\mathbf{q}})^2} (e^{i(p-q)_c}-1)(\delta_{da}\delta_{ec}-\delta_{dc}\delta_{ea}) \\
&\quad \times\Big(d_{ABC}d_{BCD}(e^{i(q_c-(p-q)_a)} - e^{iq_c} - 1 + e^{i(p-q)_a}) \\
&\quad -f_{ABC}f_{BCD}(e^{i(q_c-(p-q)_a)} + e^{iq_c} + 1 + e^{i(p-q)_a})\Big) \qquad \text{(A.6)}
\end{aligned}$$

Now looking at $I_{\chi_{ab}\chi_{gh}}$:

$$\begin{aligned}
I_{\chi_{ab}\chi_{gh}}(\mathbf{p}) &= \int \frac{d^4\mathbf{q}}{(2\pi)^4} \sum_{c,d,e,f,B,C} \frac{1}{32\widehat{\mathbf{q}}^2\widehat{(\mathbf{p}-\mathbf{q})}^2}\epsilon_{abcde}(\delta_{gc}\delta_{hf}-\delta_{gf}\delta_{hc}) \\
&\quad\times\left((e^{-i(p-q)_d}-1)\delta_{ef}-(e^{-i(p-q)_e}-1)\delta_{df}\right)\left(\lambda_{BCD}e^{iq_f}-\overline{\lambda}_{BCD}e^{i(p-q)_c}\right) \\
&\quad\times\Big(e^{-ik_{(a+b+c)}}\left(\overline{\lambda}_{ABC}e^{ip_c}-\lambda_{ABC}e^{-iq_{(a+b)}}\right) \\
&\quad -e^{ip_{(c+d+e)}}\left(\lambda_{ABC}e^{-i(p-q)_c}-\overline{\lambda}_{ABC}e^{-iq_{(d+e)}}\right)\Big) \\
&= \int \frac{d^4\mathbf{q}}{(2\pi)^4} \sum_{d,e,B,C} \frac{-1}{16\widehat{\mathbf{q}}^2\widehat{(\mathbf{p}-\mathbf{q})}^2}e^{ip_{(g+d+e)}}\epsilon_{abgde} \\
&\quad\times\left((e^{-i(p-q)_d}-1)\delta_{eh}-(e^{-i(p-q)_e}-1)\delta_{dh}\right) \\
&\quad\times\left(\lambda_{ABC}e^{-i(p-q)_g}-\overline{\lambda}_{ABC}e^{-iq_{(d+e)}}\right)\left(\lambda_{BCD}e^{iq_h}-\overline{\lambda}_{BCD}e^{i(p-q)_g}\right) \\
&\quad -(h\leftrightarrow g)
\end{aligned}$$

That is

$$\begin{aligned}
I_{\chi_{ab}\chi_{gh}}(\mathbf{p}) &= \int \frac{d^4\mathbf{q}}{(2\pi)^4} \sum_{d,B,C} \frac{1}{8\widehat{\mathbf{q}}^2\widehat{(\mathbf{p}-\mathbf{q})}^2}e^{ip_{(g+d+h)}}\epsilon_{abdgh}(e^{-i(p-q)_d}-1) \\
&\quad\times\big(d_{ABC}d_{BCD}(e^{-i(p_g-q_{(g+h)})}-1-e^{-iq_d}+e^{i(p_g-q_{(g+d+h)})}) \\
&\quad -f_{ABC}f_{BCD}(e^{-i(p_g-q_{(g+h)})}+1+e^{-iq_d}+e^{i(p_g-q_{(g+d+h)})})\big) \\
&\quad -(h\leftrightarrow g)
\end{aligned} \tag{A.7}$$

(Note that we also need to take into account the diagram where the internal $\psi\chi$ is flipped. It is the same as what we have but with $a\leftrightarrow g$, $b\leftrightarrow h$ and $\mathbf{p}\leftrightarrow-\mathbf{p}$. We may for convenience take $\mathbf{q}\leftrightarrow-\mathbf{q}$. We pick up an additional minus sign in the $f_{ABC}f_{BCD}$ term due to the differing order of the group factors.)

Appendix B

The vanishing of one-loop fermion propagators at zero momentum

We show that the one loop fermion propagators given in given in (5.54)-(5.57) vanish in the limit of vanishing external momentum. Starting with the first diagram and using the simplified forms of the integrals derived in Appendix A (assuming an IR regulator), we have:

$$\begin{aligned} I_{\eta\psi_d}(\mathbf{0}) &= \int \frac{d^4\mathbf{q}}{(2\pi)^4} \sum_{BC} \Big[\frac{1}{8\widehat{\mathbf{q}}^2\widehat{\mathbf{q}}^2}(1-e^{-iq_d}) \Big] \\ &\quad \times \Big[-2 \sum_{a\neq d} f_{ABC} f_{BCD} (1+e^{iq_d}) \Big] = 0 \ , \end{aligned} \tag{B.1}$$

as $(1-e^{-iq_d})(1+e^{iq_d}) = 2i \sin q_d$ and then the integrand is the combination of an odd and an even function.

Next we calculate:

$$\begin{aligned} I^{(1)}_{\psi_a\chi_{gh}}(\mathbf{0}) &= \int \frac{d^4\mathbf{q}}{(2\pi)^4} \sum_{d,m} \sum_{B,C} \frac{1}{8\widehat{\mathbf{q}}^2\widehat{\mathbf{q}}^2} (e^{-iq_m}-1) \Big[\delta_{ag}\delta_{mh} + \delta_{ah}\delta_{md}\delta_{dg} + \delta_{ad}\delta_{mg}\delta_{dh} \\ &\quad -\delta_{ah}\delta_{mg} - \delta_{ag}\delta_{md}\delta_{dh} - \delta_{ad}\delta_{mh}\delta_{dg} \Big] \times \Big(d_{ABC} d_{BCD} (e^{iq_{(g+h)}} \\ &\quad -1 - e^{iq_{(g+h-a)}} + e^{-iq_a}) - f_{ABC} f_{BCD} (e^{iq_{(g+h)}} + 1 + e^{iq_{(g+h-a)}} + e^{-iq_a}) \Big) \\ &= \int \frac{d^4\mathbf{q}}{(2\pi)^4} \sum_{m} \sum_{B,C} \frac{1}{8\widehat{\mathbf{q}}^2\widehat{\mathbf{q}}^2} (e^{-iq_m}-1) \Big(\delta_{ah}\delta_{mg} - \delta_{ag}\delta_{mh} \Big) \\ &\quad \times \Big(d_{ABC} d_{BCD} (e^{iq_{(g+h)}} - 1 - e^{iq_{(g+h-a)}} + e^{-iq_a}) \\ &\quad - f_{ABC} f_{BCD} (e^{iq_{(g+h)}} + 1 + e^{iq_{(g+h-a)}} + e^{-iq_a}) \Big) \ . \end{aligned} \tag{B.2}$$

Then, we can use the fact that if $a \neq g$ and $a \neq h$ then the expression disappears. If $a = g = h$, again the expression disappears. So, assuming $a = h$ and $a \neq g$ we get:

$$\begin{aligned} I^{(1)}_{\psi_a\chi_{gh}}(\mathbf{0}) &= \int \frac{d^4\mathbf{q}}{(2\pi)^4} \sum_{B,C} \frac{1}{8\widehat{\mathbf{q}}^2\widehat{\mathbf{q}}^2}(e^{-iq_g}-1)\Big(d_{ABC}d_{BCD}(e^{iq_{(g+a)}}-1-e^{iq_g}+e^{-iq_a}) \\ &\quad -f_{ABC}f_{BCD}(e^{iq_{(g+a)}}+1+e^{iq_g}+e^{-iq_a})\Big) \\ &= \int \frac{d^4\mathbf{q}}{(2\pi)^4} \sum_{B,C} \frac{2i}{8\widehat{\mathbf{q}}^2\widehat{\mathbf{q}}^2}\Big(d_{ABC}d_{BCD}(\sin q_a+\sin q_g-\sin q_{(a+g)}) \\ &\quad -f_{ABC}f_{BCD}(\sin q_a-\sin q_g-\sin q_{(a+g)})\Big) \\ &= 0\ , \end{aligned} \tag{B.3}$$

which vanishes term by term.

We then move onto the second $\psi\chi$ diagram.

$$\begin{aligned} I^{(2)}_{\psi_a\chi_{de}}(\mathbf{0}) &= \int \frac{d^4\mathbf{q}}{(2\pi)^4} \sum_{c,B,C} \frac{1}{8\widehat{\mathbf{q}}^2\widehat{\mathbf{q}}^2}(e^{-iq_c}-1)(\delta_{da}\delta_{ec}-\delta_{dc}\delta_{ea}) \\ &\quad \times\Big(d_{ABC}d_{BCD}(e^{iq_{(c+a)}}-e^{iq_c}-1+e^{-iq_a}) \\ &\quad -f_{ABC}f_{BCD}(e^{iq_{(c+a)}}+e^{iq_c}+1+e^{-iq_a})\Big) \end{aligned} \tag{B.4}$$

In a similar way to the previous diagram, if $a \neq d$ and $a \neq e$, then the diagram vanishes. If $a = d = e$, it also vanishes, so we only need to deal with the case $a = d$, $a \neq e$:

$$\begin{aligned} I^{(2)}_{\psi_a\chi_{de}}(\mathbf{0}) &= \int \frac{d^4\mathbf{q}}{(2\pi)^4} \sum_{B,C} \frac{1}{8\widehat{\mathbf{q}}^2\widehat{\mathbf{q}}^2}(e^{-iq_e}-1)\Big(d_{ABC}d_{BCD}(e^{iq_{(e+a)}}-e^{iq_e}-1+e^{-iq_a}) \\ &\quad -f_{ABC}f_{BCD}(e^{iq_{(e+a)}}+e^{iq_e}+1+e^{-iq_a})\Big) \\ &= \int \frac{d^4\mathbf{q}}{(2\pi)^4} \sum_{B,C} \frac{2i}{8\widehat{\mathbf{q}}^2\widehat{\mathbf{q}}^2}(e^{-iq_e}-1)\Big(d_{ABC}d_{BCD}(\sin q_a+\sin q_{(a+e)}+\sin q_e) \\ &\quad -f_{ABC}f_{BCD}(\sin q_a+\sin q_{(a+e)}-\sin q_e)\Big) \\ &= 0\ , \end{aligned} \tag{B.5}$$

which again vanishes term by term.

Finally we show that $I_{\chi\chi}(\mathbf{0}) = 0$.

$$\begin{aligned}
I_{\chi_{ab}\chi_{gh}}(\mathbf{0}) &= \int \frac{d^4\mathbf{q}}{(2\pi)^4} \sum_{d,B,C} \frac{1}{8\widehat{\mathbf{q}}^2\widehat{\mathbf{q}}^2} \epsilon_{abdgh} (e^{iq_d} - 1) \\
&\quad \times \Big(d_{ABC} d_{BCD} (e^{iq_{(g+h)}} - 1 - e^{-iq_d} + e^{-iq_{(g+d+h)}}) \\
&\quad - f_{ABC} f_{BCD} (e^{iq_{(g+h)}} + 1 + e^{-iq_d} + e^{-iq_{(g+d+h)}}) \Big) \\
&\quad - \Big(h \leftrightarrow g \Big) \\
&= \int \frac{d^4\mathbf{q}}{(2\pi)^4} \sum_{d,B,C} \frac{2i}{8\widehat{\mathbf{q}}^2\widehat{\mathbf{q}}^2} \epsilon_{abdgh} \\
&\quad \times \Big(d_{ABC} d_{BCD} (\sin q_{(d+g+h)} - \sin q_d - \sin q_{(g+h)}) \\
&\quad - f_{ABC} f_{BCD} (\sin q_{(d+g+h)} + \sin q_d - \sin q_{(g+h)}) \Big) \\
&= 0 \; . \qquad \text{(B.6)}
\end{aligned}$$

Appendix C

Coupling constant independence in $\mathcal{N} = 4$ SYM

The twisted $\mathcal{N} = 4$ SYM in the continuum possesses a privileged set of operators whose expectation values can be shown to be independent of the background metric and, hence, topological. (See (2.31) and (2.32) in Chapter 2.) The condition for this to be true is that the operator be annihilated by the charge $\mathcal{Q}$. In addition, the expectation values of these operators can be shown to be independent of the coupling constant. As we will see, this property remains true in the lattice theory and provides powerful constraints on the renormalization of such operators. To see this result, consider the twisted lattice action, which is the sum of $\mathcal{Q}$-exact and $\mathcal{Q}$-closed terms. The coupling constant dependence of the $\mathcal{Q}$-closed term can be removed, without disturbing the $\mathcal{Q}$ BRST transformation, by rescaling the fields in appropriate ways. We show this below.

The twisted action is:

$$\begin{aligned} S &= \frac{1}{g^2} S_{exact} + \frac{1}{g^2} S_{closed} \\ &= \int \mathrm{Tr} \left\{ \frac{1}{g^2} \Big(\overline{\mathcal{F}}_{ab} \mathcal{F}_{ab} + \frac{1}{2} [\overline{\mathcal{D}}_a, \mathcal{D}_a]^2 - \chi_{ab} \mathcal{D}_{[a} \psi_{b]} - \eta \overline{\mathcal{D}}_a \psi_a \Big) \right. \\ &\quad \left. - \frac{1}{g^2} \Big(\frac{1}{2} \epsilon_{abcde} \chi_{ab} \overline{\mathcal{D}}_c \chi_{de} \Big) \right\} . \end{aligned} \tag{C.1}$$

A simple rescaling of the fields:

$$\chi_{ab} \to \chi_{ab}/g, \quad \psi_a \to g\psi_a, \quad \eta \to \eta/g \ , \tag{C.2}$$

gives the action

$$\begin{aligned} S &= \frac{1}{g^2}\int \mathrm{Tr}\left(\overline{\mathcal{F}}_{ab}\mathcal{F}_{ab} + \frac{1}{2}[\overline{\mathcal{D}}_a, \mathcal{D}_a]^2 - \chi_{ab}\mathcal{D}_{[a}\psi_{b]} - \eta\overline{\mathcal{D}}_a\psi_a\right) \\ &\quad -\frac{1}{2}\int \mathrm{Tr}\,\epsilon_{abcde}\chi_{ab}\overline{\mathcal{D}}_c\chi_{de} \\ &= \frac{1}{g^2}S_{exact} + S_{closed} \end{aligned} \tag{C.3}$$

Calling $\beta = \frac{1}{g^2}$ and writing the action as $S = \mathcal{Q}\Lambda + S_{\text{closed}}$ the expression for the expectation value of a $\mathcal{Q}$-invariant operator $\mathcal{O}$ becomes

$$\langle\mathcal{O}\rangle_\beta = \frac{1}{Z}\int \mathcal{O}e^{-(\beta\mathcal{Q}\Lambda + S_{closed})}, \quad Z = \int e^{-(\beta\mathcal{Q}\Lambda + S_{closed})}\ . \tag{C.4}$$

Differentiating this expression with respect to β leads to

$$\begin{aligned} \frac{\partial}{\partial\beta}\langle\mathcal{O}\rangle_\beta &= \langle\mathcal{Q}\Lambda\rangle_\beta\langle\mathcal{O}\rangle_\beta - \langle\mathcal{O}\mathcal{Q}\Lambda\rangle_\beta \\ &= \langle\mathcal{Q}\Lambda\rangle_\beta\langle\mathcal{O}\rangle_\beta - \langle\mathcal{Q}(\mathcal{O}\Lambda)\rangle_\beta \\ &= 0\ , \end{aligned} \tag{C.5}$$

where we have used the fact that as long as the BRST symmetry is not broken spontaneously, the expectation value of the $\mathcal{Q}$ variation of some operator vanishes. Thus, expectation values of $\mathcal{Q}$-invariant observables are independent of β and, hence, can be computed exactly in the semi-classical limit $\beta \to \infty$. In this limit, we need only do one loop calculations around the classical vacua.

Bibliography

[1] J. M. Maldacena, "The Large N limit of superconformal field theories and supergravity," Adv. Theor. Math. Phys. **2**, 231-252 (1998). [hep-th/9711200].

[2] L. Brink, J. H. Schwarz, J. Scherk, "Supersymmetric Yang–Mills Theories," Nucl. Phys. **B121**, 77 (1977).

[3] F. Gliozzi, J. Scherk, D. I. Olive, "Supersymmetry, Supergravity Theories and the Dual Spinor Model," Nucl. Phys. **B122**, 253-290 (1977).

[4] J. Polchinski, "String theory. Vol. 2: Superstring theory and beyond," Cambridge, UK: Univ. Pr. (1998) 531 p.

[5] S. Weinberg, "The quantum theory of fields. Vol. 3: Supersymmetry," Cambridge, UK: Univ. Pr. (2000) 419 p.

[6] A. S. Schwarz, "The Partition Function of Degenerate Quadratic Functional and Ray-Singer Invariants," Lett. Math. Phys. **2**, 247-252 (1978).

[7] E. Witten, "Supersymmetry and Morse theory," J. Diff. Geom. **17**, 661-692 (1982).

[8] C. Becchi, A. Rouet, R. Stora, "Renormalization of Gauge Theories," Annals Phys. **98**, 287-321 (1976).

[9] M. Z. Iofa, I. V. Tyutin, "Gauge Invariance of Spontaneously Broken Nonabelian Theories in the Bogolyubov-Parasiuk-HEPP-Zimmerman Method," Teor. Mat. Fiz. **27**, 38-47 (1976).

[10] D. Birmingham, M. Blau, M. Rakowski, G. Thompson, "Topological field theory," Phys. Rept. **209**, 129-340 (1991).

[11] E. Witten, "Topological Quantum Field Theory," Commun. Math. Phys. **117**, 353 (1988).

[12] L. Baulieu, I. M. Singer, "Topological Yang–mills Symmetry," Nucl. Phys. Proc. Suppl. **5B**, 12-19 (1988).

[13] R. Brooks, D. Montano, J. Sonnenschein, "gauge-fixing And Renormalization In Topological Quantum Field Theory," Phys. Lett. **B214**, 91 (1988).

[14] J. M. F. Labastida, M. Pernici, "A Gauge Invariant Action in Topological Quantum Field Theory," Phys. Lett. **B212**, 56 (1988).

[15] I. A. Batalin, G. A. Vilkovisky, "Quantization of Gauge Theories with Linearly Dependent Generators," Phys. Rev. **D28**, 2567-2582 (1983).

[16] J. P. Yamron, "Topological Actions From Twisted Supersymmetric Theories," Phys. Lett. **B213**, 325 (1988).

[17] C. Vafa, E. Witten, "A Strong coupling test of S duality," Nucl. Phys. **B431**, 3-77 (1994). [hep-th/9408074].

[18] N. Marcus, "The Other topological twisting of N=4 Yang–Mills," Nucl. Phys. **B452**, 331-345 (1995). [hep-th/9506002].

[19] M. Blau, G. Thompson, "Aspects of $N_T \geq 2$ topological gauge theories and D-branes," Nucl. Phys. **B492**, 545-590 (1997). [hep-th/9612143].

[20] S. Elitzur, E. Rabinovici, A. Schwimmer, "Supersymmetric Models On The Lattice," Phys. Lett. **B119**, 165 (1982).

[21] N. Sakai, M. Sakamoto, "Lattice Supersymmetry And The Nicolai Mapping," Nucl. Phys. **B229**, 173 (1983).

[22] V. A. Kostelecky, J. M. Rabin, "Supersymmetry On A Superlattice," J. Math. Phys. **25**, 2744 (1984).

[23] D. M. Scott, "Lattices, Supersymmetry, And Kahler Fermions," J. Phys. A **A17**, 1123 (1984).

[24] H. Aratyn, A. H. Zimerman, "Lattice Supersymmetry For N=4 Yang–mills Model," J. Phys. A **A18**, L487 (1985).

[25] N. Kawamoto, T. Tsukioka, "N=2 supersymmetric model with Dirac-Kahler fermions from generalized gauge theory in two-dimensions," Phys. Rev. **D61**, 105009 (2000). [hep-th/9905222].

[26] J. Kato, N. Kawamoto, Y. Uchida, "Twisted superspace for N=D=2 super BF and Yang–Mills with Dirac-Kahler fermion mechanism," Int. J. Mod. Phys. **A19**, 2149-2182 (2004). [hep-th/0310242].

[27] A. D'Adda, I. Kanamori, N. Kawamoto, K. Nagata, "Twisted superspace on a lattice," Nucl. Phys. **B707**, 100-144 (2005). [hep-lat/0406029].

[28] S. Catterall, "Lattice supersymmetry via twisting," Nucl. Phys. Proc. Suppl. **140**, 751-753 (2005). [hep-lat/0409015].

[29] S. Catterall, "A Geometrical approach to N=2 super Yang–Mills theory on the two dimensional lattice," JHEP **0411**, 006 (2004). [hep-lat/0410052].

[30] S. Catterall, "Lattice formulation of N=4 super Yang–Mills theory," JHEP **0506**, 027 (2005). [hep-lat/0503036].

[31] S. Catterall, "Dirac-Kahler fermions and exact lattice supersymmetry," PoS **LAT2005**, 006 (2006). [hep-lat/0509136].

[32] M. Ünsal, "Twisted supersymmetric gauge theories and orbifold lattices," JHEP **0610**, 089 (2006) [hep-th/0603046].

[33] S. Catterall, "From Twisted Supersymmetry to Orbifold Lattices," JHEP **0801**, 048 (2008) [arXiv:0712.2532 [hep-th]].

[34] S. Catterall and A. Joseph, "Lattice actions for Yang-Mills quantum mechanics with exact supersymmetry," Phys. Rev. D **77**, 094504 (2008) [arXiv:0712.3074 [hep-lat]].

[35] S. Catterall, D. B. Kaplan, M. Ünsal, "Exact lattice supersymmetry," Phys. Rept. **484**, 71-130 (2009). [arXiv:0903.4881 [hep-lat]].

[36] E. Witten, "Phases of N = 2 theories in two dimensions," Nucl. Phys. B **403**, 159 (1993) [arXiv:hep-th/9301042].

[37] D. B. Kaplan, E. Katz, M. Ünsal, "Supersymmetry on a spatial lattice," JHEP **0305**, 037 (2003). [hep-lat/0206019].

[38] A. G. Cohen, D. B. Kaplan, E. Katz, M. Ünsal, "Supersymmetry on a Euclidean space-time lattice. 1. A Target theory with four supercharges," JHEP **0308**, 024 (2003). [hep-lat/0302017].

[39] A. G. Cohen, D. B. Kaplan, E. Katz, M. Ünsal, "Supersymmetry on a Euclidean space-time lattice. 2. Target theories with eight supercharges," JHEP **0312**, 031 (2003). [hep-lat/0307012].

[40] D. B. Kaplan, M. Ünsal, "A Euclidean lattice construction of supersymmetric Yang–Mills theories with sixteen supercharges," JHEP **0509**, 042 (2005). [hep-lat/0503039].

[41] T. Banks, Y. Dothan, D. Horn, "Geometric Fermions," Phys. Lett. **B117**, 413 (1982).

[42] J. M. Rabin, "Homology Theory Of Lattice Fermion Doubling," Nucl. Phys. **B201**, 315 (1982).

[43] A. D'Adda, I. Kanamori, N. Kawamoto, K. Nagata, "Exact extended supersymmetry on a lattice: Twisted N=2 super Yang–Mills in two dimensions," Phys. Lett. **B633**, 645-652 (2006). [hep-lat/0507029].

[44] A. Kapustin, E. Witten, "Electric-Magnetic Duality And The Geometric Langlands Program," [hep-th/0604151].

[45] P. Becher, "Dirac Fermions On The Lattice: A Local Approach Without Spectrum Degeneracy," Phys. Lett. **B104**, 221 (1981).

[46] P. Becher, H. Joos, "The Dirac-Kahler Equation and Fermions on the Lattice," Z. Phys. **C15**, 343 (1982).

[47] H. Aratyn, M. Goto, A. H. Zimerman, "A Lattice Gauge Theory For Fields In The Adjoint Representation," Nuovo Cim. **A84**, 255 (1984).

[48] P. H. Damgaard, S. Matsuura, "Geometry of Orbifolded Supersymmetric Lattice Gauge Theories," Phys. Lett. **B661**, 52-56 (2008). [arXiv:0801.2936 [hep-th]].

[49] S. Catterall, E. Dzienkowski, J. Giedt, A. Joseph, R. Wells, "Perturbative renormalization of lattice N=4 super Yang-Mills theory," JHEP **1104**, 074 (2011). [arXiv:1102.1725 [hep-th]].

[50] S. Matsuura, "Exact Vacuum Energy of Orbifold Lattice Theories," JHEP **0712**, 048 (2007) [arXiv:0709.4193 [hep-lat]].

[51] T. Reisz "A Power Counting Theorem for Feynman Integrals on the Lattice" Commun. Math. Phys. **116**, 81 (1988)

[52] T. Reisz "A Convergence Theorem for Lattice Feynman Integrals with Massless Propagators" Commun. Math. Phys. **116**, 573 (1988)

[53] T. Reisz "Renormalization of Feynman Integrals on the Lattice" Commun. Math. Phys. **117**, 79 (1988)

[54] T. Reisz "Renormalization of Lattice Feynman Integrals with Massless Propagators" Commun. Math. Phys. **117**, 639 (1988)

[55] H. Kawai, R. Nakayama and K. Seo "Comparison of the Lattice Λ Parameter with the Continuum Λ Parameter in Massless QCD" Nucl. Phys. B **189**, 40 (1981)

[56] S. Capitani "Lattice Perturbation Theory," Phys. Rept. **382**, 113 (2003) [arXiv:0211.036v2 [hep-lat]].

[57] S. Duane, A. D. Kennedy, B. J. Pendleton, D. Roweth, "Hybrid Monte Carlo," Phys. Lett. **B195**, 216-222 (1987).

[58] F. Fucito, E. Marinari, G. Parisi, C. Rebbi, "A Proposal for Monte Carlo Simulations of Fermionic Systems," Nucl. Phys. **B180**, 369 (1981).

[59] M. A. Clark, "The Rational Hybrid Monte Carlo Algorithm," PoS **LAT2006**, 004 (2006). [hep-lat/0610048].

[60] A. Frommer, B. Nockel, S. Gusken, T. Lippert, K. Schilling, "Many masses on one stroke: Economic computation of quark propagators," Int. J. Mod. Phys. **C6**, 627-638 (1995). [hep-lat/9504020].

[61] B. Jegerlehner, "Krylov space solvers for shifted linear systems," [hep-lat/9612014].

[62] J. C. Sexton, D. H. Weingarten, "Hamiltonian evolution for the hybrid Monte Carlo algorithm," Nucl. Phys. **B380**, 665-678 (1992).

[63] S. Catterall, A. Joseph, T. Wiseman, "Gauge theory duals of black hole - black string transitions of gravitational theories on a circle," [arXiv:1009.0529 [hep-th]].

[64] S. Catterall, A. Joseph, T. Wiseman, "Thermal phases of D1-branes on a circle from lattice super Yang–Mills," JHEP **1012**, 022 (2010). [arXiv:1008.4964 [hep-th]].

[65] N. Itzhaki, J. M. Maldacena, J. Sonnenschein, and S. Yankielowicz, *Supergravity and the large N limit of theories with sixteen supercharges*, *Phys. Rev.* **D58** (1998) 046004, [hep-th/9802042].

[66] M. Hanada, J. Nishimura, and S. Takeuchi, *Non-lattice simulation for supersymmetric gauge theories in one dimension*, *Phys. Rev. Lett.* **99** (2007) 161602, [0706.1647].

[67] S. Catterall and T. Wiseman, *Towards lattice simulation of the gauge theory duals to black holes and hot strings*, *JHEP* **12** (2007) 104, [0706.3518].

[68] K. N. Anagnostopoulos, M. Hanada, J. Nishimura, and S. Takeuchi, *Monte Carlo studies of supersymmetric matrix quantum mechanics with sixteen supercharges at finite temperature*, *Phys. Rev. Lett.* **100** (2008) 021601, [0707.4454].

[69] S. Catterall and T. Wiseman, *Black hole thermodynamics from simulations of lattice Yang–Mills theory*, *Phys. Rev.* **D78** (2008) 041502, [0803.4273].

[70] M. Hanada, A. Miwa, J. Nishimura, and S. Takeuchi, *Schwarzschild radius from Monte Carlo calculation of the Wilson loop in supersymmetric matrix quantum mechanics*, *Phys. Rev. Lett.* **102** (2009) 181602, [0811.2081].

[71] M. Hanada, Y. Hyakutake, J. Nishimura, and S. Takeuchi, *Higher derivative corrections to black hole thermodynamics from supersymmetric matrix quantum mechanics*, *Phys. Rev. Lett.* **102** (2009) 191602, [0811.3102].

[72] S. Catterall and T. Wiseman, *Extracting black hole physics from the lattice*, *JHEP* **04** (2010) 077, [0909.4947].

[73] M. Hanada, J. Nishimura, Y. Sekino, and T. Yoneya, *Monte Carlo studies of Matrix theory correlation functions*, *Phys. Rev. Lett.* **104** (2010) 151601, [0911.1623].

[74] S. Catterall and G. van Anders, *First Results from Lattice Simulation of the PWMM*, 1003.4952.

[75] G. Ishiki, S.-W. Kim, J. Nishimura, and A. Tsuchiya, *Deconfinement phase transition in N=4 super Yang–Mills theory on $R \times S^3$ from supersymmetric matrix quantum mechanics*, *Phys. Rev. Lett.* **102** (2009) 111601, [0810.2884].

[76] G. Ishiki, S.-W. Kim, J. Nishimura, and A. Tsuchiya, *Testing a novel large-N reduction for N=4 super Yang–Mills theory on $R \times S^3$*, *JHEP* **09** (2009) 029, [0907.1488].

[77] O. Aharony, J. Marsano, S. Minwalla, and T. Wiseman, *Black hole-black string phase transitions in thermal 1+1- dimensional supersymmetric Yang–Mills theory on a circle*, *Class. Quant. Grav.* **21** (2004) 5169–5192, [hep-th/0406210].

[78] O. Aharony *et al.*, *The phase structure of low dimensional large N gauge theories on tori*, *JHEP* **01** (2006) 140, [hep-th/0508077].

[79] R. Gregory and R. Laflamme, *Black strings and p-branes are unstable*, *Phys. Rev. Lett.* **70** (1993) 2837–2840, [hep-th/9301052].

[80] R. Gregory and R. Laflamme, *The Instability of charged black strings and p-branes*, *Nucl. Phys.* **B428** (1994) 399–434, [hep-th/9404071].

[81] L. Susskind, *Matrix theory black holes and the Gross Witten transition*, hep-th/9805115.

[82] M. Li, E. J. Martinec, and V. Sahakian, *Black holes and the SYM phase diagram*, *Phys. Rev.* **D59** (1999) 044035, [hep-th/9809061].

[83] E. J. Martinec and V. Sahakian, *Black holes and the SYM phase diagram. II*, *Phys. Rev.* **D59** (1999) 124005, [hep-th/9810224].

[84] B. Kol, *Topology change in general relativity and the black-hole black-string transition*, *JHEP* **10** (2005) 049, [hep-th/0206220].

[85] T. Harmark and N. A. Obers, *New phases of near-extremal branes on a circle*, *JHEP* **09** (2004) 022, [hep-th/0407094].

[86] T. Harmark and N. A. Obers, *New phases of thermal SYM and LST from Kaluza-Klein black holes*, *Fortsch. Phys.* **53** (2005) 536–541, [hep-th/0503021].

[87] H. Kudoh and T. Wiseman, *Properties of Kaluza-Klein black holes*, *Prog. Theor. Phys.* **111** (2004) 475–507, [hep-th/0310104].

[88] H. Kudoh and T. Wiseman, *Connecting black holes and black strings*, *Phys. Rev. Lett.* **94** (2005) 161102, [hep-th/0409111].

[89] M. Headrick, S. Kitchen, and T. Wiseman, *A new approach to static numerical relativity, and its application to Kaluza-Klein black holes*, *Class. Quant. Grav.* **27** (2010) 035002, [0905.1822].

[90] B. Kol, *The Phase Transition between Caged Black Holes and Black Strings - A Review*, *Phys. Rept.* **422** (2006) 119–165, [hep-th/0411240].

[91] T. Harmark and N. A. Obers, *Phases of Kaluza-Klein black holes: A brief review*, hep-th/0503020.

[92] T. Harmark, V. Niarchos, and N. A. Obers, *Instabilities of black strings and branes*, *Class. Quant. Grav.* **24** (2007) R1–R90, [hep-th/0701022].

[93] T. Eguchi and H. Kawai, *Reduction of Dynamical Degrees of Freedom in the Large N Gauge Theory*, *Phys. Rev. Lett.* **48** (1982) 1063.

[94] T. Banks, W. Fischler, S. H. Shenker, and L. Susskind, *M theory as a matrix model: A conjecture*, *Phys. Rev.* **D55** (1997) 5112–5128, [hep-th/9610043].

[95] N. Kawahara, J. Nishimura, and S. Takeuchi, *Phase structure of matrix quantum mechanics at finite temperature*, *JHEP* **10** (2007) 097, [0706.3517].

[96] G. Mandal, M. Mahato, and T. Morita, *Phases of one dimensional large N gauge theory in a 1/D expansion*, *JHEP* **02** (2010) 034, [0910.4526].

[97] D. J. Gross and E. Witten, *Possible Third Order Phase Transition in the Large N Lattice Gauge Theory*, *Phys. Rev.* **D21** (1980) 446–453.

[98] S. Wadia, *A STUDY OF U(N) LATTICE GAUGE THEORY IN TWO-DIMENSIONS*, . EFI-79/44-CHICAGO.

[99] S. Catterall, *First results from simulations of supersymmetric lattices*, *JHEP* **01** (2009) 040, [0811.1203].

[100] T. Wiseman, *Static axisymmetric vacuum solutions and non-uniform black strings*, *Class. Quant. Grav.* **20** (2003) 1137–1176, [hep-th/0209051].

[101] T. Harmark, *Small black holes on cylinders*, *Phys. Rev.* **D69** (2004) 104015, [hep-th/0310259].

[102] D. Gorbonos and B. Kol, *A dialogue of multipoles: Matched asymptotic expansion for caged black holes*, *JHEP* **06** (2004) 053, [hep-th/0406002].

[103] D. Gorbonos and B. Kol, *Matched asymptotic expansion for caged black holes: Regularization of the post-Newtonian order*, *Class. Quant. Grav.* **22** (2005) 3935–3960, [hep-th/0505009].

[104] D. Karasik, C. Sahabandu, P. Suranyi, and L. C. R. Wijewardhana, *Analytic approximation to 5 dimensional black holes with one compact dimension*, *Phys. Rev.* **D71** (2005) 024024, [hep-th/0410078].

VITA

NAME OF AUTHOR: Anosh Joseph

PLACE OF BIRTH: Anthinadu, Kerala, India

DATE OF BIRTH: September 23, 1980

DEGREES AWARDED:

M.Sc., Physics, Indian Institute of Technology–Madras, Chennai, India (2004)

B.Sc., Physics, Mahatma Gandhi University, Kottayam, India (2001)

PROFESSIONAL EXPERIENCE:

Syracuse University, Department of Physics, Graduate Student Instructor/Assistant & Graduate Student Researcher (2005-2011)

Syracuse University, The Graduate School, Future Professoriate Program participant (2010-2011)

HONORS AND AWARDS:

Certificate in University Teaching, Syracuse University (April 2011)

Outstanding Teaching Assistant Award, Syracuse University (April 2009)

Gold Medalist, Indian Institute of Technology–Madras, Chennai, India (July 2004)